Danica Bugarski BSc

Clinical benefit and visualization of baroreceptor sensitivity (BRS) in a non-invasive medical device using spectral methods

MASTER'S THESIS

to achieve the university degree of

Master of Science

Master's degree programme:

Biomedical Engineering

submitted to

Graz University of Technology

Supervisor

Ao.Univ.-Prof. Dipl.-Ing. Dr.techn. Hermann Scharfetter

Institute of Biomedical Imaging

Co-Supervisor

Dipl.-Ing. Dr. Jürgen Fortin

Graz, November 2024

AFFIDAVIT

I declare that I have authored this thesis independently, that I have not used other than the declared sources/resources, and that I have explicitly indicated all material which has been quoted either literally or by content from the sources used. The text document uploaded to TUGRAZonline is identical to the present master's thesis.

Date, Signature

Abstract

This thesis explores the Baroreflex Sensitivity (BRS), a cardiac parameter, emphasizing its clinical relevance, computational methodologies and visualization techniques. The thesis is divided into two phases: a literature review and a practical phase. The literature review identifies three primary clinical roles of BRS - outcome prediction, risk stratification, and disease diagnosis in cardiovascular-related conditions such as congestive heart failure (CHF), post-myocardial infarction (POST-MI), diabetes mellitus, and hypertension. Among computational methods, the sequence method is the most cited, while spectral methods, including the transfer function and alpha coefficient, offer unique capabilities such as tracking BRS changes across time and frequency domains. Strengths and limitations of these methods are discussed, with an emphasis on their non-interchangeability and the impact of parameter variations on outcomes.

The practical phase involved implementing the transfer function-based spectral method for BRS computation and comparing two spectral decomposition techniques: the Welch method (frequency domain) and the Short-Time Fourier Transform (STFT, time-frequency domain). Key spectral parameters affecting BRS calculations, such as sampling frequency, window size, FFT size, and overlap, are analyzed, revealing their influence on BRS variability and visualization. This phase also introduces normalized 3D spectrograms for STFT-based BRS visualizations.

The thesis underscores the need for future work reflecting standardized protocols, larger studies, optimized algorithms, and tailored parameter settings to enhance BRS research and facilitate its integration into clinical practice. Suggestions for further research and potential incorporation into medical devices are also provided, paving the way for improved BRS-related healthcare applications.

Keywords: baroreflex sensitivity, transfer function analysis, baroreflex sensitivity visualization, time-frequency domain, short-time fourier transform

Zusammenfassung

In dieser Arbeit wird die Baroreflex-Sensitivität (BRS), ein Herzparameter, untersucht, wobei seine klinische Relevanz, Berechnungsmethoden und Visualisierungstechniken im Vordergrund stehen. Die Arbeit gliedert sich in zwei Phasen: eine Literaturübersicht und eine praktische Phase. In der Literaturübersicht werden drei primäre klinische Anwendungen von BRS identifiziert: Ergebnisvorhersage, Risikostratifizierung und Diagnose bei kardiovaskulären Erkrankungen wie kongestiver Herzinsuffizienz (CHF), Post-Myokardinfarkt (POST-MI), Diabetes mellitus und Hypertonie. Unter den Berechnungsmethoden wird die Sequenz Methode am häufigsten genannt, während spektrale Methoden, einschließlich der Übertragungsfunktion und des Alphakoeffizienten, einzigartige Möglichkeiten bieten, wie z. B. die Verfolgung von BRS-Änderungen über Zeit- und Frequenzbereiche hinweg. Die Vorteile und Nachteile dieser Methoden werden diskutiert, wobei der Schwerpunkt auf ihren Unterschieden und den Auswirkungen von Parametervariationen auf die Ergebnisse liegt.

Die praktische Phase umfasste die Implementierung der auf Übertragungsfunktionen basierenden Spektralmethode für die BRS-Berechnung und den Vergleich zweier spektraler Dekompositionstechniken: die Welch-Methode (Frequenzbereich) und die Kurzzeit-Fourier-Transformation (STFT, Zeit-Frequenz-Bereich). Die wichtigsten spektralen Parameter, die die BRS-Berechnungen beeinflussen, wie die Abtastfrequenz, die Fenstergröße, die FFT-Größe und die Überlappung, werden analysiert und ihr Einfluss auf die BRS-Variabilität und die Visualisierung aufgezeigt. In dieser Phase werden auch normalisierte 3D-Spektrogramme für STFT-basierte BRS-Visualisierungen eingeführt.

Die Arbeit unterstreicht die Notwendigkeit zukünftiger Forschungen mit standardisierten Protokollen, größeren Studien, optimierten Algorithmen und angepassten Parametereinstellungen, um die BRS-Forschung zu verbessern und ihre Integration in die klinische Praxis zu erleichtern. Es werden auch Vorschläge für die weitere Forschung und die mögliche Integration in medizinische Geräte gemacht, die den Weg für verbesserte BRS-Anwendungen im Gesundheitswesen erleichtern.

Schlüsselwörter: Baroreflex-Sensitivität, Übertragungsfunktionsanalyse, Visualisierung der Baroreflex-Sensitivität, Zeit-/Frequenzbereich, Kurzzeit-Fourier-Transformation

Acknowledgement

First and foremost, I would like to express my deepest gratitude to Ao.Univ.-Prof. Dipl.-Ing. Dr.techn. Hermann Scharfetter for his guidance and support through all phases of the development and drafting of this thesis. Despite his demanding responsibilities as Dean of Studies, he was an excellent thesis supervisor, generous with his time and offering valuable insight and encouragement whenever needed along the way.

I am also thankful for the support received from CNSystems Medizintechnik GmbH for providing me with the opportunity to undertake both the research and practical phases of this project. I extend special thanks to Dipl.-Ing. Dr. Jürgen Fortin for making this collaboration possible and serving as my thesis co-supervisor, Dr. Julian Grond for his personal and professional support in the technical areas addressed here, and Dr. Doris Flotzinger, whose many contributions to the early literature and research phases of the project were much appreciated and provided a strong foundation for the entire work.

My heartfelt gratitude goes to my parents, whose unconditional love, encouragement, and sacrifices made my studies in Austria - and this thesis - possible. Their support over so many years has provided countless contributions to both my life and my academic journey.

Finally, I want to express my infinite gratitude to Mark, who was always there for me as a constant source of strength and motivation.

Table of contents

List of Abbreviations

BRS Baroreflex sensitivity

BEI Baroreflex effectiveness index

BP Blood pressure

SBP Systolic blood pressure

RRI RR interval

HR Heart rate

BPV Blood pressure variability

HRV Heart rate variability

ANS Autonomic nervous system

HF High frequency

LF Low frequency

VLF Very low frequency

TF Transfer function

VM Valsalva maneuver

WBA Weighted band average

FFT Fast Fourier Transformation

STFT Short Time Fourier Transform

AR Autoregressive

CHF Chronic heart failure

MI Myocardial infarction

AD Autonomic dysfunction

CAN Cardiovascular autonomic neuropathy or AN (interchangeably used with AD)

AN Autonomic neuropathy (interchangeably used with AD)

PRSA Bivariate phase-rectified signal averaging

ARMA Autoregressive Moving Average

PSD Power spectral density (Auto-spectrum)

CSD Cross-spectral density (Cross-spectrum)

f_s Sampling frequency

f_{res} Frequency resolution

t_{res} ‘Quasi’ time resolution

1 Introduction

1.1 Definition of baroreceptor sensitivity

Baroreceptors are mechanoreceptors (stretch receptors, sensors) located mainly in the carotid sinus, aortic arch and the lungs. [1], [2], [3] They are major players in the arterial baroreflex system which is involved in the short and long-term regulation of the arterial blood pressure (BP) homeostasis.

These receptors sense small and large changes in blood pressure pulsation (rises and falls) occurring in daily life under different circumstances, and send information signals to the higher centers in the brain stem. These centers react responsively to these changes, allowing the whole baroreflex system to keep the BP constant around a reference value. [2], [4], [5]

More specifically, when BP increases, the baroreflex mechanism reacts by increasing the vagal activity which slows down the heart rate (HR) to protect the heart. [6] This response is termed cardiac, vagal or parasympathetic response. On the other hand, sympathetic responses occur when the BP drops and HR increases. [5], [7], [8] Nevertheless, the effect on the HR is not the only way the baroreflex system controls BP buffering. [6] More about the baroreflex physiology is explained in Chapter 1.2.

Hence, the cardiac or vagal 'baroreceptor sensitivity', 'baroreflex sensitivity (BRS)' or 'blood pressure-heart rate reflex' represents a physiological parameter (biomarker) - first described in the late 1960s [9] - that quantifies the amount of change in the heart rate (HR) provoked by the changes in the systolic blood pressure (SBP). [7], [10] Given that it represents the change in the interval between successive heart beats (termed RRI as the interval from one of an ECG's R-waves to the next) triggered by the change in SBP, its derived unit is a millisecond per millimeter of mercury (ms/mmHg). [11]

In general, a high BRS value seems to reflect high stability of the autonomic control of the cardiovascular system in humans [7], [8], [12], [13] More precisely, it actually describes the efficiency of the vagal-mediated HR response. [14], [15]

BRS has proven its clinical value in research as well as in clinical studies as a strong prognostic and predictive marker of autonomic dysfunction (AD) and when being measured intravenously as a risk stratification parameter in various cardiovascular diseases. [3], [16]

However, for any given physiological parameter to become a useful clinical index and to be deployed in routine clinical practice, in addition to its proven clinical value [17], its measurability, reproducibility and reliability are crucial. [18] How many of these crucial characteristics are fulfilled for BRS – and to what extent – was assessed in the course of this thesis.

Another significant BRS characteristic that makes it potentially useful in clinical application is the possibility of its improvement (leading to higher BRS values) by diverse treatment options. [10], [19], [20], [21] According to research, various therapies such as a specific drug therapy [22], nocturnal home dialysis [23], slow breathing sessions applied in yoga [24], chronic

baroreceptor stimulation by implantable device [21] etc. are currently targeted to improve BRS and possibly prevent future cardiovascular events.

1.2 Baroreflex physiology

The baroreflex mechanism portrays a complex closed-loop physiological phenomenon [25] that consists of three separate baroreflex branches: [1], [14]

1. Cardiac
2. Vascular
3. Myocardial

The cardiac branch regulates BP swings by manipulating the HR, the vascular branch modulates the contraction and relaxation of the blood vessels and the myocardial branch is responsible for myocardial contractility. [1]

Notably, it has been reported that the cardiac BRS and the BP buffering capacity are actually mainly unrelated, since BP buffering is primarily controlled by the vascular branch and is achieved by regulating the peripheral resistance. In contrast, cardiac BRS measures the baroreflex response to the sinus node. [6], [12], [14]

Furthermore, because measuring peripheral resistance is a more complex procedure and is not currently feasible in clinical practice, the cardiac component of the baroreflex is predominantly used in research due to its ease of measurement. [4]

Therefore, the topic of this thesis is focused only on the cardiac baroreflex branch; the other two branches were not addressed further in this thesis.

1.2.1 Baroreflex time delay

Due to its closed loop negative feedback nature (see Chapter 1.7.1), one more baroreflex feature that seems to be physiologically relevant is the baroreflex time delay. [5], [25]

As mentioned before, following a rise in BP, baroreceptors activate, stimulating vagal nerve discharge to the sinus node, and the HR decreases (bradycardic or parasympathetic effect). On the other hand, when BP drops, baroreceptors deactivate, leading to vagal withdrawal and sympathetic response activation, increasing HR (tachycardic effect). Hence, the time difference between the SBP change and subsequent RRI reaction in each direction is termed the baroreflex delay – it is the response time the baroreflex needs. [5]

In healthy humans, the vagal (parasympathetic) response acts quickly (200-600 ms). Yet the reaction of the sympathetic response is slower - usually taking 2-3 seconds to reach its full effect. [5] It has been reported that a standard baroreflex delay period suitable for all individuals does not exist. [25]

Nevertheless, it appears that a longer baroreflex delay seems to be relevant in certain pathologies. For example, it is present in chronic renal failure (CHF) [25], diabetes [26] and syncope patients with low orthostatic tolerance. [27] It can also appear after spinal cord injury [28]. Thus, the phenomenon could indicate some issue in the autonomic stability even if the

BRS index is still preserved. [28] Hence, this delay should also be determined in addition to the BRS value.

1.3 BRS behavior

BRS is a highly individualistic attribute [29] and, similarly to BP and HR, fluctuates constantly during a 24-hour cycle. [30], [31] On two consecutive days, when measured under the same conditions with the same procedure, BRS index can vary between 0.5 to more than 2 times. On some days it varies within relatively narrow limits, on others the differences can be wide or even occur in different distribution ranges. [32], [33]

This behavior and average value differ between healthy subjects and those suffering from disease because the BRS has been found to be reduced in various diseases. [30], [34] It is also proven that its magnitude declines with age. [7] Specifically, the biggest drop in BRS value in healthy individuals is observed during the fifth decade of life, after which it stays predominantly constant until death. [35], [36], [37], [38]

Furthermore, this parameter is reported as sensitive to external influences of different kinds (e.g., respiration) that affect both BP variability (BPV) and HR variability (HRV). [39] It is negatively affected by poor lifestyle choices, such as obesity [22], as well.

In terms of daily BRS fluctuations, research suggests that the BRS value increases during sleep/night hours [30], [40] and its behavior changes during different activities and in various body postures [39]. (Fig. 1.1, 1.2)

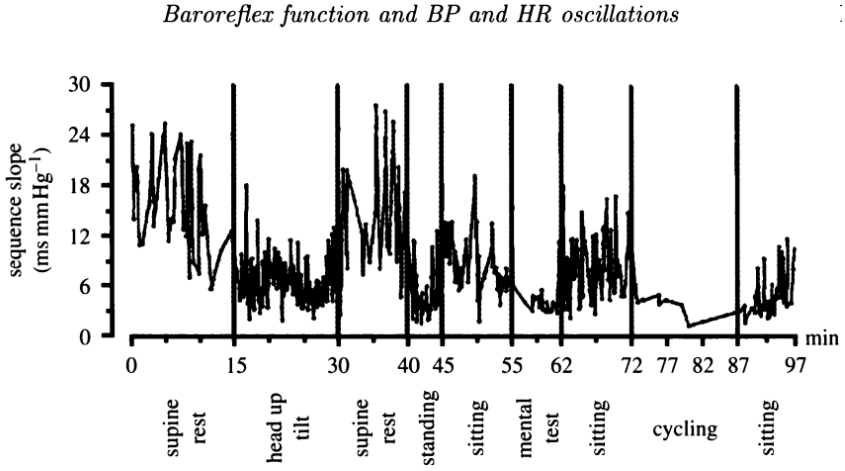

Figure 1.1: Time modulation of BRS (determined via sequence method) in a subject undergoing a series of different activities. Adapted from Di Rienzo et al. (1997) [4]

The BRS index measured in older and younger subjects during 24h. (Fig. 1.2)

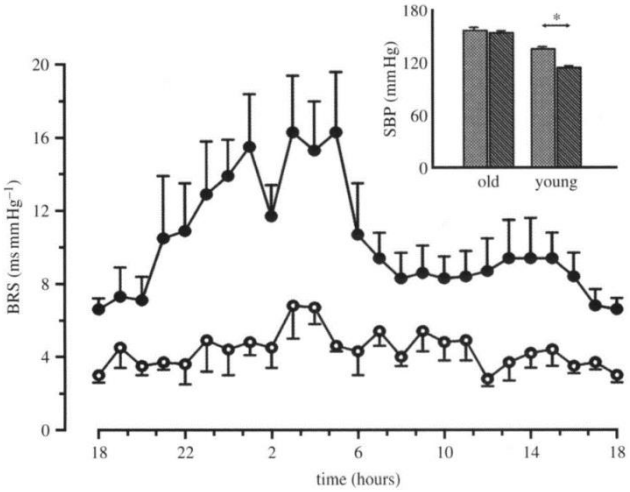

Figure 1.2: The 24-hour profile of BRS (determined via sequence method) in younger and older individuals. [30]

According to Jira et al. [29], the BRS index shows lower intraindividual variability than interindividual variability in humans, and seems to be dependent on mean RRI. If the RRI stays mostly constant, the BRS value should be more reproducible. Additionally, the BRS value appears most reproducible at lower absolute BRS values, rather than when increased.

1.4 BRS reference values

In general, it is reported that, in healthy individuals, the normal BRS range is usually between 3 – 30 ms/mmHg. In some exceptional cases, or in children and younger adults, this could be even higher, also depending on the BRS algorithm used. [29]

According to numerous studies, BRS values below 3 ms/mmHg point to a serious baroreflex impairment. [41] This ‘depressed’ BRS usually presents a high risk of cardiac mortality or adverse cardiovascular events and can lead to adverse clinical outcomes. [12]

Furthermore, there is not yet a standardized measurement protocol for BRS, although there is a clear need for this to be developed. [7], [18] The protocols differ from study to study, which makes the direct comparison of BRS results often impossible. [18]

For this reason, and due to many external influences mentioned earlier - particularly due to age and breathing pattern influences - standardized reference values for the BRS index are also missing. [7] However, since the lack of reference values was seen as a gap in useful clinical information, certain studies in following years did provide some reference values for particular subpopulations (e.g. children [42], working healthy population [43], elderly [7]) which may be valid when specific algorithms are applied.

Recently, the study by Suarez-Roca et al. [44] summarized the findings of a number of studies, grouping the BRS values into three separate ranges and providing an interpretation of the results:

- BRS range 0-3 ms/mmHg is regarded as severely impaired,
- 3-6 ms/mmHg is regarded as moderate impairment and
- Higher than 6 ms/mmHg is regarded as normal BRS.

Literature also suggests that the BRS might be better represented as a range of values, instead of being reduced to a single [45] or small number of values, as it is done by pharmacological methods (see Chapter 1.5.1), and as it is found in the majority of modern techniques. [29]

The next sections describe several techniques used to estimate BRS: one type stimulates baroreceptors' response artificially, and another quantifies the 'spontaneous' behavior of baroreceptors. Also, the most prominent challenges present in measuring BRS by these techniques were outlined.

1.5 Techniques based on artificially stimulated baroreceptor activity

1.5.1 Invasive procedure for BRS estimation

Smyth et al. [9] described an invasive procedure measuring cardiac BRS by intra-venous injection of the vasoconstrictive drug angiotensin in humans, which artificially triggers baroreceptor activity. This substance raises the SBP level by 15-20 mmHg points and simultaneously causes the prolongation of the following RRI. As a result, the linear relationship between the rise of SBP and the response of RRI (time delay of 1 beat – which is called a lag of 1) was observed; the average BRS value (BRS slope) was estimated by deploying the linear regression analysis technique between the SBP and RRI. [9]

In the majority of studies from following years, angiotensin was replaced by phenylephrine (another vasoconstrictive substance) but this procedure in some occasions was combined with injections of an additional drug - nitroprusside (a vasodilative substance) [46]. This was done as baroreceptor activity is actually triggered by both positive and negative BP changes. [19]

In multiple studies, this method was acknowledged as the 'gold standard' for BRS estimation as the BRS index measured by phenylephrine did prove its clinical value in cardiovascular diseases. [10], [16], [46]

Nonetheless, further research raised various issues associated with the phenylephrine method [46] - such as not being applicable in patients with high BP and certain other cardiovascular issues. [47] The dosage of the drug injected also differs between studies, causing variable BRS values and making results hard to compare. Furthermore, this procedure is more time-consuming [10] and the drug itself does not only affect the baroreceptors, but also other receptors (e.g., cardiopulmonary receptors). [3] As a result, further research was primarily concentrated on finding a non-invasive way of measuring BRS.

1.5.2 Non-invasive procedures for BRS estimation

For a while, the neck chamber method and the Valsalva maneuver (VM) were used to increase BP quickly and stimulate the baroreceptors, approaches mainly applied in the laboratory environment.

The VM is a procedure where a particular subject blows into a closed mouth-piece to observe the resulting short-term changes in BP and RRI. [3]

On the other hand, the neck chamber method is a procedure where a neck suction device (collar) applies controlled negative or positive pressure to a person's neck to provoke internal BP change and stimulate the carotid baroreceptors. [3]

Nonetheless, these non-invasive procedures did not manage to replace the pharmacological method as they came with their own sets of issues and additional risks. For instance, the VM technique affects some other major receptor groupings, aside from baroreceptors. Thus, it is 'not selective' enough in measuring BRS. [48] Further research finally introduced a 'spontaneous' BRS index in the 1980s.

1.6 Techniques based on spontaneous baroreceptor activity (spontaneous BRS)

Spontaneous BRS represents the foundation for all modern, computerized techniques which measure the linear changes between SBP and concurrent RRI fluctuations, but without any prior external influence on the baroreceptors. [49] Since natural BP and RRI oscillations are present at all times in humans, even at resting conditions, it was assumed that the spontaneous BRS behavior may provide meaningful information, perhaps clinically useful as well, as it provides a deeper understanding of how this parameter acts over time in humans. Thus, the spontaneous BRS estimation methods were believed to present an opportunity to determine the 'real' BRS values under normal daily conditions. [50]

Some of the major advantages these methods offer include the fact that they are non-invasive (as the BP is non-invasively measured including or excluding an additional ECG device [7], [48]), can be applied in the clinician's offices instead of only in a laboratory environment [49], constitute no discomfort for patients, provide simpler methodological procedure for clinicians to follow, and do not carry the risks connected to drug effects. The time duration of the BRS estimation is also significantly shorter. [10] In addition, the BRS estimation can be repeated numerous times if necessary and, as a result, these methods can be applied on wider populations. [10], [51]

However, there are two additional features of the baroreflex control of circulation affecting BRS measurement process: a presence of the nonlinear relationship between the RRI and SBP changes, and the baroreflex resetting phenomenon. [4], [51]

1.6.1 Nonlinearity of the baroreflex response

The baroreflex response can be described as a sigmoidal curve with two extremes at each end: a saturation level at the top, and a threshold along the bottom. [4], [10] (Fig. 1.3) Hence, the linear relationship between SBP and RRI occurs only in the central area of the curve between these two extremes.

According to this curve, 'stimulated' BRS results cannot be directly compared to spontaneous BRS results since they describe a different baroreflex behavior taking place in different regions of the curve. [51]

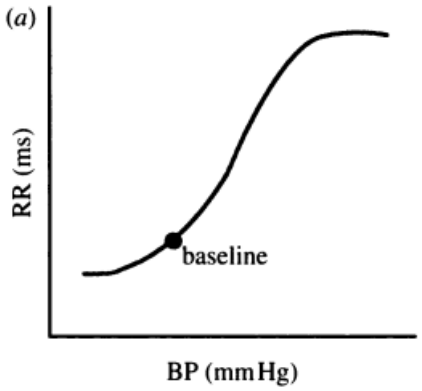

Figure 1.2: Nonlinearity of the baroreflex response [4]

Pharmacological methods or neck chamber methods [52] activate a stronger BP response and, as a result, produce larger RRI response as well. On the contrary, spontaneous BRS operates at much smaller amplitudes of RRI and SBP changes. [45] Although so far confined to research performed on canine subjects, the results showed that two different types of baroreceptors seem to be involved - one type responds to resting (spontaneous) BRS and the other to dynamic BRS stimulation. [45]

Consequently, the literature suggests that methods based on spontaneous BRS are mainly employed to estimate the BRS value within the linear range of the curve, but only the pharmacological method can explore the full baroreflex response. [51] This explains why the reported BRS values between methods based on spontaneous versus stimulated BRS correlate to some extent, but it should not be expected that they would provide identical BRS results. [51]

Another nonlinear feature of the baroreflex response is the phenomenon of "stochastic resonance" which enhances the system's ability to detect weak signals by adding limited noise to the input, thus allowing the weaker signal to cross the sensory threshold. This behavior, known in neuroscience for facilitating weak signal transmission, appears to apply to baroreceptors as well. Specifically, research has shown that when a small amount of noise is introduced to the carotid baroreceptors, an enhanced baroreflex response occurs in reaction to a subthreshold stimulus generated by an oscillating tilt table. [4]

1.6.2 The baroreflex resetting phenomenon

The baroreflex resetting can be described as a phenomenon that occurs when baroreceptors adjust their activation threshold to a higher BP reference point after being under the constant stimulation of elevated BP for some time. [4] More precisely, according to one study, complete resetting to a new reference value occurs after 48 hours in rats. [12] Furthermore, it has been reported that this phenomenon manifests mainly toward the end of the night - a time when BP, HR and sympathetic activity could shift suddenly. Thus, in the case of a person with an attenuated baroreflex function, this mechanism may partially explain the occurrence of cardiovascular events, such as a sudden death or myocardial infarction - at that same time of the day - due to poor baroreflex mechanism. [53] The presence of this resetting phenomenon is also reported in other biological receptors, not only in baroreceptors. [4]

Nevertheless, research suggests that in humans, during their day-to-day lives, the linearity of the sigmoidal curve prevails even if a sudden rise in BP occurs. [4], [30]

1.7 Overview of spontaneous BRS algorithms

In the literature, there are two fundamental types of methods used for the determination of spontaneous BRS. One is calculated in the time domain, and the other in the frequency domain – the spectral methods.

The time domain methods describe the behavior of the spontaneous BRS as a time-variant parameter, while the spectral methods explore the BRS as a frequency-dependent characteristic. [29], [45]

In the 1980s, the sequence method was developed which was the first time-domain technique. [54] This method still represents the most popular method applied in BRS research. The second time-domain technique is the cross-correlation method (xBRS) which was introduced in 2004. [55]

Regarding the spectral methods, two types are most frequently employed: the transfer function method (TF) [56] and the alpha coefficient (also known as alpha index). [20]

Over the years, newer and more exotic methods or models for the BRS calculation have been, and are continuing to be developed. [3], [57] These include the bivariate phase-rectified signal averaging (PRSA) method [58], trigonometric regressive spectral analysis (TRS) [46], Z coefficient method based on statistical dependence between SBP and HR changes [59], and impulse response function [37], among others. Additionally, in recent years, time-frequency domain algorithms have been introduced which employ: wavelet transformation [60], [61], Wigner-Wille distribution [62], Zhao-Atlas-Marks distribution (ZAM) [63] and others. However, since these methods were rarely applied in clinical research studies and some are not yet validated [46], they are not here included in subsequent discussions.

1.7.1 Closed versus open loop model for the baroreflex mechanism

In the literature, two types of models are generally used to explain the complex baroreflex physiology applied for the BRS calculation – the open loop and the closed loop model. [20], [64], [65]

From the physiological perspective, the baroreflex mechanism is a closed loop system with negative feedback that includes both the ‘feed-backward (FB)’ and the ‘feed-forward (FF)’ pathways that exist between the SBP and RRI changes (Fig 1.4). [13], [20], [64]

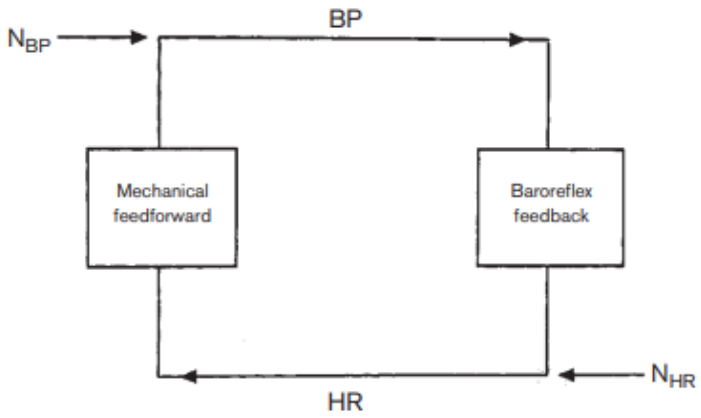

Figure 1.3: Schematic drawing of FB and FF reciprocal interactions between BP and HR; NBP and NHR refer to 'noise' influences independent from HR and BP [3]

The FB pathway takes into account only the SBP variation that leads to corresponding RRI change, while the FF pathway acts in the opposite direction from the FB; it considers the influence of the RRI variation on the following SBP change by the vasculature. [20], [64]

The FF pathway is not considered a part of the cardiac baroreflex branch and is termed 'mechanical' [19] – related to the Starling law of the heart and arterial windkessel effects. [66] For this reason, the FF pathway mainly remains ignored in the literature and disregarded in the development of the majority of BRS algorithms. [64]

Therefore, the closed baroreflex loop needs to be converted into the open loop, or to include major mathematical simplifications to make the BRS estimation possible, as performed e.g. in the alpha coefficient method. [20], [64], [67]

Nonetheless, according to Barbieri et al. [64], the correct measurements of cardiac BRS might be possible only when the FF pathway is either completely abolished or its effect is much smaller than the stimulation of the baroreceptors, hence, it would be applicable in situations when the baroreflex loop remains open - for instance, it is reported as applicable in case of pharmacological and neck chamber methods due to stronger baroreceptor stimulations.

However, according to La Rovere et al. [68], the loop seems to remain open even in supine resting individuals in the LF band and, thus, the open loop approach seems adequate in that case as well. In addition, the open loop approach is generally assumed as applied in the sequence method and in the TF method as well. [64], [67]

The closed loop approach, on the other hand, can be found in various studies that develop complex mathematical models in an attempt to describe the functioning of the whole cardiovascular system in a way closer to the real physiology. [69], [70] Some of these models include the effect of respiration on the BPV and HRV, some do not, and other studies attempt to decouple the FF and FB pathways within the baroreflex loop. These studies are mainly focused on the causality between SBP and RRI changes. [66], [70]

1.7.2 Spectral methods: Origin and frequency bands

The idea behind the development of spectral methods for the BRS estimation is based on the assumption that specific frequency regions of the HRV spectrum are regulated by the baroreflex. [71]

It is believed that the BRS spectrum - obtained from the combination of the HRV and SBPV spectra - at specific frequencies or within specific frequency bands may be able to provide meaningful information about an individual's cardiovascular health. When coupled with the right interpretation, BRS spectral analysis may give clinicians an opportunity to understand better the exact causes or severity of the baroreflex issues. [72] This information could not be derived from the time-domain methods.

In general, while the subject breaths normally, the power spectra of both RRI and SBP time series generally tend to contain three peaks - one centered between 0.1 to 0.15 Hz – the low frequency (LF) peak - and the other centered at the average breathing rate, thus centered between 0.2 to 0.4 Hz – known as the high frequency (HF) peak. [18] The third peak is usually in the very low frequency (VLF) band (below 0.04 Hz) but this peak was broadly disregarded in BRS studies (see Chapter 2.3.1.2). [18], [56]

Additionally, even though the borders of these frequency ranges tend to vary slightly in certain studies, this does not seem to have a significant impact on BRS results. [26], [34]

Hence, in most cases the ordinary BRS spectrum contains the HF and LF peak-like shapes at similar frequency ranges as well. Subsequently, the two frequency bands used most often in the literature are the LF (0.04 – 0.15 Hz) and the HF bands (0.15 – 0.4 Hz). This approach was applied in this thesis as well.

Fig. 1.5 depicts the BRS spectrum of two healthy subjects with a constant breathing rate (at 0.33 Hz). [18] As it could be seen, sizes and shapes of peaks generally vary even between healthy individuals, with the same breathing rate; however, the interplay between the two is not yet clear.

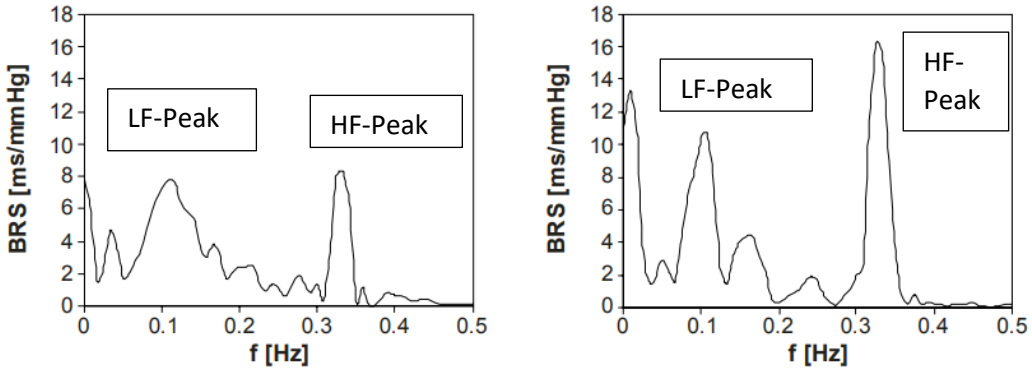

Figure 1.4: BRS spectrum calculated in two healthy subjects with paced breathing rate at 0.33 Hz. Adapted from Bothova et al. (2010) [73]

1.8 The aim of this thesis

In summary, this thesis is divided into two main phases:

1. In the first phase of this thesis, the relevant scientific literature on BRS was summarized to give an understanding of the application and estimation of BRS in clinical practice and research. In the main clinical areas where BRS has been shown to be of value, a summary of relevant information has been presented along with an outline of associated challenges in the most important areas. Also, some examples of how BRS is visualized in research were given.
2. In the second (practical) phase, the preferred spectral BRS estimation method was selected, implemented in Python, further developed in a time-frequency domain and applied to a set of actual patient data. The real-world data were used to provide suggestions for the visualization of BRS changes over time which might be of use in clinical practice and incorporated into medical devices.

2 Literature part

The questions to be addressed in the literature section of this master's thesis were the following:

- What is the clinical impact of BRS, what are potential therapeutic consequences, in which circumstances is it important?
- What algorithms for determining the BRS are present in the literature?
- What are the specific strengths/weaknesses of different algorithms in the context of medical requests?
- Which algorithms for BRS calculation are useful/indicated for which application?
- Which algorithms for BRS calculation are proven to be of medical benefit?
- What are advantages and disadvantages of the different sequence methods available today?
- What conclusions can be drawn from the literature with regard to a comparison of advantages/disadvantages of spectral vs sequence methods?
- Which algorithms are already integrated within currently available products?

This resulted in the following inclusion and exclusion criteria.
Inclusion criteria:

- Articles describing the clinical benefits of baroreflex sensitivity (BRS)
- Articles which demonstrate advantages and/or disadvantages of different BRS algorithms applied for specific medical requests
- Articles describing definition and the clinical value of the baroreflex effectiveness index (BEI)
- Articles describing the behavior of BRS during autonomic function testing
- Articles providing certain reference values for the BRS and the BEI
- Articles describing therapies specifically designed to improve BRS
- Articles investigating the progress of therapies for certain diseases by measuring the BRS improvement
- Articles using different BRS methods to explore BRS behavior during anesthesia

Exclusion criteria:

- Articles in which BRS was not mentioned in the abstract
- Articles focusing on assessing BRS in animal studies
- Articles focusing on research rather than medical benefit/clinical value of BRS:
    - Articles investigating BRS in certain ethnicities or particular groups of people (e.g. athletes, yoga practitioners)
    - Articles exploring BRS behaviors in different geographical regions (e.g. Arctic expeditions)
    - Articles focusing only on the physiology of the baroreflex system
    - Articles estimating BRS during certain daily activities (e.g. swimming)

2.1 Methods

To identify research papers which were most relevant to the topic of this master's thesis, on 05.10.2021 a systematic literature search of the Medline database was performed (https://pubmed.ncbi.nlm.nih.gov). To identify and select the relevant literature to be able to answer the questions of this thesis, four different combinations of search terms and filters were applied:

I. '("baroreflex" OR "baroreceptor") AND ("sensitivity" OR "function" OR "activity" OR "index" OR "gain") AND ("calculation" OR "algorithm" OR "method" OR "estimation" OR "analysis" OR "technique" OR "assessment") AND ("sequence" OR "sequential")'
II. '("cardiac" OR "cardiovagal" OR "vagal") AND ("baroreflex" OR "baroreceptor") AND ("sensitivity" OR "function" OR "activity" OR "index" OR "gain") AND ("calculation" OR "algorithm" OR "method" OR "estimation" OR "analysis" OR "technique" OR "assessment") AND ("spectral")'
III. '("clinical") AND ("value" OR (("useful" OR "utility") AND "index")) AND ("baroreflex" OR "baroreceptor") AND ("sensitivity" OR "function" OR "activity" OR "index" OR "gain") AND ("calculation" OR "algorithm" OR "method" OR "estimation" OR "analysis" OR "technique" OR "assessment")'
IV. '("baroreceptor" OR "baroreflex") AND "effectiveness index "'

Additional filters included in the PubMed search were articles written in English, German, French and Spanish and applied only on humans.

In total, 958 articles were found. In addition to these articles, 51 extra papers were included (supplementary articles which were referenced by a colleague at CNSystems or which were noted as key references found in the bibliography of articles present in the prior general search). The abstracts of all articles were scanned and only papers which were suitable to answer the questions of this thesis were included for further analysis. In the list of articles included, 51 were duplicates. After scanning the abstracts, 753 articles were excluded as only those papers related to clinical benefits and certain algorithm comparisons were considered relevant. The remaining 205 articles were tagged and provided the basis for deeper analysis.

2.2 Results

2.2.1 Tagging matrix (Appendix 1 - digital appendix)

The tagging matrix was the tool used for the structured analysis of all papers included. The matrix consists of 205 rows, each representing an article, and 67 columns, where each of the columns, excluding those containing the name of the article and its publication year, is used as a specific tag designed to extract the most relevant information from each paper.

The cells were primarily filled with values 0 and 1, where 1 means 'yes/present in the article', and 0 as a 'no/not present in the article'. On some occasions, the letter 'w' was also applied, which indicated 'weak evidence' or 'not fully present'. Some of the cells were, if deemed necessary, filled in with words. Some of the primary tags applied were the following:

- Disease (+ various diseases listed in different columns) – present or not
- BRS algorithm (+ each method listed in separate columns) – present or not

- Medical benefits of BRS – present or not
- Autonomic function testing – applied in the paper or not
- Anesthesia – applied in the paper or not
- Baroreflex effectiveness index – mentioned or not
- Healthy subjects – healthy subjects studied or not
- Sample size – filled in the number of subjects included in the study
- Breathing rate – spontaneous or controlled
- Body position/activity during the measurement – filled in with words
- Review – is the paper a review article or not
- Referenced paper – is the paper a referenced paper or found in the original search
- Pharmacological method – only the BRS pharmacological method applied or not

2.2.2 Algorithm clinical benefit matrix (Appendix 2 - digital appendix)

Since the baroreflex function is mainly linked to a cardiovascular system, the research is predominantly focused on medical states that could be significantly affected by BRS impairment. This would include, inter alia, the BRS value of a subject calculated in post myocardial infarction (POST-MI) state, or in cases following a diagnosis of diabetes mellitus (DM1 and DM2), chronic heart failure (CHF), coronary artery disease (CAD) and cardiomyopathy, and/or BRS value during and after an (acute) stroke, cerebral hemorrhage and others.

The research studies generally examine the advantages and/or disadvantages each BRS estimation method may have in a specific disease or in certain clinically relevant applications (e.g. during autonomic function testing, under anesthesia), or carry out a comparison of different methods applied to estimate the BRS, evaluating their success in relation to a particular clinical role of BRS.

The next step contained construction of a second matrix described as the ‘Matrix with clinical benefits’ which includes medical requests - diseases and clinical applications - with related BRS medical benefits estimated by techniques frequently referenced and analyzed in the literature. This matrix consists of 25 columns and 19 rows, with the rows organized into two sections. The first section lists various individual algorithms, including BEI computation, used to estimate BRS in selected studies, while the second section summarizes comparisons between these algorithms. The columns, meanwhile, represent medical areas - diseases and applications - where BRS is relevant. The resulting cells primarily detail the clinical benefits of BRS inc. short summary of the researched topic and/or the algorithmic benefit explored in the studies.

However, 25 review articles, as secondary sources, were not included in the second matrix since the primary sources (original research papers) were considered more relevant.

2.3 Discussion

In this section, the following two topics were discussed:
(1) the BRS algorithms used in clinical literature and
(2) the medical application fields where BRS algorithms are applied.

2.3.1 Algorithms present in the literature

From the 205 tagged articles, 129 were selected as relevant for the "Matrix with clinical benefits" in which BRS algorithms were applied in the clinical literature for different purposes. Therefore, in this section, an overview of the various methods to derive BRS used within clinical literature is presented. (Fig. 2.1)

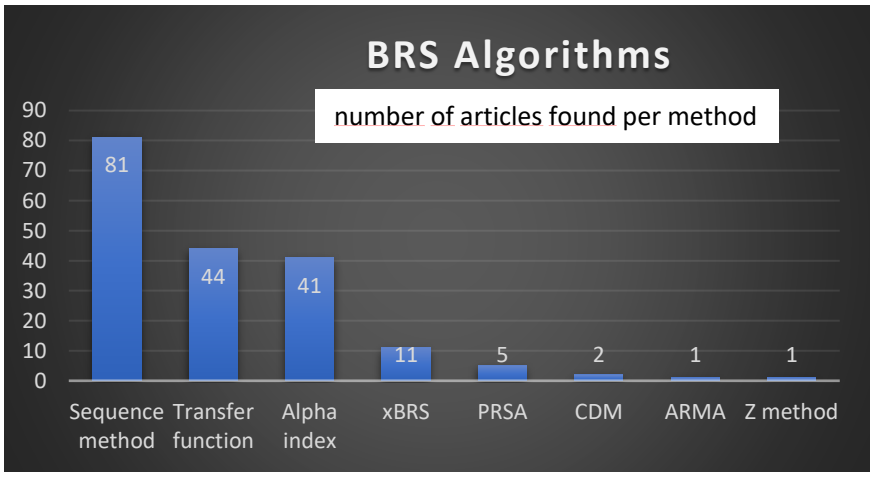

Figure 2.1: Overview of BRS algorithms present in the clinical literature

In the following paragraphs, the most important BRS algorithms are presented in detail.

2.3.1.1 Sequence method

The sequence method – a non-invasive BRS estimation method - is a time domain method. Originally, it was tested on unanesthetized cats and later applied on humans as well**.** [30] However, this technique is derived directly from the pharmacological BRS method described earlier (see Chapter 1.5.1) and is based on the linear regression analysis as well. [30]

Blaber et al. [74] proved that the spontaneous interaction between SBP and following RRI changes in the parallel direction represent 'true baroreflex events' or 'sequences' and are not accidental occurrences. [73] Therefore, the sequence technique is thus an open-loop method [64] based on the premise that spontaneous beat-by-beat fluctuations in SBP throughout the day are the sole cause of linear changes induced in RRI. [74], [75] As a result, the BRS value is estimated as a ratio between the magnitude of the RRI change and the magnitude of the SBP change, as in (1).

$$\mathrm{BRS} = \frac{\Delta\,\mathrm{RRI}}{\Delta\,\mathrm{SBP}} \tag{1}$$

This algorithm itself first identifies spontaneous sequences lasting three to six beats each. The sequences of three beats are most frequently found in humans [11], [76], while longer sequences represent a less common phenomenon. [11], [30] Additionally, it has been noted that with the increasing sequence length, BRS value decreases. [11], [30] In general, sequences are formed when progressive increases in SBP are followed by RRI prolongations (decrease in HR) or vice-versa, when both, the SBP and RRI simultaneously decrease (increase in HR). The first type of sequence is described as 'SBP+/RRI+' [30] or 'up' [77] or 'bradycardic' [78] sequences. Similarly, the second type is named 'SBP-/RRI '[30] or 'down' [77] or 'tachycardic' [78]

sequences. Furthermore, both, ‘up’ and ‘down’ sequences are also called ‘baroreflex’ type sequences [79] as they are both regulated by the cardiac baroreflex. According to Del Paso et al. [80], ‘up’ sequences represent the vagal activation, while ‘down’ sequences reflect the vagal withdrawal.

On the other hand, ‘non-baroreflex sequences’ also exist, and Di Rienzo et al. [79] described them as ‘converging (SBP-/RRI+)’ and ‘diverging (SBP+/RRI-)’ sequences. They are formed when the SBP and RRI changes occur in opposite directions. [79] However, both of these types are potentially useful in further research on baroreflex physiology. [79] Additionally, it has been reported that ’non-baroreflex’ sequences represent only ca. 30% or less of all baroreflex sequences. [65], [74], [79]

After a sequence identification, a linear regression between RRI and SBP is applied to each of the sequences discovered, and the BRS value is determined as a regression coefficient (gain) of the slope. [79] In the next step of this technique, all BRS slopes derived from each sequence detected in the recording are summarized. The estimated mean value derived from all up and down sequences represents the final BRS slope of an individual. [25]

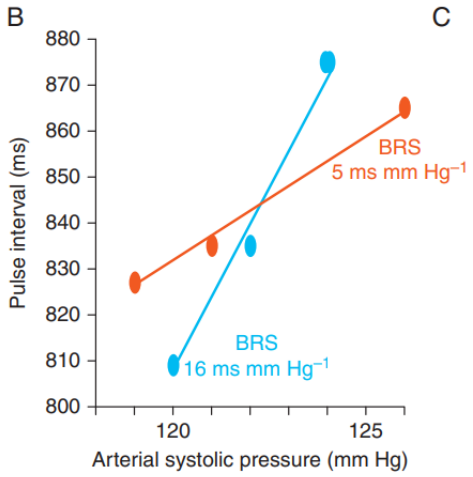

Figure 2.2: Two BRS slopes - sequence method: blue slope shows higher BRS value than the red slope [81]

The steeper the slope, the higher the BRS value of an individual. Generally, a steep slope serves as a sign for good vagal baroreflex function. On the contrary, a slope which is steep to a lesser degree, points to impaired vagal baroreflex function and indicates that there may be potential issues with the cardiovascular system. [81] (Fig. 2.2)

With regard to different visualization techniques, sequence methods present their BRS results in two different ways. In some studies, the BRS result is given separately for up and down sequences, as suggested by Martínez-García et al. [25], as two different BRS slopes (BRS_{seq+} and BRS_{seq-}). [82] In other papers, in addition to up and down slopes, the mean BRS slope is given as well. [83]

The sequence method contains five computational parameters that need to be set ahead of any BRS measurement, since depends on these parameters to determine what type of sequences the algorithm will detect in the recording and consider as valid sequences. The parameters include:

- Minimum number of beats considered as a sequence (usually ≥ 3)
- Minimum thresholds for detection of SBP and RRI variations
- Minimum threshold for required correlation coefficient between SBP and RRI
- Time delay – 'Lag' or 'time shift' - between the initial SBP change and the corresponding RRI response

The correlation coefficient describes the linearity between two signals, where a high correlation coefficient indicates high linearity. In general, the value goes from 0 (no linearity) to 1 (full linearity) and, in most cases, the required threshold is usually set in a range from 0.80 to 0.95. [84]

These parameters help the algorithm to sort out sequences retaining only the valid examples before the BRS slope is computed. However, variable parameter settings applied in the studies led to the application of numerous variations of the sequence method. [85] Furthermore, the choice of thresholds for sequence detection has a significant impact on BRS values as well as on the number of sequences found in a particular recording, affecting the measurability rate of BRS. [84], [85]

Another parameter that deserves to be mentioned – also regarded as the most controversial parameter - is the choice of the appropriate lag. In general, the RRI response to an initial SBP change could occur during the same heart cycle (lag of 0 beats), during the next heart cycle (lag of 1 beat) or during the cycle afterward (lag of 2 beats). (Fig. 2.3)

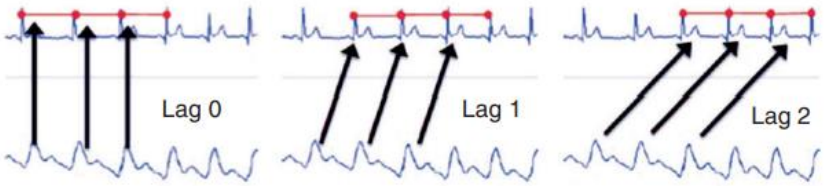

Figure 2.3: Sequence calculation with lags 0,1 or 2 [42]

It is believed that rapid coordination of HR with SBP changes at lag 0 likely reflects faster input from carotid baroreceptors, given its proximity to the heart. In contrast, lags 1 and 2 likely represent delayed HR adjustments driven by central input from the ANS. [42]

According to the relevant literature reviewed for this thesis, the lags most frequently applied in the studies are lags 0 and 1. This is due to the fact that the lag of 2 beats appears to produce smaller number of valid sequences in humans, especially in the supine position. [27] On the other hand, the lag 0 and 1 suit the majority of people. [27], [84]

When choosing between the two lags (0 or 1), the most popular solution appears consistent with adopting the lag which generates the highest number of valid sequences in a person, since that way the BRS result is less biased. [84]

Some authors have associated lags with the mean RRI in an individual – they proposed an approach to choose the right lag depending on the RRI length. [86], [87] Blaber et al. [74] stated that delay in cardiac baroreflex response in humans is around 775 ms. For shorter RRI, the response would probably manifest in the following beat (Lag 1). In contrast, in the case of

longer RRI, the response can occur during the same cycle (Lag 0). Nevertheless, this lag theory has not been confirmed as a scientifically justified solution for the whole population.

Davies et al. [84] tested different lags (-4 to +4 beat shifts) in normal as well as in patients with heart failure. They concluded that the lag choice in both groups has a visible impact on the number of sequences found, but appears to have no influence on calculated BRS results. [85], [88]

In the literature surveyed, another metric of vagal baroreflex control was also introduced in 2001. [89] It was named the baroreflex effectiveness index (BEI) and is applied in combination with the sequence method. [89] BEI is estimated as the ratio between all valid baroreflex type sequences and all SBP ramps (spontaneous successive increases or decreases in SBP values on a beat-by-beat basis, independent from the modulation of the RRI) found in a particular recording, as in (2). [4]

$$\mathrm{BEI} = \frac{\text{total number of RRI | SBP sequences}}{\text{total number of SBP ramps}} \text{ x } 100\ (\%) \qquad (2)$$

Therefore, the results could be given for all sequences (BEI) or for 'up' and 'down' sequences separately (BEI + and BEI-). This measure describes the efficiency of the cardiac baroreflex – its engagement rate; it quantifies how often the baroreflex is involved in a control of the HR within a particular time window. Although useful, this additional metric cannot replace the BRS index, since they offer different, although complementary, information about cardiac baroreflex control. [90]

For this reason, it has been recommended to estimate both BRS and BEI with the intention to extract a fuller picture of the cardiac baroreflex mechanism. [1] For instance, this index has been reported to convey a certain clinical value in cases when baroreflex dysfunction is present since, under those circumstances, the baroreflex mechanism is usually less engaged when compared to healthy individuals.

The BEI index did show certain clinical value in some studies. For instance, it was proposed as the most sensitive discriminator of cardiovascular autonomic neuropathy (CAN) in diabetes [91], and also was reported as being an independent prognostic predictor of long-term survival in chronic renal patients (when high enough). [92]

Similar to the BRS index, BEI decreases with prolonged sequence length, and also during high-paced frequency breathing as well. [93], [94]

2.3.1.2 Transfer function method

The Transfer Function (TF) method was originally introduced in 1985 and, in 1987, was also validated for BRS quantification in humans. [56]

Like other spectral methods, the TF technique is based on the spectral presentation of minor spontaneous rhythmic fluctuations of cardiovascular signals occurring around a natural set point. These oscillations occur constantly in RRI and SBP time series in humans; the TF technique describes their rhythmic co-occurrence across frequency ranges of interest, usually

within the LF and/or the HF bands as they are believed to be under baroreflex control. [56], [95]

The TF technique is often employed to describe the response of a linear time-invariant system in relation to gain, coherence and phase shift at various frequencies. It is considered one of the most extensively utilized techniques in short-term investigations of BP, HR and respiration signals. [96]

As mentioned earlier, this technique's fundamental assumption is a linear open-loop relationship between input and output signals. [96] However, this assumption may be seriously compromised in the coupling of HR and BP signals, unless specific conditions are met (e.g. small signal variations**,** analysis of fluctuations in selected frequency bands). [96]

The modulus of the transfer function ($G_{xy}(f_k)$) or transfer gain at a specific frequency (f_k) is calculated as the cross-spectral density (CSD) ($S_{xy}(f_k)$) between SBP and RRI variabilities divided by the power spectral density (PSD) of the SBP ($S_{xx}(f_k)$) variability alone, as in (3). [56], [73], [97]

$$\left|G_{xy}(f_k)\right| = \frac{S_{xy}(f_k)}{S_{xx}(f_k)} \tag{3}$$

In general, PSD (or 'auto-spectrum') portrays the signal's power distribution across different frequency regions. It thus reveals how much variability exists in signals across different frequencies. Hence, the PSD of RRI is expressed in units ms^2/Hz, while the PSD of SBP is expressed in $mmHg^2/Hz$ [72] On the other hand, the CSD represents the relationship between two signals across a range of frequencies expressed in the units ms*mmHg/Hz. [96]

The 'coherence' or 'magnitude squared coherence' portrays the linear correlation between the fluctuations of two signals at a given frequency, calculated as in (4). [56] This parameter has the same function as the correlation coefficient from the regression analysis. [56], [98] Generally, the coherence is a normalized value and ranges between the values of 0 and 1, and is dimensionless. A value 0 indicates there is no linearity between the two signals and value of 1 indicates full linearity. [56], [99] Additionally, any value below 1 also indicates that nonlinearities or noise could be present in the signal which is a normal occurrence in cardiovascular signals. [96]

$$\mathrm{Coh}(f_k) = \frac{|S_{xy}(f_k)|^2}{S_{xx}(f_k)\ \mathrm{x}\ S_{yy}(f_k)} \tag{4}$$

Additionally, from the CSD of RRI and SBP variabilities, the coherence spectrum and the phase spectrum (often excluded) can be derived. [56], [95], [100] (Fig. 2.4)

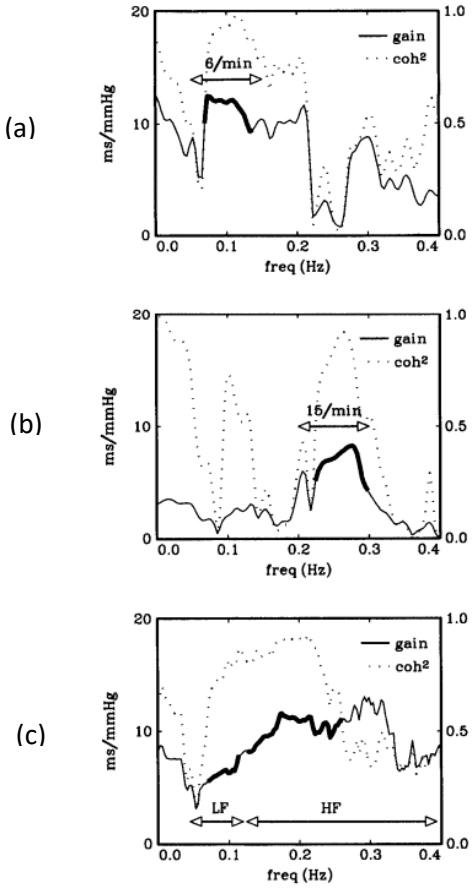

Figure 2.4: BRS gain and coherence spectrum of a 57-year-old woman computed by TF method - (a) during slow breathing, (b) during fast breathing and (c) during spontaneous breathing. The strong black line represents the high coherence (coh^2) area. It can also be seen that BRS and coherence shift constantly. [7]

Furthermore, the phase, computed as the argument (angle) from the CSD between the signals, illustrates the temporal relationship between SBP and RRI fluctuations across different frequency regions. [72], [94] However, the issue with the phase estimation is the ambiguity in determining which signal in the cross-spectrum leads the other. Therefore, determining the most suitable description relies on relevant physiological considerations (Chapter 2.5.4). [72] If necessary, the phase displayed in degrees at specific frequency could be transformed into seconds. [100]

The requirement for a reliable phase calculation, in literature, is a high coherence threshold, usually set above 0.5. [56], [60], [97]

TF modifications: BRS value and coherence criterion interplay

It is important to distinguish between transfer gain computations, as in (3) and the BRS value derivation. Specifically, the determination of the BRS value often follows one of three approaches when employing the TF method, which leads to variations in the resulting output of this method in the literature. (Table 2.1)

Reference	BRS value computation method	Coherence criterion	Frequency bands
Robbe et al. 1987 [56] 'Original' TF method	BRS value as the mean of all included transfer gain points which satisfy the coherence criterion in a specific frequency band	Accepts only transfer gain points where coherence between SBP-RRI > 0.5 (arbitrary threshold)	LF and HF band
Pinna et al. (WBA-TF) [95]	BRS as the mean of all transfer gain points across the whole LF band independent from any coherence criterion	Excluded from BRS computation	LF band
Bothova et al. [73]	BRS value as the single transfer gain in the LF band occurring at the highest coherence value in that frequency band	Usually highest coherence > 0.5	LF band

Table 2.1: Three methods of BRS value determination found in the literature

Robbe et al. [56] approach, termed 'Original TF' method, typically takes the coherence criterion into account during BRS calculations. This entails incorporating only TF gain points where the coherence at specific frequency points exceeds the chosen threshold, arbitrarily set above 0.5. In contrast, frequency points generating coherence values below the threshold are excluded from further computations. Thus, the ultimate BRS value is calculated as the mean of all transfer gain points integrated into the analysis for the LF and HF bands separately.

Additionally, Robbe at al. [56] concluded that the coherence spectrum shows the highest values in healthy adults in the LF range and lowest values in the frequency range below 0.07 Hz (VLF band) pointing to low linearity between SBP and RRI in this region. [95], [98] For this reason - in all BRS studies - frequencies below 0.04 Hz are never applied in the BRS evaluation procedures, since the VLF range seems not to be associated with the baroreflex function, but rather with other long-term processes, such as body temperature regulation, etc. [56]

One study by James et al. [101] pointed out an interesting finding that, after drug injection to estimate BRS in elderly subjects, the power, phase and coherence between SBP and RRI actually increased in the VLF band. Thus, longer (> 10 beats) baroreflex type sequences which usually do not occur in a normal daily life – generated via artificial stimulation of SBP - are part of the VLF region, not LF and HF bands. For this reason, the direct comparison of the pharmacological BRS results with daily spontaneous BRS results - obtained via spectral or sequence methods – may not be desirable approach, as it appears that these do not occur at same frequency regions assumed to be under the baroreflex control.

However, the observation regarding high coherence values in the LF band, agrees with the majority of other studies which also indicate that only the LF band - not the HF band - seems to be the appropriate frequency area for the short-term spontaneous BRS calculation. [33], [73], [95]

For this reason, Bothova et al. [73] narrowed their focus exclusively to a single transfer gain point within the LF band determined at the frequency with the highest coherence value and adopted this gain as the BRS index. Pinna et al. [95], on the other hand, introduced another variation of the TF method – termed the 'weighted band average' TF (WBA-TF). This TF variation disregards the coherence criterion altogether and calculates the BRS value in the LF range by averaging all BRS transfer gains across the whole LF band.

This WBA-TF approach was described as particularly valuable in patients with an established baroreflex dysfunction who, due to physiological changes caused by their disease, lack higher coherence between the RRI and SBP necessary for traditional BRS estimation.

In general, due to low coherence values, the original TF method produces fewer transfer gain points available for BRS calculation in the LF band if the coherence threshold is set too high; thus, their results end up being more scattered around the mean. Consequently, the resulting BRS estimate may not be considered reliable. [95]

Hence, the major advantage of the WBA-TF approach, compared to the 'original' TF method, lies in the fact that the BRS index calculated produces more points necessary for BRS calculations, filters out higher variation of BRS values by averaging gains across the whole LF band and, in turn, generates more stable results. [95]

The TF method in the relevant literature was computed either by employing the FFT (nonparametric) approach or the autoregressive modeling procedure (AR model - parametric approach). [102]

In the studies selected for deeper analysis this thesis, the TF method was mainly computed by employing the FFT algorithm (33 papers) while the AR model was employed less often (8 papers). However, overall literature did not establish definitively which method is superior in BRS estimations.

The only study to compare these two spectral estimators in the TF method application - conducted by Pinna et al. [102] in 2017 - found that the BRS value calculated using the FFT-based TF method had greater prognostic value in POST-MI patients compared to the value derived from the AR approach. However, the authors suggested that this outcome was likely to have been influenced more by the differences in how BRS values were calculated, rather than the choice of the spectral estimator, as each method used a distinct BRS value computation technique.

On point, research comparing different spectral estimators for the BRS TF analysis is generally lacking in literature from all periods. Therefore, it is reasonable to suggest that the most appropriate method (FFT or AR) can only be determined once more comprehensive research, employing a consistent BRS determination technique, is available. This would facilitate a clearer comparison of the clinical relevance of BRS obtained by both methods across various populations, including both healthy and diseased subjects.

More details on different spectral estimators are provided in the following chapter (see Chapter 2.5).

2.3.1.3 Alpha coefficient method

The alpha coefficient [103] method was first introduced in 1988 by Pagani et al. [20], [104] It is based on TF as well, but the alpha gain is estimated as the square root of the ratio between power spectra of RRI (P_{RRI}) and SBP (P_{SBP}) in a specific frequency band. In this technique, indices α_{LF} and α_{HF} are calculated separately by using (5). [20]

$$\alpha_{LF} = \sqrt{\frac{P_{RRI_{LF}}}{P_{SBP_{LF}}}} \text{ and } \alpha_{HF} = \sqrt{\frac{P_{RRI_{HF}}}{P_{SBP_{HF}}}} \quad (5)$$

The RRI is perceived as output and the SBP as the input signal. Power spectra of RRI and SBP are computed by integrating the PSD within HF and LF bands separately. [33]

The BRS gain in LF and HF bands is computed under the assumption that the coherence between the signals is high (> 0.5). However, coherence is not always computed when using this method.

In some studies, the average of α_{LF} and α_{HF} is estimated to indicate the total BRS gain. [38] In others, the gain is calculated only in one of the bands. [49], [75], [76], [78]

Generally, the alpha method in literature - as is the TF method - is calculated either by employing the FFT approach or the AR model. [105] However, according to Clyton et al. [105], the results obtained by this technique do not differ significantly if the BRS gain is averaged across the whole frequency band of interest.

2.3.1.4 Cross-correlation baroreflex sensitivity (xBRS)

This algorithm is a time domain method first introduced in 2004. [55] The technique is also based on SBP and RRI variabilities - it calculates their cross-correlation and regression slope over fixed time - although sliding - windows. The window length usually lasts 10 seconds with an intention to include fully the whole baroreflex frequency range. As mentioned prevoiusly, this frequency range includes both slow and fast frequencies.

The method also incorporates a variable time delay (shift) of 0 - 5 seconds between associated SBP-RRI changes, as the most suitable time delay varies between persons. This approach is taken since, according to Westerhof et al. [55], 5 seconds are adopted as long enough to accommodate the sympathetic portion of the baroreflex response to the RRI as well. The delays expressed in lags and beats in the sequence method here are converted to seconds.

During computation, however, the thresholds for the minimal required SBP and RRI changes are disregarded; the cross-correlation is estimated six times per window.
After the highest cross-correlation coefficient is selected, the regression slope is calculated. Requirements for an accepted BRS slope mean that it has to be positive and the probability of it being a random regression must be below 1%.

Finally, the particular regression slope is divided by the cross-correlation coefficient to determine the BRS result. This approach is intended to filter out any random noise that could have been included in SBP and RRI signals. The time delay which best fits the particular regression slope is selected as the appropriate time delay. [55]

2.3.2 Spectral methods: TF versus Alpha coefficient method

The key distinction between the alpha coefficient and the TF lies in their underlying assumptions. According to the alpha coefficient method, it is suggested that all RRI variability is exclusively driven by changes in SBP, although this assertion may not be entirely accurate.

Conversely, the TF method adopts a more nuanced perspective, restricting its consideration to the portion of RRI variability that is shared between SBP and RRI for the BRS estimation.[106] For this reason, the alpha coefficient always generates higher values than the TF method and is reported to have a c. 41% positive bias. [7], [64], [67]

According to Gerritsen et al. [7] the TF method is preferable as it, in part, corrects for the 'non-correlating' noise and estimates the phase shift. This preference is not absolute, as it should be noted that the alpha index could also produce the phase shift, (if necessary) although this is very rarely seen in the studies from the literature relevant to this thesis. [20]

The alpha coefficient appears to be a simpler method for the calculation than the TF, but the coherence criterion may represent an issue if it is set too high for the alpha index (> 0.5). [7] This criterion limits its use on pathological subjects who lack high linearity between SBP and RRI. [95] In contrast, the WBA-TF method variation disregards this issue and could be applied to larger populations. [95]

In general, both methods produce similar values in situations where the coherence is high; this is true mainly in healthy subjects. Yet, in cases where the coherence is lower, the difference in results is more noticeable. [64]

The difference between methods is also less visible when slow metronomic breathing is used, since this type of breathing increases the coherence, but also overestimates the BRS result. [7]

2.3.3 Overview of general advantages/disadvantages of BRS algorithms

All non-invasive methods for measuring BRS involve not only pure baroreflex, but also other cardiovascular and thoracic stretch reflexes. [107] In more recent times, it is reported that the BRS assessment demonstrated in certain health issues (e.g. reflex syncope, atrial fibrillation, and CHF) appears to improve its specificity by applying various inducive maneuvers (e.g., standing, HUT). [108] However, the major requirement for any acceptable BRS estimation is the presence of the sinus rhythm. [109]

The disadvantage of the BRS algorithms is reflected in the fact that they cannot be applied on all individuals. They must contain specific exclusion criteria to provide valid output such as the presence of atrial fibrillation [84], [110], [111], atrial flutter [108], permanent pacemakers [107], [108], frequent supraventricular or ventricular ectopic beats. [108], [111]

According to Barthel et al. [109], some of the other issues include non-stationarities (see Chapter 3.1.2.2.1) and noise that BP and RRI usually contain. Efforts have been made to reduce these influences by applying different filters, yet the filters may, on the other hand, potentially affect the predictive ability of the results.

Another important point is that different algorithms seem to focus on different parts of baroreflex physiology. [45] The sequence method uses only short sequences (3-6 beats in length) and focuses on parasympathetic baroreflex breach, reflecting fast vagal increase or withdrawal, while spectral methods are believed to have a chance to investigate also the sympathetic (slower) component of the baroreflex. For this reason, it is assumed that sequence BRS results are more associated with the HF band, and less with the LF band of spectral estimates. [101]

On the other hand, the VLF band had not been used for BRS determination since the coherence value between SBP-RRI was reported as lowest in that range as explained earlier. Therefore, spectral results could not be accepted as reliable in that band. Yet the recording period used for the spectral analysis in that study by Robbe et al. [56] was only 4.5 minutes long. Thus, the short time period may have limited their ability to analyze the VLF band properly.

Additionally, as mentioned earlier, phenylephrine injections used for invasive BRS estimation, whose prognostic clinical usefulness was already proven in the ATRAMI study (see Chapter 2.3.5), trigger longer sequences in SBP and provoke a stronger RRI response in return; this procedure thus actually appears to increase the coherence in the VLF band between SBP and RRI. [101]

In contrast to these findings, the study by Eckberg et al. [33] investigated baroreflex physiology in a recording of 20 minutes by employing the alpha coefficient method (time-frequency analysis) in nine healthy supine resting adults, and concluded that spontaneous major and constant oscillations of cardiac BRS, without any artificial stimulation of baroreceptors, do occur mainly in the VLF band (central frequency of all subjects was reported to be close to 0.01 Hz, or every 90 seconds).

Therefore, the limitations of BRS algorithms may not lie solely in their inconsistent results in different studies or be related to unclear parameter settings. A significant issue is that by excluding the VLF band, researchers may struggle to define (and agree) on the full spontaneous baroreflex operating range, the physiological aspects behind it and on relations between BRS indices produced by different algorithms. This state of research makes it more difficult to establish the clinical usefulness of spontaneous BRS indices.

General strengths and weaknesses of the sequence and spectral methods (TF and alpha coefficient) are given in tables 2.2 and 2.3.

Sequence method General properties	
Strengths	**Weaknesses**
• Dynamic measure of the parasympathetic (vagal) activity on the heart [10] • Method likely indicates baroreceptor effects on the sinus node with high specificity: it is supported by the near-total disappearance of both positive and negative baroreflex sequences following sinoaortic denervation in animals [76] • Discriminate baroreflex and non-baroreflex activities: separates baroreflex type and non-baroreflex type sequences [65] • Separate analysis of up and down sequences: follows both positive and negative SBP changes [25] • Linear regression is easier to apply than spectral methods and easier to interpret [112] • Does not require external stimulation [113] • Not operator-dependent [113] • Does not require stationarity as do spectral methods [32] • Not time-consuming, but longer recordings recommended [113] • BEI could be added as a complementary parameter which seems useful in specific medical fields: in that it expresses the engagement rate of the baroreflex [89]	• May miss the sympathetic part of BRS due to short sequences [6], [102] • Separate analysis of BRS changes in LF and HF bands not possible [112] • Baroceptors probably do not modulate the sinus node only in sequence-like form, but also trigger a beat-to-beat change in RRI in relation to a beat-to-beat change in the SBP [20] • Relies on invariant time delay (lag) between RRI and BP changes across all subjects [107] • Choosing the right parameters (sequence length, thresholds for RRI changes, SBP changes, correlation coefficient, lags) is very important and influences results [84], [101] • Sequence length effect: BRS and BEI values decrease when sequence length increases [30] • Non-causal method: based on a simple open-loop model between SBP and RRI without taking into account respiration and other influences [101] - can overestimate the BRS value [69], [101] • High correlation coefficient between RRI and SBP does not formally confirm causality between RRI and SBP [69] • Limited value in individuals who lack high correlations between RRI and SBP [114]

Table 1.2: General strengths and weaknesses of the sequence method

Spectral methods General properties	
Strengths	**Weaknesses**
• **Spectral methods:** Not time consuming: 3 minutes are sufficient for LF and HF band analysis [41] • **Spectral methods:** Offer a chance to follow BRS changes over time in LF and HF bands: allowing more in-depth analysis of BRS differences between subjects and their autonomic mechanisms [112] • **TF:** Computes phase spectrum [67]: describes a temporal relationship between RRI and SBP oscillations in LF and HF band • **TF:** Computes coherence spectrum: describes the extent of the linear relationship between RRI and SBP in LF and HF band • **TF:** Computes BRS spectrum: useful for spectrum shape interpretations (see Chapter 2.5.1) • **WBA-TF variation:** Computes BRS value even when coherence between signals is lower than 0.5 [95], [102] • **Alpha:** Easier to compute than the TF method	• **Spectral methods:** Sensitive to ectopic beats and other artifacts which reduce their measurability and applicability in clinical practice: requires visual inspection of signals before the analysis begins [115] • **Spectral methods:** Operator dependent**:** Subjective choice of RRI and SBP signal segments used for spectral analysis • **Spectral methods:** Sensitive to noise in SBP and RRI signals [109] • **Spectral methods:** Require excessive preprocessing of data to ensure signal stationarity: editing and filter applications could lead to different results (Chapter 3.1.2.3) [101], [109] • **Spectral methods:** Noncausal methods: SBP-RRI causality is not taken into account when BRS is computed [69], [101] • **Spectral methods:** BRS values could not be calculated if no LF or HF components in the power spectrum of SBP are detected [102] • **Spectral methods:** BRS results are dependent on the spectral algorithm used and parameter settings (type and size of the spectral window, order of the autoregressive model, threshold for coherence) [96], [101] • **Alpha:** Assumption that there is always high coherence (> 0.5) present between RRI and SBP [116] (add 40) • **Alpha:** The phase between SBP and RRI can be calculated but rarely performed [20] • **Alpha:** Positive bias against the TF method [7], [67]: includes respiration effects

Table 2.2: General strengths and weaknesses of the spectral methods (TF and alpha coefficient)

2.3.4 Algorithms for medical requests/applications

The BRS index serves mainly as autonomic dysfunction (AD) marker in different diseases; however, types of BRS analyses vary depending on the specific medical characterizations of each disease, and according to the clinical value that BRS offers (Digital Appendix 2). Thus, to be able to discuss the strengths and weaknesses of different methods in relation to various health issues, this section of the thesis relates to the specific diseases that are most often found in the literature, ranked by the number of articles found for each disease.

Four bar charts below reflect the number of times each method has been applied in the selected literature for the four most popular BRS-associated diseases: diabetes mellitus, hypertension, CHF and POST-MI. (Fig. 2.5 and 2.6)

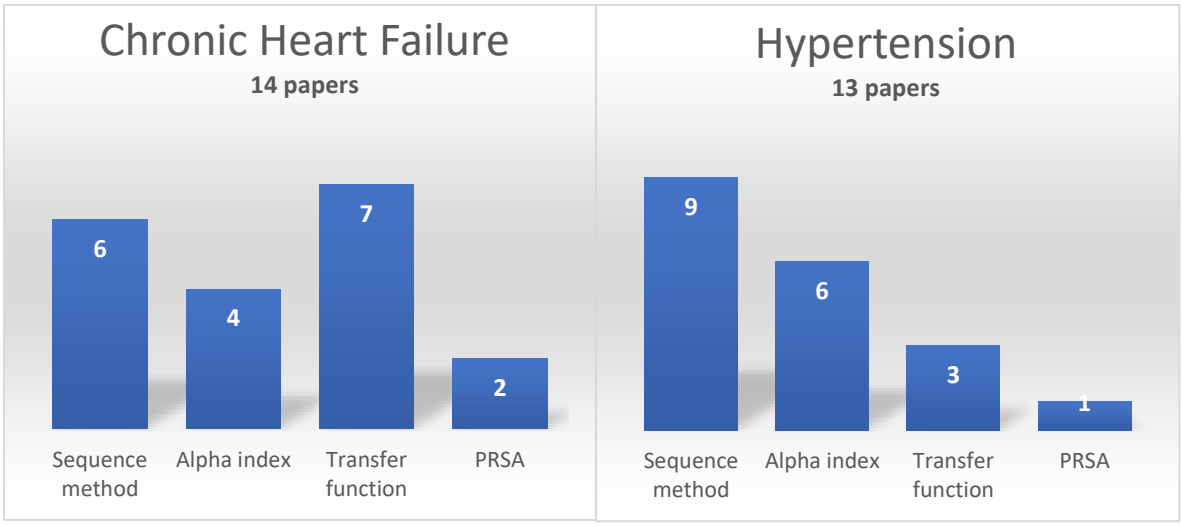

(a) (b)

Figure 2.5: Bar charts for (a) CHF and (b) hypertension with a number of times each method was applied in studies

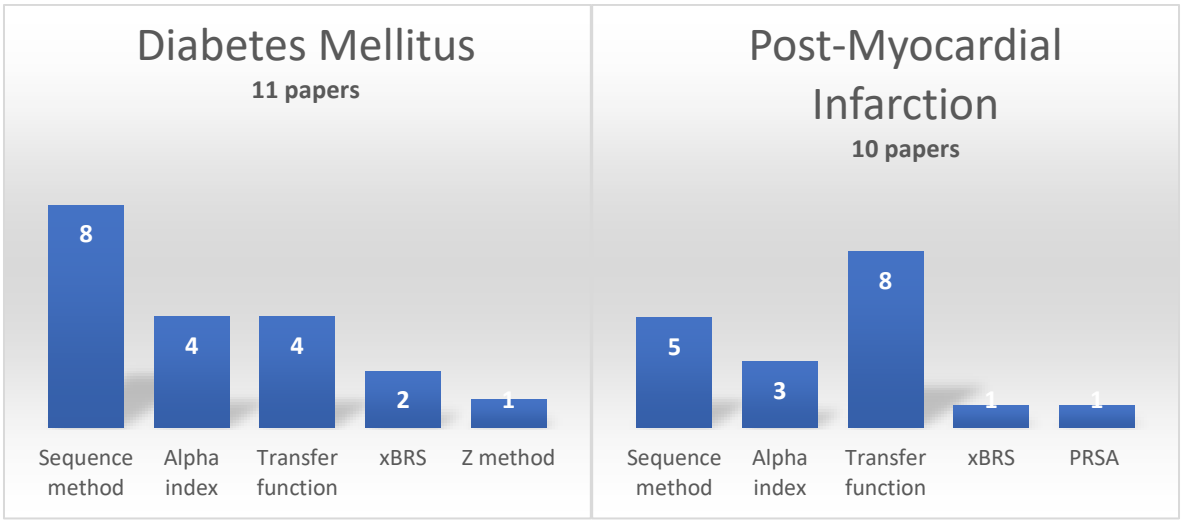

(a) (b)

Figure 2.6: Bar charts for (a) diabetes and (b) POST-MI with a number of times each method was applied in studies

In addition to cardiovascular diseases, BRS algorithms were most frequently applied in two key areas: assessing BRS during autonomic function tests in healthy individuals under various body postures or physical activities, including different breathing patterns (27 papers), and evaluating BRS in subjects under different types of anesthesia (8 papers). Anesthesia usually reduces BRS and changes the relationship between SBP and RRI, thus making the assessment of BRS more challenging. [117], [118], [119]

2.3.4.1 Chronic heart failure

Articles included

Overall, for CHF there were 14 relevant articles found in the time span 1999-2020. These papers focus on heart failure and, in most cases, exclude other diseases from consideration.

Clinical value of BRS in CHF

Heart failure is a critical medical event associated with AD. [102], [108] As a result, BRS as a marker of AD is often reduced, suggesting that a more precise BRS assessment could lead to better risk stratification and outcome prediction, as well as to better care for CHF patients.

Some of the proposed therapies to improve autonomic function and increase BRS include different medication therapies [111], cardiac resynchronization therapy (CRT) [108], baroreflex activation therapy (BAT) [110], vagus nerve stimulation [21] and slow breathing sessions. [120]

Since reduced BRS serves as a high-risk predictor of negative outcomes such as sudden death, cardiac mortality and morbidity, major adverse cardiovascular events (MACE) and frequent hospital admissions, the quantity of reduction in BRS also has prognostic value, although the actual value may depend on the BRS algorithm used. [102], [108], [110] The prognostic value of BRS depends on the measurement timing as well (before or after any treatment), as it seems to have a different prognostic power in untreated versus optimally managed patients, as well as in different types of heart failure. [110]

Challenges associated with the BRS measurement in CHF patients

In CHF patients, the presence of nonlinear dynamics of baroreflex due to their pathology, together with frequent ectopic activity, restrict the power of the algorithms to measure BRS accurately. [102], [108], [115]

Additionally, the BPV in the LF region is distinctly depressed [102], as well as the HRV in both LF and HF ranges [102]. This leads to a low signal-to-noise ratio (SNR). [102] For this reason, the algorithms face difficulty in differentiating what is due to the real baroreflex mechanism and what is due to noise.

Moreover, abnormal breathing patterns are often present in this patient population – in up to 50% of CHF patients according to Pinna et al. [115] - and these patients are usually prone to a higher breathing frequency. [107] The different respiratory rates, which are also present during spontaneous breathing, act as a confounding factor on cardiovascular variability measurements. [107], [115], [121] That is the main reason why measurements by spectral analysis are preferrable in the LF band with paced breathing recordings. [102]

Specific advantages and disadvantages of BRS algorithms in the CHF population are presented in tables 2.4-2.6.

2.3.4.1.1. Advantages and disadvantages of different BRS methods in CHF

Sequence method CHF application	
Advantages	**Disadvantages**
• **Reproducibility (same-day):** Good reproducibility in CHF patients, less in the controls [107]	• **Measurability:** Frequent ectopic beats hinder 3-beat sequences occurrence which causes the failure of the method [107] • **Reproducibility (same-day):** Irregular or differing respiratory rates worsen the reproducibility [107] • **Reproducibility and success rate:** Wrong thresholds (lags choice, thresholds for RRI and SBP changes, threshold for correlation coefficient) lead to poor results and to high failure rate (low measurability) - limits use in clinical practice [84], [102], [107] • **Thresholds recommendation:** RRI and SBP variation thresholds influence BRS result – caution when setting them (high RRI and low SBP threshold select sequences which deliver high BRS, which is rare in CHF patients). Advised that it is best to use the lag which produces the most valid sequences (Lag 0 produced most sequences in controls and CHF patients) and avoid putting any correlation coefficient threshold to avoid bias in BRS results; optimal thresholds vary between controls and CHF patients and influence agreement with other BRS algorithms [107] • **Prognosis:** BRS value did not show prognostic value in CHF patients since prognostic information appear only connected to the LF band [102]

Table 2.3: Sequence method: advantages and disadvantages in CHF application

TF method: WBA-TF (no coherence criterion) versus original TF (coherence > 0.5) CHF application	
Advantages	**Disadvantages**
WBA-TF (nonparametric) • **Measurability:** 100% - BRS was computed in all CHF patients [102] • **Parameters:** No coherence criterion issue [121], [122] • **Critical BRS value:** Proposed critical value of BRS < 3ms/mmHg reflects the complete baroreflex impairment - this BRS value seems to be a biological threshold for the functioning of the baroreflex, below which RRI changes are not any more linearly related to SBP changes [122], [123] • **Risk stratification:** Improved risk stratification classification when it was added to the clinical prognostic model and showed an acceptable stability of results [102]	**WBA-TF** • **WBA-TF (nonparametric):** Cannot replace the phenylephrine method in the risk stratification classification, but can be integrated with it [115] • **WBA-TF**: **Prognosis:** Non-baroreflex information is present in the calculated BRS value so the prognostic information cannot be directly associated to the baroreflex function [68] **Original TF** • **Measurability:** Reduced due to high ectopic rate in CHF patients [121],[115] • **Parameters:** Coherence threshold > 0.5 is an issue - in CHF patients it was common to have coherence value < 0.4 [102] • **Prognosis (parametric):** Provided some prognostic value in CHF patients but not good stability, or did not help to improve risk stratification: recommended to do averaging procedure over the whole LF band to enhance stability of measurements [102] • **Measurability (parametric)**: Low SBP variability of CHF patients in the LF band limited the application of the method (Measurability was 96% but still lower than for the nonparametric WBA-TF which was 100 %) [102]

Table 2.4:TF method: advantages and disadvantages in CHF applications

Alpha coefficient CHF application	
Advantages	**Disadvantages**
• Nothing specific mentioned	• **Measurability:** Not always computable in CHF patients [102] • **Prognosis:** aHF (parametric) did not show any prognostic information in CHF patients [102] and has poor reproducibility [107] • **Prognosis:** aLF (parametric) did provide prognostic information for CHF patients, but did not significantly improve the risk classification when added to the clinical prognostic model, and didn't demonstrate good stability (poor reproducibility) in the validation procedure [102]

Table 2.5: Alpha coefficient: advantages and disadvantages in CHF application

2.3.4.2 Hypertension

Articles included

Overall, for hypertension, there are 13 relevant articles found in the time span 1988-2015. These papers focus only on hypertension or on hypertension mixed with some other health issues, such as stroke. [12]

Clinical value of BRS in hypertension

The presence of hypertension per se in an individual indicates a significant risk factor for cardiovascular disease as it was confirmed that BRS, as AD marker [12], [22] as well as BEI [92] - in case the renal failure was additionally present - could be used as an independent risk indicator and predictor for mortality and the development of major advanced cardiac events (MACE) in hypertensive patients. [53]

Since hypertensive patients have decreased BRS in the early stages of hypertension, it was originally believed that hypertension causes baroreflex impairment. [30] Evidence now reported from more recent studies indicate that lower BRS is actually a factor that plays a role in the development of hypertension. [53]

Reduced BRS in hypertension cases is further reduced in patients with stroke history [12], metabolic syndrome [12], [22] and chronic renal failure (CRF) [92], making hypertensive patients with different comorbidities more easily prone to sudden death and higher mortality rates. [92]

For this reason, appropriate assessment of BRS in hypertension, or identifying hypertension [124], is the goal of numerous studies. [101], [112] In addition, in some studies, specific therapy efforts, such as slow breathing sessions [24] or physical training [20] were also tested while monitoring BRS, trying to find opportunities to improve the BRS in that patient population.

Specific BRS characteristics in hypertensive patients

BRS is reduced in hypertension [53], [125] approximately 35 [112] - 40% [30] when compared to normotensive patients.

In older hypertensive patients (> 40+) the night/day variation of BRS is small or absent, but in younger patients the modulation is still present; the BRS slope increases at night, while the number of valid baroreflex sequences decreases. [30], [76]

Reduction in BRS slope of ‘up’ (slowing down the HR) sequences seems to be of particular relevance in prognosis of cardiovascular events. ‘Up’ sequences reflect parasympathetic activation, while down sequences reflect parasympathetic deactivation. [53]

In addition, the baroreflex seems to be less engaged (lower BEI) in hypertensive patients as the number of valid baroreflex type sequences discovered in measurements is lower than in normal subjects. [30] Moreover, the number of valid sequences is even lower in older hypertensive patients in comparison to younger hypertensives when the same thresholds for both groups are applied in setting the ‘valid sequence’. [76] On the other hand, in younger patients BRS is directly connected to HR while in older subjects this connection disappears. [76]

Specific advantages and disadvantages of BRS algorithms in hypertensive population are presented in tables 2.7-2.9.

2.3.4.2.1. Advantages and disadvantages of different BRS methods in hypertension

Sequence method Hypertension	
Advantages	**Disadvantages**
• **Diagnosis:** Suitable method to diagnose hypertension and to be used for risk stratification for MACE and mortality [30], [92], [112] • **Risk stratification:** 'Up' sequences appear more relevant for the risk of mortality [53] • **Risk stratification:** BRS measured in a supine position most correlated with other risk factors in hypertension; BRS slope may assess risks of cardiovascular events [124] • **Risk stratification and outcome prediction:** BEI as additional support and an independent risk factor can be calculated in hypertensives with the renal disease - BRS and BEI are not interchangeable since BRS predicted sudden death, but BEI predicted the all-cause mortality in this patient population [92] • **Algorithm:** Differentiates 24-hour BRS behavior between older and younger hypertensives and also between hypertensives and age-matched controls: same thresholds set for young and older subjects [30], [76] • **Parameters:** Lag 1 used in all selected research papers: no reasons given	• **Parameters:** Different thresholds settings influence results, the caution is required with different age populations (e.g. in elderly, if RRI threshold is set, there is high tendency to bias BRS results) – advised that thresholds should be relaxed in elderly population to allow better measurability [101]

Table 2.6: Sequence method: advantages and disadvantages in hypertension

Alpha coefficient method Hypertension	
Advantages	**Disadvantages**
• **Diagnosis:** Suitable method to diagnose hypertension [76], [101], [125] • **Diagnosis**: Mean alpha index (mean of aLF and aHF) at rest may identify hypertension when age and sex data are added to the model: accuracy was c. 80%, but more evidence is required before a final conclusion can be determined [125] • **Diagnosis**: aLF showed reduced BRS in hypertensives and displayed day/night variations [76] • **Risk stratification:** aLF index seems useful in assessing the risk of cardiovascular events [124] • **Diagnosis:** The alpha method may be useful when SBP is relatively stable and the recording is of shorter duration [76]	• **Parameters:** Coherence threshold is an issue when set above 0.5 in hypertensives [101]

Table 2.7: Alpha coefficient: advantages and disadvantages in hypertension

TF method Hypertension	
Advantages	**Disadvantages**
• **Diagnosis:** Suitable method to diagnose borderline hypertension: BRS - TF (LF) [112] • **Risk stratification**: BRS-TF (LF) (with HF breathing) may be marker of high cardiovascular risk in hypertensive patients with stroke history (BRS most reduced when metabolic syndrome added < 3ms/mmHg) [12]	• **Diagnosis:** Breathing at 6bpm overestimates BRS in the LF band and should be avoided for diagnostic purposes [73]

Table 2.8:Transfer function: advantages and disadvantages in hypertension

2.3.4.3 Diabetes mellitus

Articles included

Overall, for diabetes mellitus (DM1 and DM2) there are 11 relevant articles found in the time span 1997-2020. Three articles focus solely on DM1, two on DM2, and the rest include both types concurrently.

Clinical value of BRS in diabetes

In diabetes mellitus, there is a substantial need for a detection of cardiovascular autonomic neuropathy (CAN or AN or AD) [26] which affects around 20% of all diabetic cases [126] and represents a high risk for cardiovascular mortality, even doubling it, according to Javorka et al. [26] For this reason, the measurement of spontaneous BRS could act as a possible non-invasive solution for early diagnosis. It offers a less complicated clinical procedure than other standardized clinical tests, for patients as well as for clinicians. [78] Furthermore, BRS is recommended as a potential AD diagnosis marker which could be useful in times when even regular diagnostic tests still show a negative result [78], or in asymptomatic diabetic cases that show no evidence of CAN. [91], [127]

Characteristics of diabetes (DM1 and DM2)

It is reported that DM1 and DM2 have different onset times, prevalence, treatment options and the development of AN. [91] Diabetic patients usually, aside from DM, deal with additional health issues such as obesity, hypertension and CRF, which influence and reduce BRS values even further. [91]
Specific advantages and disadvantages of BRS algorithms in a diabetic population are presented in tables 2.10-2.12.

2.3.4.3.1. Advantages and disadvantages of different BRS methods in diabetes mellitus

Sequence method Diabetes mellitus	
Advantages	**Disadvantages**
• **DM1: Diagnosis (age ± 21):** Up and down sequences useful: Reduced slope of up sequences (implies longer baroreflex time delay in DM1), preserved slope of down sequences: asymmetric baroreflex impairment noticeable - sequence method more sensitive than others [26] • **Diagnosis**: Number of up and down baroreflex sequences is reduced in diabetics; this is relevant [78], [91], [128], but also the number of SBP ramps increases (BP varies more) in this group • **Diagnosis:** BRS slope showed mixed results: in some cases was relevant [127], in others not [128] • **(Mixed DM) Diagnosis (age 22-54**): Sequence number (used > 4 beats sequence) and/or BRS slope were enough to detect early AD [78] • **(Mixed DM) Diagnosis (middle age)**: BRS slope was sensitive enough to detect CAN [91] • **BEI is clinically useful: (mixed DM - middle age)** BEI was the most sensitive discriminator of AD [91] • **Parameters**: Lag 1 mostly applied in studies: no reasons given	• **Algorithm:** Assumes a linear relationship between SBP and RRI changes which may not be valid in diabetics [26] • **Measurability:** Appropriate number of sequences must be found in diabetics for this technique to work [103] • **Measurability:** Frequent premature beats and atrial fibrillation present in diabetics made the BRS estimation often unfeasible [103] • **(DM2) Diagnosis:** In middle-aged and older patients, the reduction of BRS in the supine position is harder to measure or not detected at all [103], [126]; wrong thresholds could be the issue • **(DM1) Diagnosis**: in children and adolescents BRS must be combined with HRV metrics for better diagnosis [129] • **(Mixed DM) Diagnosis**: BRS slope values show large variability in DM patients – reduces the physiological relevance [128]

Table 2.9: Sequence method: advantages and disadvantages in diabetes mellitus

Alpha coefficient method Diabetes mellitus	
Advantages	**Disadvantages**
• **(Mixed DM) Diagnosis (age 22-54):** Shows progressive reduction of BRS (aLF) with higher degrees of CAN able to detect CAN, coherence > 0.5 [78] • **(DM2) Diagnosis (age ± 50):** Mean alpha, aLF and aHF were sensitive in early detection of CAN more than the sequence method, coherence > 0.5 [126] • **(Mixed DM) Diagnosis (age 20-54):** Mean alpha detected CAN, no info if coherence criterion was applied [130] • **DM1: Diagnosis (age ± 35):** Significant BRS (mean alpha) impairment determined in supine and standing positions, coherence set above 0.4 [131] • **Diagnosis:** Mean alpha was most used BRS index in DM	• **Parameters:** Coherence criterion (> 0.5) reduced the number of patients in whom BRS could be measured [126]

Table 2.10: Alpha coefficient: advantages and disadvantages in diabetes mellitus

TF method Diabetes mellitus	
Advantages	**Disadvantages**
• **(mixed DM) Diagnosis (age ± 48):** HF and LF gain didn't' reach significance but were lower than in controls [128] • **(mixed DM) Diagnosis (age ± 45):** HF gain detects patients labeled as without AD or in early stages only in a standing position, gain computed at maximum coherence in each frequency band [127] • **DM 1: Diagnosis (age ± 21):** Time delay in SBP-RRI was reported as important: the phase should be computed [26] • **DM 1: Diagnosis (age ± 21):** Coherence was > 0.5 in patients but didn't reach the level of statistical significance [26] • **DM 1: Diagnosis (age ± 22):** LF gain detected BRS decrease and longer recordings (3-42 min) proved more useful to make the method more reliable, coherence > 0.5 – used different LF band limits, HF breathing [34]	• **Diagnosis:** In supine position spectral results do not seem useful [127] • **DM 1: Diagnosis (age ± 21):** LF gain showed lower sensitivity to detect changes in BRS in this group of patients, coherence set > 0.5, 60 min recording, HF breathing [26] • **Parameters:** Coherence criterion could be an issue in diabetics; it lowers measurability [128] • **Diagnosis:** Clinical value of the LF gain shows controversial results [26], [34], [128]

Table 2.11: Transfer function: advantages and disadvantages in diabetes mellitus

2.3.4.4 Post-myocardial infarction (POST-MI)

Articles included

Overall, for POST-MI population, there were 10 relevant articles in the time span 1998-2014. These papers all focus only on myocardial infarction in the acute [83] and 2-4 weeks post-infarction phase. [41], [109], [132]

Clinical value of BRS in POST-MI population

Individuals who survived the first myocardial infarction were categorized as having a higher risk for cardiac mortality after their first event than those who had not suffered from a previous heart attack. [41], [109] According to research, the BRS has clinical value as the detector of AD, and thus is able to predict the risk of cardiac mortality occurring in subsequent years. [109], [132] Furthermore, it is also suggested that BRS could be particularly useful for the risk stratification procedure - to identify POST-MI subjects, who have moderate risk for cardiac

mortality. However, when estimated BRS is combined with other standard risk factors - e.g. with HRV indices or with reduced LVEF – their combination can improve the prognosis. [41]

On the other hand, in the acute phase – only a few hours after MI - one particular study described the role of BRS as a prognostic factor for the successful tissue reperfusion after the primary percutaneous coronary intervention (a therapy treatment). It has been reported that the change in BRS can separate the individuals who are improving from others whose condition is worsening after the intervention. [83] Additionally, according to Barthel et al. [109] the baroreflex function could be improved in POST-MI cases with rehabilitation programs (e.g. with exercise), but studies confirming the improvement in survival rates have yet to be provided.

Specific BRS characteristics in POST-MI population

The BRS index is usually reduced in POST-MI patients compared to normal subjects since the baroreflex is weak in this group of patients. According to Honzikova et al. [41], [132], their LF peak presented in spectral methods is usually shifted to lower frequencies (0.07 – 0.12 Hz) and the lack of SBP variability at 0.1 Hz in some of the patients has been reported as well. [32], [41] Furthermore, the coherence value between SBP and RRI appears to be low in this population [41], [67]; yet the prolonged baroreflex delay has not been reported. The BRS index estimated via phenylephrine method cannot be replaced with the spectral BRS index in this group, as there is a bigger difference in results between patients with depressed and more preserved LVEF. [67]

Specific advantages and disadvantages of certain BRS algorithms in POST-MI population are presented in tables 2.13-2.15.

2.3.4.4.1. Advantages and disadvantages of different BRS methods in POST-MI

Sequence method POST-MI application	
Advantages	**Disadvantages**
• **Outcome prediction:** BRS slope predicted mortality (12.5 years follow-up): no information was provided on algorithm parameters used [133] • **Parameters:** Lag 0 was used once (other studies did not provide information on lags) • **Measurability:** Recordings longer than 8 minutes are recommended in POST-MI to improve measurability and reliability [102] • **After PCI therapy (acute-MI):** BRS slope was able to differentiate between BRS recovery and early worsening after treatment; BRS is present in the acute MI phase, was not lost due to medical condition [83] • **Measurability (acute-MI):** Full – considered as reliable method, but no information provided on lag used [83]	• **Measurability:** Lack of valid sequences could be found due to small amplitudes and fast changes in SBP and RRI [32], [69], hence not a reliable method [32] • **Parameters:** Invariant lag delay used (not clear which lag) - it might be better to use variable delay (lags) to improve measurability [32] • **Risk stratification:** BRS slope provided poor prediction for all-cause mortality [109] • **Acute-MI phase:** BRS shows a high variance in this phase [83]

Table 2.12: Sequence method: advantages and disadvantages in POST-MI applications

Alpha coefficient method POST-MI application	
Advantages	**Disadvantages**
• Nothing specific mentioned	• **Measurability:** Low in POST-MI [32] • **Reliability:** Less reliable than WBA-TF method and aHF shows the worst reliability in POSTI-MI – aHF improved with paced breathing [32] • **Algorithm:** non-causal method - Possibility that aHF and aLF overestimate the real BRS value in patients with impaired LVEF [32]

Table 2.13: Alpha coefficient: advantages and disadvantages in POST-MI applications

TF method: WBA-TF (no coherence threshold) and TF (coherence > 0.5 or measured at the highest coherence) POST-MI application	
Advantages	**Disadvantages**
TF • **Risk stratification:** Critical value of 3ms/mmHg in POST-MI was estimated; mortality increased 5 times in patients with moderate risks (BRS gain in LF measured at the highest coherence) [41], [132] • **Outcome prediction:** BRS LF and HF gain predicted mortality in POST-MI (12.5 years follow-up): no information on algorithm parameters [133] **WBA-TF** • **Reliability:** Reliable method in POST-MI [32] • **Measurability:** Full in POST-MI [32], [95] • **Parameters**: Coherence criterion exclusion better for POST-MI cases (especially with depressed LVEF) [32], [95] **TF and WBA-TF** • **Frequency band:** Only the LF band was applied and considered relevant in POST-MI studies, with some small variations in band limits • **Algorithm:** Short recording time (3 minutes) required [41], [132]	**TF** • **Measurability:** Low - high failure rate (30%) due to strict coherence criterion and due to lack of variability at 0.1 Hz in some of the patients; low SBP variability in the LF band leads to low coherence if noise is assumed as constant [32], [41], [132] • **Parameters:** High coherence threshold SBP-RRI is an issue in POST-MI cases [32], [41]

Table 2.14: Original TF and WBA-TF methods: advantages and disadvantages in POST-MI applications

2.3.5 Algorithms proven to be of medical benefit?

In the tagging matrix there is a tag labelled 'medical benefit'– the column is then filled with the options 0 (indicating no medical benefit), 1 (indicating evidence of medical benefit/claim for the medical benefit) or 'w' (standing for weak evidence). Weak evidence was tagged in studies that had a cohort with less than 10 subjects, or if the final conclusion included words like 'may' be of clinical value or 'needs further conformations' from larger studies.

The sequence method, including all of its variations, is widely used in clinical studies and it has proven its value many times. For instance, value could be seen in the data related to hypertensive patients with CRF [92], in the vasovagal syncope recurrence during HUT [113], in dynamic assessment of the cardiac anticholinergic drug effects [10], in detecting AN in DM [91], and in following recovery after an intervention during the acute phase of POST-MI. [83]

On the other hand, the spectral methods have also shown their clinical value in the following instances: the alpha coefficient (solely aLF index) acting as an independent predictor of acute kidney disfunction and low cardiac outflow state [134]. This method is also useful in the detection of hypertension - although with a c. 80% success rate [125]. This technique also appears to be useful in following the BRS variations during the day. [20]

Particularly in cases of CHF, the WBA-TF method seems to offer useful independent prognostic information but it should be noted - due to lower measurability - its use could be expanded in a combination with the 'new risk index'. [121], [123] The study by Pinna et al. [102], for instance, confirmed the value of the prognostic information derived from the WBA-TF approach. However, all these studies worked with a cohort that had below 400 patients and thus larger multicentral studies, with preferably current cohorts, are needed to validate the clinical benefit.

The cross-correlation method (xBRS) showed its clinical value in the stroke outcome prediction - acute intracerebral hemorrhage [135] – although the sample size was below 50 subjects. The other useful clinical value can be seen in discovering that longer baroreflex delay is essentially found in cardiac patients who are not treated with beta blockers. [136]

The bivariate phase-rectified signal averaging (PRSA) method has been confirmed to generate the independent prognostic information in the CHF and POST-MI patients. [58], [102], [109] However, according to the literature selected for this thesis, the number of research studies applying it is still very low.

Of these, the ATRAMI study [16], using the phenylephrine method to estimate BRS, examined close to 1,300 individuals. This study appears to be accepted by the broader research community as providing real clinical evidence for their BRS-related findings in the prediction of total cardiac mortality after myocardial infarction. [132]

2.3.6 Algorithms on the market

The Task Force Monitor (CNSystems Medizintechnik GmbH, Graz, Austria) includes the sequence method. [1], [137]

The time cross-correlation (xBRS) method has proven its value in the BRS estimation and was validated in 2017. [138] Additionally, it is this BRS algorithm that is currently incorporated into an operational medical device – FINAPRES NOVA (Finapres Medical Systems B.V., Enschede, The Netherlands) - which is currently on the market. (Fig. 2.7)

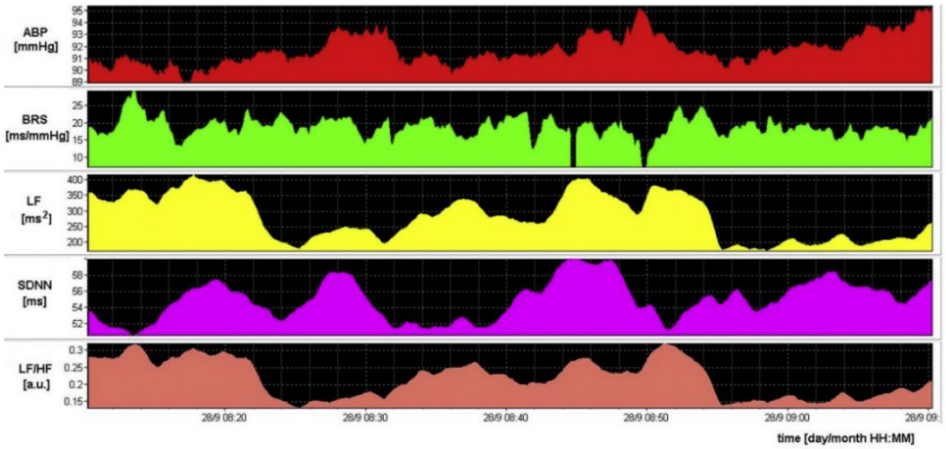

Figure 2.75: The Cross-correlation method (xBRS) [139]

Other software options are also available for purchase. For instance, the sequence method is incorporated into the following software packages:

- Heart Scope Software (AMPS Ltd, NY, USA) [83]

- BRS Analysis software (Nevrokard, Slovenia) [126]
- Small Animal Baroreflex Sensitivity Analysis SA-BRS software (Nevrokard, Slovenia) (Fig. 2.8)
- CardioSeries v2.1 or v2.4 (Brazil) [140], [141]
- Spike2 (v.2, Cambridge Electronics Design, Cambridge, UK) [52]

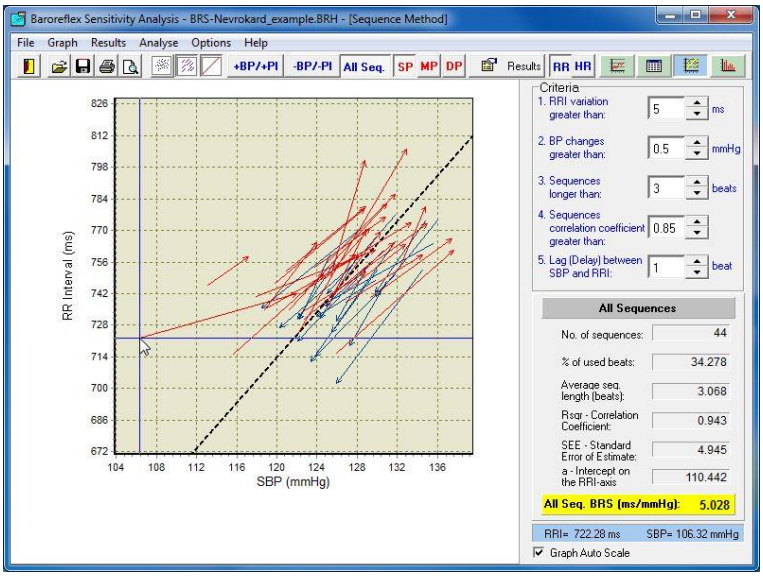

Figure 2.8: Nevrokard BRS software - Sequence method (source: http://www.nevrokard.eu/maini/brs.html)

Software packages using spectral methods (used for research) include:

- Nevrokard® BRS Analysis software (Nevrokard Kiauta, Izola, Slovenia) [126] (Fig. 2.9)
- Small Animal Baroreflex Sensitivity Analysis SA-BRS software (Nevrokard, Slovenia)
- HemoLab Software (Harald Stauss Scientific, Dunuggan, USA) [142]
- Ponemah® Software (Data Sciences International, USA) [142]

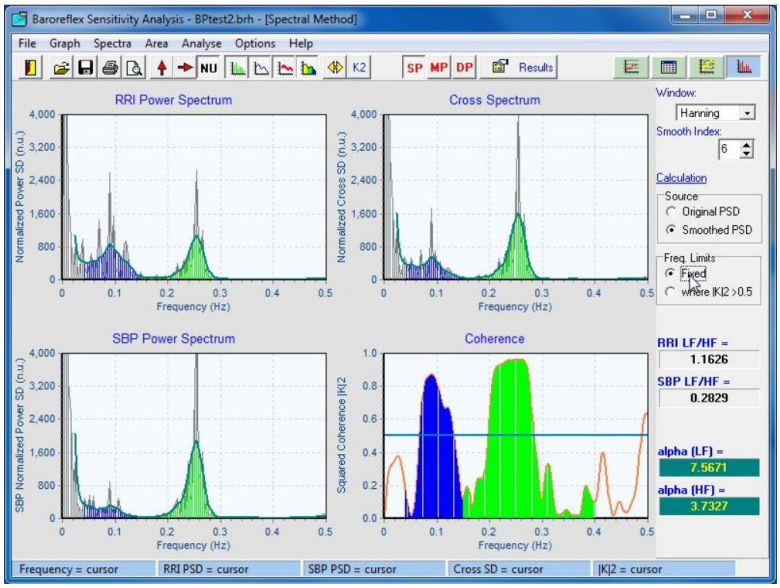

Figure 2.9: Nevrokard BRS software - Spectral method (Source: http://www.nevrokard.eu/maini/brs.html)

2.4 Conclusions

In summary, it appears that the main clinical benefits of BRS emerging from the literature are:

- its role in outcome prediction, risk stratification and diagnosis of certain cardiovascular and neurological diseases;
- it can also play a role in measuring the effects of the different therapy options (inc. physical exercise and medications) on BRS by using it as a valid measure for the assessment of therapeutic progress.

However, while the studies address a broad spectrum of diseases, they often lack focus on the rationale behind the selection of specific algorithms, types of spectral estimators or the identification of optimal parameter settings. As a result, the research appears fragmented and typically yields only a limited number of studies on specialized topics with direct relevance to the specific clinical value of BRS.

Overall, the spontaneous BRS index has a potential as a clinically useful index in a prognosis/risk stratification of cardiovascular diseases, and/or to detect AD when applied alone or analyzed in conjunction with standard risk factors for a better prognosis. However, a full validation of its clinical value requires stronger evidence from larger and more consistent clinical studies.

As can be seen in Chapter 2.3.3 regarding the advantages and disadvantages of methods applied in different diseases, the reliability and measurability of algorithms depend upon the population selected (healthy or ill subjects, specific disease characteristics) and the settings of algorithmic parameters. Outcomes also vary based upon the types of spectral estimators used that differ in studies. Definitive and reliable results are hence often impossible to derive, compare and form strong conclusions.

According to the literature, a first issue arises in measurability which is additionally affected in cardiac patients due to the presence of ectopic beats, thus leading to the rejection of many patients from relevant studies. Abnormal breathing patterns also influence results.

A second issue lies in the fact that the majority of algorithms are based on high linearity between SBP and RRI signals. This, per se, limits the BRS use in clinical conditions of patients who suffer from poor cardiovascular health and have a less linear SBP-RRI relationship. [17]

2.4.1 General advantages/disadvantages of spectral vs sequence methods

Overall, both types of methods – spectral and sequence – have their advantages and limits; so far, a universally agreed ‘best’ method for BRS estimation does not exist.

The sequence method assumes that all SBP variations linearly related to the RRI are of baroreflex origin. Thus, it also includes in the BRS calculation other influences (e.g. respiration) that independently drive the fluctuation of the two signals. [69], [82] For this reason, it often overestimates the BRS value. [69]

In most cases, the sequence method BRS results correlate more with the spectral BRS which is determined within the respiratory rate-related HF band, and correlates less with the spectral

BRS estimated in the LF band - which is attributed more to its assumed sympathetic influence. [101]

Overall, the sequence method primarily measures fast vagal nerve traffic to the heart and ignores slower sympathetic activity due to shorter sequences being employed. [6] Spectral methods, in contrast, cover both frequency bands. However, the sequence algorithm is based on a simpler mathematical model (linear regression) than the spectral methods and is generally regarded as easier to use, and the BRS slope as easier to interpret.

On the other hand, the sequence method requires appropriate threshold setting before BRS measurement, as the thresholds affect the results considerably, also varying between different groups of individuals. [84] If the thresholds are incorrectly chosen, the sequence algorithm often generates missing slots (no BRS values) as the sequences are undetectable in a particular recording. On the contrary, spectral techniques produce more BRS points during the calculation. They include smaller beat-to-beat changes of SBP and RRI in their calculations, not only sequence-shaped changes (lasting few beats); they also do include some noise. [30], [109] (Fig. 2.10 and 2.11)

This noise could be problematic when the subjects have a very low BRS value, since in those circumstances it could be hard to separate the noise from the real signal. [6] Spectral methods offer phase calculation between SBP and RRI and are thus useful in estimating baroreflex time delay, a topic of potential interest which needs to be further researched. This phase computation is not usually pursued using the traditional sequence method.

Finally, the sequence method has the advantage that it does not require signal preprocessing steps before BRS estimation and is able to separate positive and negative SBP changes (up and down sequences), explaining the fast vagal activation and withdrawal on HR better. Yet spectral methods seem to provide more accurate BRS results than the time-domain techniques when applied with the noninvasive measurement of the pressure waves signals alone - without the need for an additional ECG. [48]

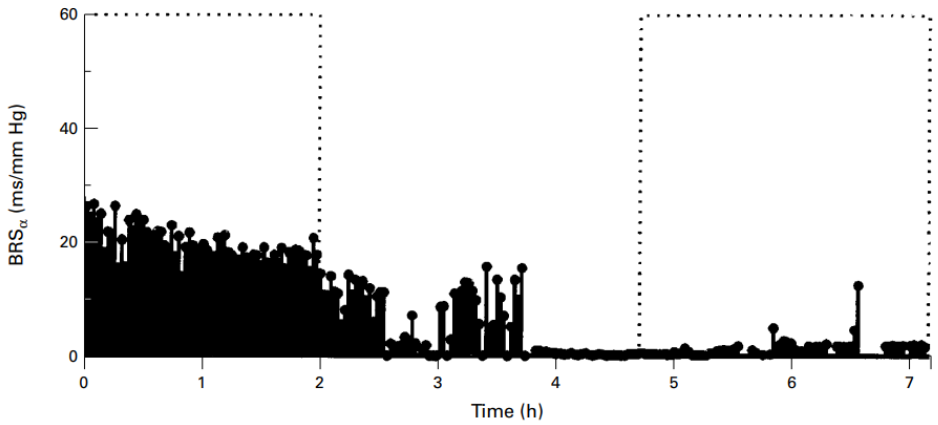

Figure 2.10: Diagnosis of brain death by the spectral method (alpha coefficient method) [99]

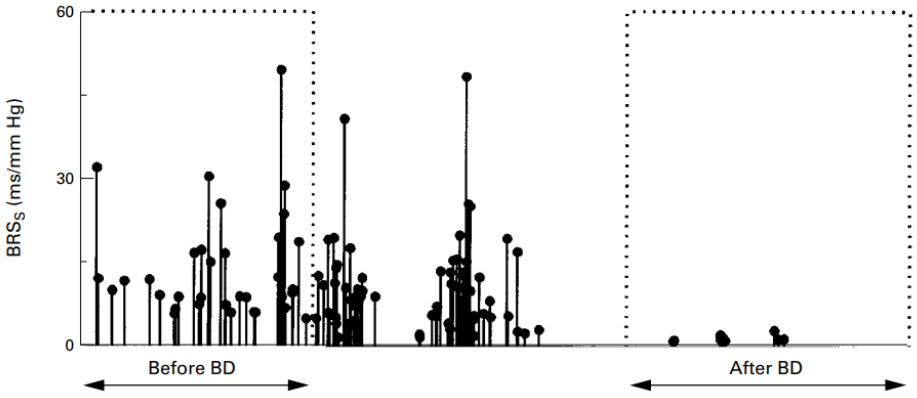

Figure 2.11: Diagnosis of brain death (BD) by the sequence method [99]

Both types of methods tend to provide parallel trends regarding BRS fluctuations (Fig. 2.12) However, they are not interchangeable, although the information they provide is similar between the two. [71]

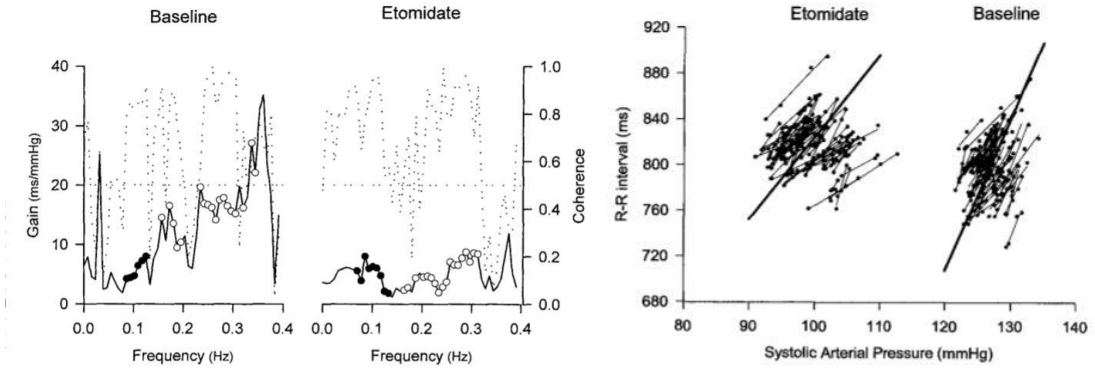

(a) (b)

Figure 2.12: Same BRS behavior expressed by the (a) spectral and (b) sequence methods during the etomidate anesthesia. As it can be seen, baseline BRS is higher than etomidate BRS in both cases. In the sequence method the slope is steeper in the baseline stage, however, the spectral method shows that the change in BRS comes mainly from the HF band, not the LF band [45]

2.4.2 Issues with the literature analysis

Comparison of BRS techniques in the literature was difficult for numerous reasons: sample sizes were considered small, according to some sources. [23], [129] As a result, it was hard to decide on the real clinical value of claims based on these studies. According to Gerritsen et al. [7] there is a need for larger studies on BRS reproducibility and a need to confirm the predictive power of various algorithms to reach full agreement on early claims for clinical use.

Moreover, direct comparison and value assessment was made difficult by a range of body positions employed (supine, standing, passive head up tilt test (HUT)), varying recording times of SBP and RRI time series during measurements, patient breathing rates which were both spontaneous and/or controlled above or below 0.2 Hz, the algorithms (especially the sequence method) applied numerous different thresholds, and often did not disclose the full information about the algorithm applied. In addition, in many studies there was no clear explanation given

why any of the parameters and thresholds were applied. For these reasons, the results of many studies could not be directly compared.

As explained earlier, the differences in results between different BRS algorithms go beyond unclear parameter settings. A further major issue arising is the exclusion of the VLF band, which complicates defining the full baroreflex operating range, understanding the physiological mechanisms behind it, and correlating BRS indices across different algorithms. This uncertainty hinders the establishment of the clinical utility of spontaneous BRS indices.

The BRS estimation protocol (inc. the BRS algorithm, parameter settings and frequency bands) would benefit from being standardized for different medical requests (diseases and applications), so the results from numerous studies would be easier to compare and the BRS clinical value extracted with more evidence and hence greater confidence. [48] In addition, the BRS reference values should be determined with agreed protocols and then be used for determining the clinical use or continuous research.

A short summary of recommendations regarding experimental protocols for BRS measurement procedures and different algorithm settings for the four pathological states described above are given in Appendix A.

2.4.3 What is still unknown in the research

Throught the full period covered by the literature, many theories have been put forward as to the physiological sources of regulation of the LF and HF bands in the BRS spectrum, and how the BRS spectral results should be interpreted for diagnostic purposes. According to more recent studies, it is believed that the LF band is controlled by both the sympathetic and parasympathetic effects on the heart, while the HF band is regulated only by the parasympathetic system and respiration.

Thus, the physiological foundation of the BRS spectrum across different frequency bands has not yet been fully researched and requires further clarifications. This may be particularly relevant to the VLF band, and it should be decided whether this band should also be included in BRS estimations.

Another issue lies in the fact that none of the BRS estimation methods measures pure BRS, although many mathematical models have been developed with the intention to describe how the baroreflex complex mechanism operates. Yet, it is still the fact that the majority of the BRS methods applied in clinical studies to this day are not capable to separate FF from FB pathways in the baroreflex loop, not able to completely avoid respiration or other neural and humoral influences on the BRS, or even develop an easier-to-use BRS method that incorporates the SBP-RRI causal relationship. [76]

Overall, the autonomic nervous system (ANS) control is also a significant research topic as it is a complex regulatory system influenced by numerous different interconnected variables. In the literature, it is described as a potential treatment target for cardiovascular diseases. Yet, as there are many unknowns in this field, the physiology of the autonomic control and how it could be improved upon also requires further research. [8]

2.5 Objective of the practical part

Building upon the insights provided in preceding chapters, the objective of the practical phase of this thesis as explained above (see Chapter 1.8) was to implement (using Python (Version 3.9) with the Spyder editor installed on the Lenovo p53 laptop) a chosen spectral method suited for offline (ad hoc) BRS determination sourced from relevant literature. Therefore, taking into account the differences between the alpha coefficient and the TF method described in Chapter 2.3.2, the TF method became the preferred choice for computing and visualizing BRS.

As previously mentioned, BRS spectral analyses (both alpha coefficient and TF method) commonly employ either FFT or AR algorithms. However, due to missing BRS related literature providing deeper insights into the TF analysis and discussing the difference between these two spectral estimators, another collection of articles (n=18) was gathered specifically for the practical phase. These articles were obtained using the snowball method inspired by the methodology outlined by Meel-van den Abeelen et al. [143]; they were thus primarily sourced from references within BRS literature or from studies focused on the HRV spectral analysis (in frequency and time-frequency domain).

In general, the AR model describes signal dynamics as a linear combination of p past samples of that signal, each weighted by constant coefficients, along with a zero-mean white noise term. It was shown recently that AR modeling fits the HRV behavior well, and that 3 minutes of past beat values, influence the current beat in healthy humans. [144]

In the context of BRS, a bivariate AR model is used since SBP and RRI are analyzed jointly. This AR model characterizes the dynamics of the output series (RRI) as a linear combination of p past samples from both the output series itself and the input series (SBP), each weighted by constant coefficients, along with a zero-mean white noise term. Here, p represents the model order of the bivariate process. [20], [70] Overall, the AR modeling approach seems well-suited for BRS computations when the sympathetic component of the baroreflex is considered, as the current BRS value is influenced by previous beats. In contrast, the vagal component acts more rapidly, affecting the current or subsequent beat. [60]

The primary challenge in most AR model studies as reported by Li et al. [145] lies in the use of different algorithms to compute coefficients, the application of various criteria for selecting appropriate model orders, and the use of differing model orders themselves. This makes direct comparisons between studies difficult. In BRS studies this topic has not yet been researched.

When focusing specifically on HRV studies, the FFT and AR methods tend to yield notably different results in terms of power calculation across frequency bands and the careful interpretation of results is generally advisable. These differences between methods appear further amplified when varying body postures or patient populations (healthy versus e.g. diabetics, with non-linearities present, are considered. [146], [147]

In terms of BRS computation methods, power estimation is more closely linked to the alpha coefficient method, as power computations of RRI and SBP are central aspects of the method. Thus, one might expect more pronounced differences between the two approaches when the alpha method is applied.

Yet the BRS results generated by the two techniques in supine position via the alpha coefficient method show only minor differences, especially when transfer function estimates are averaged over the relevant frequency range. [105]

Finally, due to a lack of BRS studies focusing on differences between AR and FFT approaches when the TF method is applied, due to a higher number of BRS studies employing the FFT approach, and given the built-in integration of the FFT package in Python, the nonparametric approach was chosen as the preferred method for the TF approach in this thesis.

Further information on the distinctions in a spectrum shape between these two methodologies (AR and FFT) is provided in Appendix C.

2.5.1 BRS visualization motivations

Understanding clinicians' and researchers' needs is crucial for analyzing and presenting biomarkers such as BRS. Some clinicians prioritize clear numeric representations, especially BRS magnitude (value), as important for differentiating health statuses from potential pathologies. [60] For this reason, the BRS value in the LF band seem more clinically relevant, particularly if BRS falls below 3ms/mmHg, while the BRS behavior in the HF band is currently considered optional for visualization due to limited research and clinical validity.[15]

Certain literature sources also observe and comment on BRS spectrum shape differences between healthy and pathological subjects, but this approach is not yet utilized diagnostically. Some examples are given in Fig. 2.13 and 2.14 below.

It must be noted that unlike in HRV and BPV studies, the importance of the spectrum's power in the LF and HF band of HRV and BPV is not critical for the BRS calculation, except in the case of the alpha coefficient method. [33]

In contrast, in the TF approach, the key focus lies on individual transfer gain points across frequencies within these bands. [56], [96] The objective is to evaluate the shape of TF across a spectrum of frequencies that envelop a relevant physiological region. In all cases it is crucial to acknowledge that TF spectral estimate is susceptible to errors and its uncertainty is particularly heightened in regions of low coherence. [96]

The BRS spectrum, in short, represents a spectrum of transfer gains (BRS points) across various frequencies, and it is not a power spectrum. Thus, the total spectral power in each frequency band is not calculated as a separate parameter.

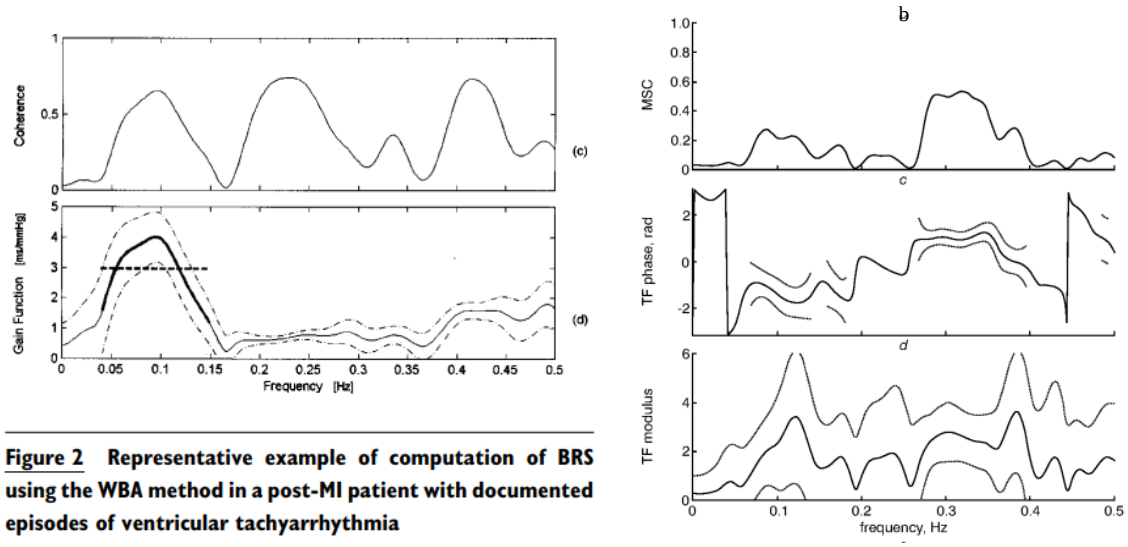

Figure 2 **Representative example of computation of BRS using the WBA method in a post-MI patient with documented episodes of ventricular tachyarrhythmia**

(a) (b)

Figure 2.13: TF: (a.c and b.c) coherence (or MSC) and (a.d and b.d) BRS spectrum as well as (b.c) phase spectrum of two subjects. Both subjects are categorized as POST-MI patients. MSC – magnitude squared coherence [95], [96]

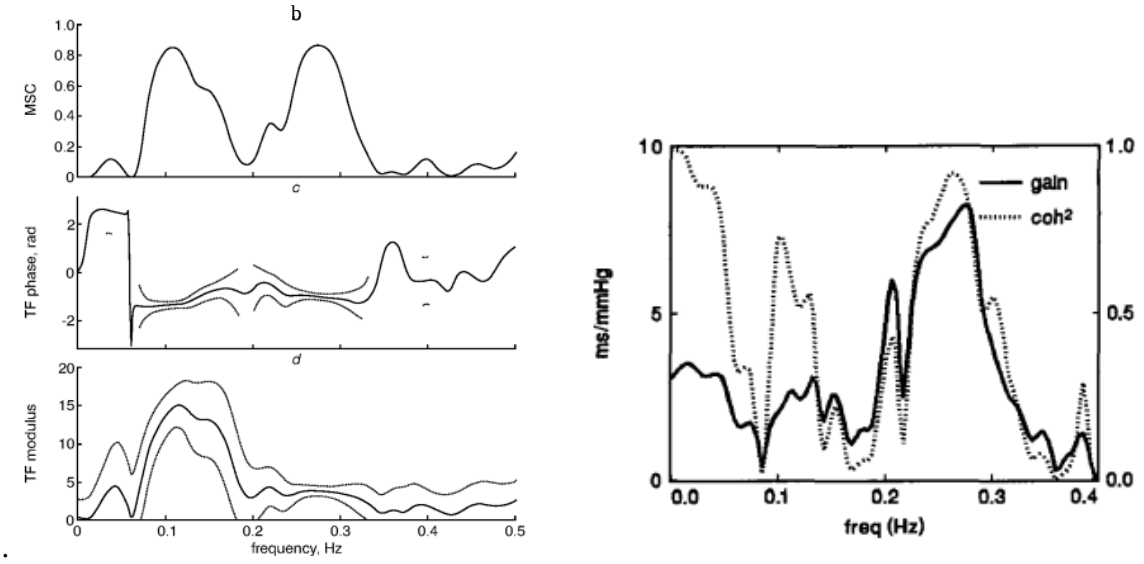

(a) (b)

Figure 2.14: TF: (a.b and b) coherence and (a.d and b) BRS spectrum and (a.c) phase spectrum of two healthy subjects; (b) subject is healthy 57-year-old woman. [96], [148]

As can be seen in Fig. 2.13, regarding interpretation, the POST-MI patient (b) in the LF band displays both low BRS gain and very low coherence in contrast to another POST-MI patient (a) who has low BRS but higher coherence.

Interestingly, as can be seen in Fig. 2.14, the healthy subject (a) has normal BRS with high coherence, while a healthy woman (b) - probably due to her age - has mainly higher coherence (> 0.5), but low BRS. Also, the shape of the phase spectrums between the healthy subject in Fig. 2.14(a) and POST- MI subject in Fig 2.13(b) – whose data display a more unstable phase – differs as well. The coherence and phase spectrums offer supplementary insights to BRS; hence they were also visualized beside the BRS spectrum in this thesis.

More recently, researchers studying the ANS would rather focus on real-time dynamics which go beyond traditional FFT-based methods [60]. Of late, non-stationary signal processing methods are increasingly recognized as more applicable for biomedical signals and are also recommended to be used even in the 'steady-state' conditions. [62], [63], [149] Therefore, visualizing BRS with an additional time dimension seems important to capture its changes over time. This approach is also recommended by literature sources since it has been shown that BRS behavior varies continuously during the day, in various body positions and in a range of activities as explained in Chapter 1.3. [33]

For this reason, the Short Time Fourier Transform (STFT) algorithm was also included in this thesis for its simplicity and ease of implementation compared to other time-frequency methods.

However, it must be noted that the STFT- based TF method has not been utilized in any BRS studies to date, making this thesis the first work known to do so.

Finally, Fig. 2.15 illustrates an example of BRS time-frequency visualizations conducted using the wavelet transform.

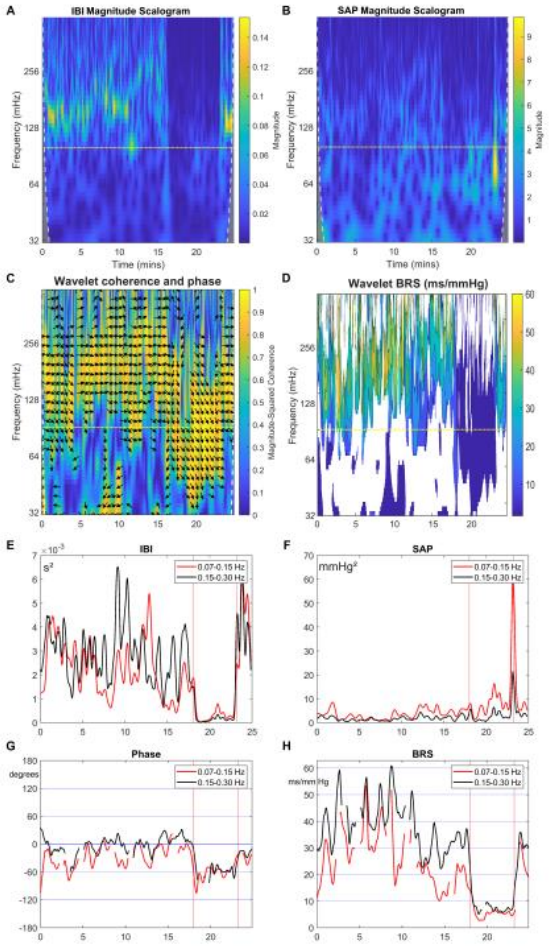

Figure 2.15**:** BRS behavior in a healthy individual across three experimental phases: supine, HUT, supine (red dashed lines indicate timings of different experimental stages) [60]

2.5.2 Computational background of FFT-based approaches

The computational background of FFT-based methods incorporated into this thesis is presented here.

2.5.2.1 Welch method

The Welch technique utilizes the FFT algorithm to estimate the power spectra of signals (static spectra). [150] Unlike the regular periodogram method, this approach segments the signal length into sections of varying sizes (segment or window size), applies a certain window shape to them (window type), allows overlap between adjacent segments (overlap percentage) and computes modified periodograms for these sections. Finally, it averages computed PSDs to generate a single mean PSD for the entire signal length. Consequently, the resulting PSD exhibits a smoother appearance due to the reduced non-stationarities in the shorter segment sizes compared to the whole signal length. This segmentation also proves advantageous when working with devices with limited storage, as it processes shorter signal sections. The parameters relevant for the Welch spectral analysis are:

- Segment size (FFT size)
- Window size (fixed length)
- Zero padding: it is applied if FFT size is longer than the window size
- Window type
- Overlap percentage between windows

2.5.2.2 Short-time Fourier Transform

The STFT method involves computing the PSDs of a signal over time. It achieves this objective by segmenting the signal into short segments (segment size), applying a window function (window type) to each segment, sliding this window by a specified number of data points (hop size), and repeating the process iteratively. Similar to the Welch method, the STFT method captures signal behavior over time and frequencies, storing the resulting PSDs as columns in a time-frequency matrix.

Unlike Welch, however, there is no averaging of PSDs, only preserving individual PSDs for each time instance.

Key parameters for STFT spectral analysis include:

- Segment size (FFT size)
- Window size (fixed length)
- Window type
- Overlap percentage between windows

However, an inherent challenge to STFT is the time-frequency resolution tradeoff, often called the ‘Heisenberg uncertainty principle’. [151], [152] This tradeoff dictates that, as the window size increases, frequency resolution improves at the expense of time resolution, and vice versa. Optimal solutions vary across applications, demanding a balance between time and frequency resolutions tailored to specific needs.

2.5.3 Coherence evaluation and visualization

To estimate coherence the threshold influence on BRS results, Jira et al. [29] applied various coherence estimation alternatives and concluded that they do not influence individual BRS values significantly. [28] However, in the pursuit of better understanding of the mechanisms and internal dynamics of the ANS, it seems reasonable to represent visually the coherence behavior between RRI and SBP signals, even if the coherence threshold is not integrated into the estimation of BRS values.

For example, while the main focus of this article was not on BRS, but rather on two other signals: diastolic pressure versus muscle sympathetic burst amplitude, the observed coherence behavior across time and frequency has provided significant additional insights into the dynamics of the ANS system (Fig. 2.16): "*Conversely, the subject on the right panel had weak coherence, not because his diastolic pressure and muscle sympathetic nerve activity were uncoordinated, but because his strong coherence came and went and shifted over a range of frequencies […] Thus, in resting humans, autonomic coordination is not qualitative, present or absent, significant or insignificant, or above or below squared coherence values of 0.50, but is quantitative and is based on the probability that strong coherence will persist over time at more or less constant frequencies."* [153]

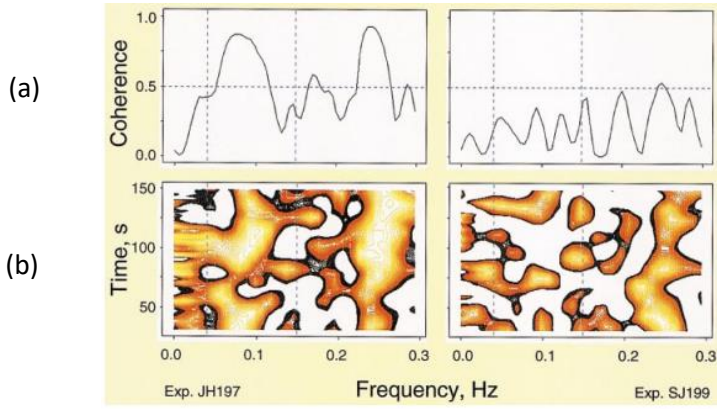

Figure 66: Greater and more consistent coherence over time and frequency observed in the subject on the left, compared to the subject on the right. (a) 2D visualization: Coherence behavior (y-axis) over frequency (x-axis); (b) 3D visualization: Coherence over time in seconds (y-axis) and frequency in Hz (x-axis); strength of the coherence is emphasized by colored shapes (z-axis). [153]

For this reason, coherence should be included as a separate parameter to potentially improve the understanding of ANS behavior.

2.5.4 Phase evaluation and visualization

Regarding phase interpretation, various scientists assume that a 'negative phase' points to an SBP signal leading RRI signal changes, indicating a baroreflex function. [15], [60], [72], [153] The phase could be visualized in the LF and the HF frequency band separately.

The literature also indicates that the LF band phase is more frequently negative overall. [15] However, it is important to note that this effect occurs primarily during 'steady-state' conditions. [60], [153]

In contrast, literature sources also note a more frequent change in signs of the phase in the HF band, suggesting that, in this frequency range, RRI may often precede SBP changes. [153] Additionally, there is a suggestion that this behavior of the HF band phase could also be an age-dependent phenomenon, with aging potentially leading to a more positive HF phase. [37]

Finally, Pitzalis et al. [154] proposed to include phase variations between RRI and SBP in both frequency bands since this approach might offer further insights into cardiovascular rhythm control. Given these considerations, it seems reasonable to explore and visualize the phase variations within both the HF and LF bands.

3 Practical part

3.1 Spectral analysis in Python: Step by step implementation

In the context of BRS computation, the spectral analysis is constituted by simultaneous spectral analysis of both RRI and SBP time series before BRS is computed. According to literature sources, both signals are first processed in the same way before the BRS calculation takes place, and they must be time-synchronized with each other. [49]

A short summary of steps included in the analysis performed within this thesis would highlight three phases:

(1) Data collection
(2) Data preprocessing
(3) Spectral analysis of RRI and SBP signals and BRS computation consisting of:
    a. Computation of PSDs of RRI and SBP separately
    b. Computation of CSD: coherence and phase between RRI and SBP
    c. TF computation: BRS values and BRS spectrum

3.1.1 Data collection and data characteristics

In the context of this thesis, CNSystems Medizintechnik GmbH supplied three representative patient datasets necessary for developing BRS visualizations. Notably, these datasets are valuable as they cover a spectrum of BRS values: high BRS from patient CU066, medium BRS from patient CU076, and low BRS from patient CU045.

Each dataset, provided in a distinct xls-file, consists of three informative columns. The first column records the temporal duration of measurements in seconds. The second column contains the mean values of RRI (ms), while the third column contains mean SBP values (mmHg). These measurements were taken during three experimental stages:

a. **Baseline values**: These were recorded while the subjects were resting and breathing spontaneously.
b. **Stress conditions**: Two of the datasets (CU045 and CU076) underwent mental stress induction through mental arithmetic, whereas another dataset (CU066) involved a cold pressor test, performed by putting a hand in ice water. The stress stage was intended to evoke increased sympathetic and diminished parasympathetic activity of the ANS, resulting in an expected increase in heart rate and SBP.
c. **Recovery period**: This phase encompassed deep breathing at a fixed rate of six breaths per minute (bpm) (at 0.1 Hz).

The patients were assessed while seated (sitting position for all three stages), with their hands resting comfortably on a table in front of them. Blood pressure was noninvasively measured using a CNAP finger sensor (CNAP® Monitor 500, CNSystems Medizintechnik GmbH, Graz, Austria), which was placed on the subject's right hand (index and middle fingers). Intervention markers were placed on each device to enable post-hoc synchronization of the data sets.

Considering the inherent physiological responses linked to each experimental stage, it was anticipated that there would not only be variations in RRI and SBP values but also consequential fluctuations in BRS values throughout the measurement process. However, this experimental protocol was not specifically designed to provoke significant BRS changes.

Additionally, while the device Task Force Monitor (TFM, CNSystems Medizintechnik GmbH, Graz, Austria) computed absolute BRS values using the sequence method exclusively during the baseline period (first experimental stage), these values served as a reference for the subsequent implementation of the spectral method. As per the data derived from TFM, the range of BRS values included a low of 3 ms/mmHg for CU045, a medium of 11.3 ms/mmHg for CU076, and the highest being 26.9 ms/mmHg for CU066.

Nevertheless, despite the low BRS value of 3 ms/mmHg potentially indicating a pathological condition, it is noteworthy that all three subjects were confirmed to be in good health. Moreover, it is essential to underline that other personal and clinical information of the patients (e.g. age, gender) was kept confidential to ensure anonymity.

Table 3.1 outlines the record length characteristics for each patient individually, while Table 3.2 offers time stamps (start and end) for each experimental stage in seconds.

Patient data	Record length (sec)	Record length (min)	Baseline period length (sec)	Stress period length (sec)	Recovery period length (sec)
CU045	818.39	13.64	301.77	182.07	300.68
CU076	814.42	13.57	299.89	180.43	300.32
CU066	822.81	13.71	299.53	181.80	304.04

Table 3.1**:** Record length characteristics for all patients (CU045, CU076, CU066) during each experimental stage: baseline, stress, recovery

Patient data	Time stamps for baseline period (sec)	Time stamps for stress period (sec)	Time stamps for recovery period (sec)
CU045	384.35 – 686.12	719.37 - 901.44	902.06 - 1202.74
CU076	454.36 – 754.25	787.45 - 967.88	968.46 - 1268.78
CU066	612.09 - 911.62	948.05 - 1129.85	1130.86 - 1434.9

Table 3.2**:** Time stamps (start - end) of each experimental stage for patients: CU045, CU076, CU066

3.1.2 Data preprocessing

Data preprocessing procedures diverge between the FFT and STFT approaches. The FFT approach requires stationary time series as input, unlike the STFT approach, where the stationarity is assumed in short segment lengths.

Hence, a brief outline of the preprocessing steps is presented in Fig. 3.1 with further elaboration provided below to explain each step in more detail.

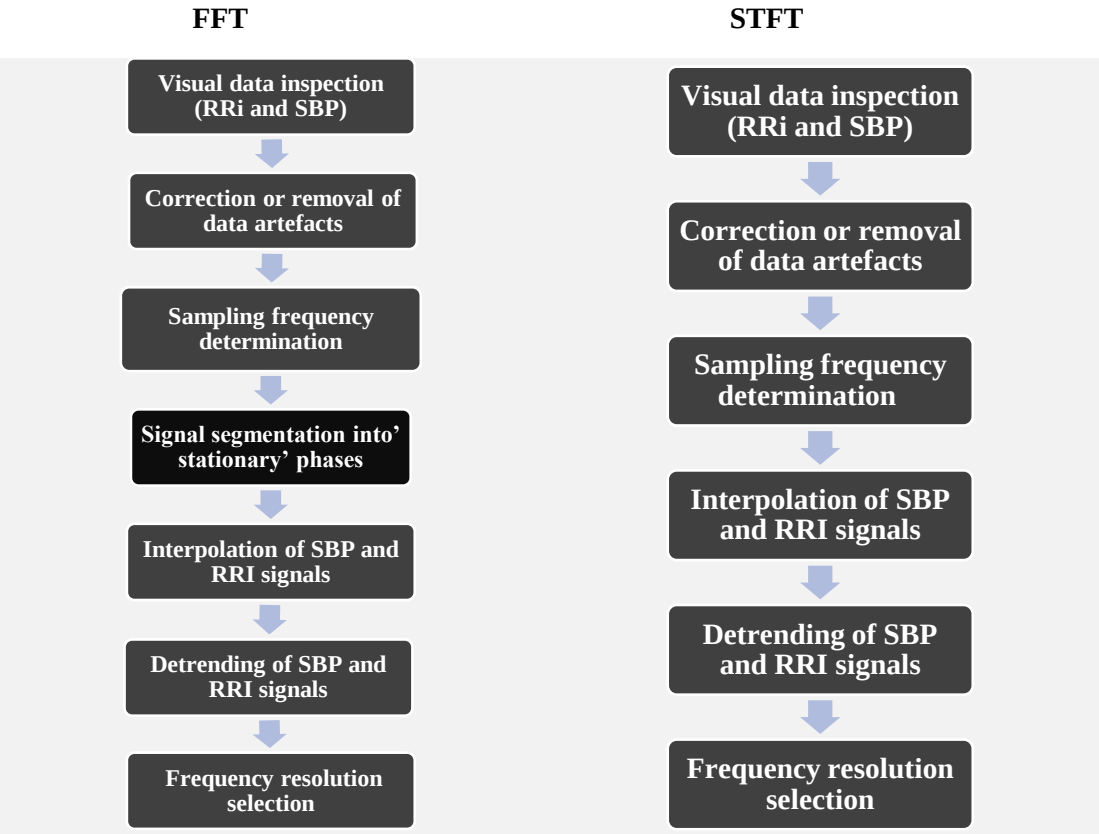

Figure 3.1: Data preprocessing steps for FFT versus STFT-based analysis

3.1.2.1 Visual data inspection

In most instances in the literature, a careful visual inspection of both RRI and SBP signals is deemed mandatory and was performed in this thesis. Particularly, the check of the RRI time series for irregular heartbeats or missing beats and other artefacts is essential. [149]

3.1.2.2 Correction or removal of data artifacts

Following a careful visual inspection, no editing was deemed necessary in this case.

3.1.2.2.1. Welch: Signal segmentation into 'stationary' phases

The notion and definition of 'stationarity' present a complex issue in the literature. [155] Fulfilling the requirement of record length stationarity for the FFT approach in physiological signals proves challenging, given the numerous unknown physiological states of uncertain origin embedded in each recording, applicable to both RRI and SBP signals. Therefore, as a practical compromise, it is assumed that stationarity is more likely to be approximated in shorter recordings than longer ones. [149]

In the literature on BRS, many studies assumed a stationary condition of signals preceding spectral analysis, especially when individuals maintained a consistent body posture for some time, thereby inferring signal stationarity. [156] In this context, stationarity in each 'steady-state' condition implies that the signal remains free from unexpected transient changes (e.g. subject movements) or artefacts (e.g. ectopic beats, missing beats, damping) that could have a significant impact on spectral analysis. [72], [149]

Therefore, the signals in this thesis were solely segmented into three assumed stationary phases: Baseline, Stress, Recovery - according to time stamps given previously.

3.1.2.3 Sampling frequency determination

Given the irregular sampling of the beat-to-beat RRI and SBP time series provided at a natural HR, and recognizing the FFT algorithm's reliance on uniformly spaced samples for reliable results, the necessity for equidistant resampling and interpolation of signals became apparent.

In general, the literature recommends interpolating and resampling data by using equal sampling rates before signal processing, mitigating potential biases in inter-individual and inter-task comparisons between different subjects. [157] This thesis adopted this approach, ensuring for signal interpolation a sufficiently high sampling frequency to prevent the aliasing effect. This approach safeguards that the Nyquist frequency, defining the spectrum's upper limit remains outside the relevant frequency range (0.04 – 0.4 Hz) for BRS spectral analysis.

Therefore, to identify the suitable uniform sampling frequency for all three datasets, the mean sample rate of individual signals was first determined for each subject separately by using (6) below.

$$\text{Mean sample rate} = \frac{\text{Maximum sample rate} + \text{Minimum sample rate}}{2} \tag{6}$$

The determination of a uniform sampling frequency for all subjects relied upon the selection of the time series for a subject with the highest mean sample rate, adhering to the condition that the sampling frequency should be at least twice the mean sample rate or even twice the maximum sample rate, to be on a safe side. Both of these conditions were fulfilled in this case.

Table 3.3 presents details regarding sample rate calculations for each subject, whereas Table 3.4 offers information on signal length after resampling.

Patient data	Maximum sample rate (sec)	Maximum sample rate (Hz)	Minimum sample rate (sec)	Mean sample rate (sec)	Mean sample rate (Hz)
CU045	0.53	1.887	0.73	0.655	1.527
CU076	0.5	2.000	0.8	0.79	1.266
CU066	0.68	1.470	1.31	0.995	1.005

Table 3.3**:** Mean sample rate computed for each subject: CU045, CU076, CU066

Consequently, the sampling frequency for spectral analysis was set at $f_s = 4$ Hz (with a sampling period T = 0.25 seconds).

Typically, a sampling frequency in the range of 2-5 Hz is also considered an appropriate choice for the HRV spectral estimates. [149]

Patient data	Sampling frequency (Hz)	Original signal length (samples)	Interpolated signal length (samples)
CU045	4	1234	3271
CU076	4	1138	3255
CU066	4	882	3289

Table 3.4**:** Comparison of original and interpolated whole signal lengths at sampling frequency of 4 Hz

3.1.2.4 Interpolation of SBP and RRI signals

Following the sampling frequency choice, both RRI and SBP signals commonly undergo different interpolation and detrending processes in the literature. The rationale for using

different interpolation methods in BRS studies was not further elaborated. However, Kuusela [149] reported that the choice of interpolation methods for RRI time series in HRV spectral analysis has no impact on the results. Therefore, in this thesis, linear interpolation was selected.

The function **'**Interpolation**'** was manually implemented.

This function takes as input a signal (RRI and SBP series), its corresponding time values and the desired sampling frequency (fs). It uses 'linear' interpolation (interp1d function from 'NumPy', but this could be changed to 'cubic spline' etc.) to estimate the signal values at regularly spaced intervals based on the given time values.

3.1.2.5 Detrending of SBP and RRI signals

Linear trends were removed following established literature practices (Appendix B). The **scipy.signal.detrend** function from the Python's package '**Scipy**' is used for detrending a signal, which involves removing trends or baseline variations from the data.

rri_interpolated_detrended = signal.detrend(data, axis=-1, type='linear', bp=0, overwrite_data=False)

Function 1: Detrending function

The most relevant parameters of the Function 1 selected for this thesis were:

data: The input signal or array: Interpolated RRI and SBP time series

Type = 'linear': Specifies the type of detrending to be applied. It can be 'linear' (default) or 'constant'. The 'linear' option removes a linear trend, while 'constant' removes only the mean.

3.1.2.6 Frequency resolution determination

In the context of investigating the BRS spectrum within the 0.04-0.4 Hz frequency band, employing the frequency resolution smaller than 0.04 Hz was selected as an appropriate choice for the FFT-based anaylsis.

In Python, three parameters play a critical role in defining both the frequency and 'actual' time resolution:

- FFT size or segment size (nfft)
- Window size (nperseg)
- Sampling frequency (fs)

The FFT algorithm performs most efficiently when the number of samples in the segment size used for the analysis is a power of 2. However, it is worth noting that this is not a strict requirement, especially when applying the STFT method.

The frequency resolution is computed by using (7) and depends on the number of samples in a given window or segment size. The window size or FFT size parameters should be set appropriately to attain the desired frequency resolution and the 'actual' time resolution at the same time.

$$f_{res} = \frac{f_s}{nfft} \text{ or } f_{res} = \frac{f_s}{nperseg} \quad (7)$$

$$t_{res\,(actual)} = \frac{nfft}{f_s} \text{ or } t_{res(actual)} = \frac{nperseg}{f_s} \quad (8)$$

Therefore, the 'actual' time resolution, as in (8), remains approximately equal to the chosen window size in seconds. [35]

3.1.2.6.1. 'Actual' vs 'Quasi' time resolution

However, in STFT applications, it is important to distinguish between 'actual' time resolution and 'quasi' time resolution, wherein the 'quasi' time resolution (t_{res}) is determined by using (9).

$$t_{res} = \frac{(nperseg - noverlap)}{f_s} \text{ or } t_{res} = \frac{\text{hop size}}{f_s} \quad (9)$$

Overall, the 'overlap' (noverlap) parameter dictates the number of points to overlap between windows and is determined by subtracting a chosen hop size from the fixed window size, as in (10), thus, it primarily depends on the chosen hop size.

$$noverlap = nperseg - \text{hop size} \quad (10)$$

The 'quasi' time resolution is primarily influenced by the selected hop size. Altering the 'overlap' parameter (noverlap) per se has no impact on the 'actual' time/frequency resolution tradeoff.

'Quasi' time resolution solely determines the number of BRS points computed for a specific frequency resolution by introducing a certain number of interpolated points. In general, more BRS values are computed when the hop size is smaller.

In summary, the number of computed BRS values when applying various hop-sizes remains unaffected by 'actual' chosen time-frequency resolutions.

3.1.2.6.2. Welch: Frequency resolution

The Table in Appendix B shows the most common frequency resolutions employed for RRI and SBP signals, namely 0.00781 Hz, 0.00195 Hz and 0.015 Hz, yet these studies lack explanations for that selection.

However, recent sources suggest Mayer waves, affecting RRI and SBP oscillations in the LF band in humans, could begin even around 0.03 Hz, implying a cycle duration of about 33.33 seconds.[158] Additionally, coherence calculations via the Welch method require at least three nonoverlapping segments, suggesting a desired frequency resolution close to 0.01 Hz (1/(3*33.33)) for the TF analysis. [159]

For this reason, in this thesis, frequency resolutions of 0.008 Hz (with zero padding) and 0.015 Hz (no zero padding) were applied for the BRS computation and visualization (Table 3.5), with window sizes and overlap parameters chosen as powers of two for efficient FFT processing.

Frequency resolution (Hz)	FFT size (samples)	Window size (samples)	Overlap (samples)	Zero padding performed
0.015	256	256	128	No
0.008	512	256	128	Yes

Table 3.5**:** Welch method - Parameter settings: FFT size, window size, overlap, zero padding

3.1.2.6.3. STFT: Time-frequency resolution tradeoff

There is a gap in BRS studies regarding the optimal tradeoff between the time and frequency resolution for STFT-based BRS estimation via the TF method. However, as discussed earlier, BRS is known for its frequency-dependent and quasi-periodic nature, presenting constant fluctuations in various conditions [33], [60]. Thus, the goal of time-dependent BRS estimation was to ensure a generation of an adequate number of BRS values (adjusting hop size parameter) without sacrificing RRI/SBP signal frequency resolution (adjusting window size parameter) in the LF band.

For instance, Martinmaki et al. [160] recommend that the segment length for spectral analysis of HRV should be at least five times the duration of the period of the slowest frequency being analyzed. Thus, to meet this guideline, a 125-second time window was chosen (5*1/0.04 Hz), resulting in a frequency resolution of 0.008 Hz for the LF band. On the other hand, the study by Eckberg et al. [33], employed a frequency resolution of 0.033 Hz for their BRS calculations in the LF band with a hop size of 2 seconds; they did not rely on HRV guidelines.

For this reason, the thesis evaluated four different frequency resolutions (0.008 Hz, 0.011 Hz, 0.17 Hz and 0.33 Hz) with diverse ‘quasi’ time resolutions (hop sizes) to examine and compare both visual and estimated BRS results in the LF band. (Table 3.6)

Frequency resolution (Hz)	Actual time resolution (sec)	Window size (samples)	Hop sizes tested (sec)	Zero padding performed
0.008	125	600	2/5/15/30/60	No
0.011	90	360	2/5/15/30	No
0.017	60	240	2/5/15/30	No
0.033	30	120	2	No

Table 3.6**:** STFT method - Parameter settings: window size, hop size, overlap, zero padding

3.1.2.6.4. Window type selection

Another parameter that can be easily adjusted in Python, although one that does not have a direct impact on frequency or time resolution, is window type.

According to literature sources (see Appendix B) the Hanning window (‘hann’), used with a 50% overlap, is frequently chosen in studies that employ the Welch algorithm. Thus, this preference was also followed in the thesis.

In the context of the STFT, despite literature emphasizing that changing window types for HRV spectral analysis yields little to no difference in spectral estimates, various window types were still employed in this thesis, specifically Hanning, Hamming, Triangular, Blackman and Parzen windows. [149] This approach was taken to test if different window types made an impact on generated BRS values in the LF band.

3.1.3 Computing PSD of RRI and SBP

3.1.3.1 Welch

For this purpose, the Python function '**signal.welch'** from the package '**Scipy**' was used to estimate the PSD in ms²/Hz for RRI and in mmHg²/Hz for SBP using the Welch method already incorporated.

f, Pxx = scipy.signal.welch(input signal,
fs=4, **window='hann', nperseg=128, noverlap=256, nfft=512**, detrend='False', return_onesided=True, scaling='density', axis=-1, average='mean')

Function 2: Welch PSD computation

Function 2 returns an array of sample frequencies (f) and PSD of the input signal (Pxx).

This function processes an input signal - measurements of a time series such as the interpolated signal of RRI and SBP with real values. The function requires additional parameters such as the sampling frequency of the signal (fs), the type of window applied to the signal (window), the window size (nperseg), and the number of points (samples) to overlap between adjacent windows (noverlap).

Optional input parameters include the FFT length (nfft), which should be specified when the FFT size is different from the window size. This parameter is applied when the zero padding for each data segment is preferred.

In this context, default values were retained for the list of following parameters:

- **window = 'hann':** As per literature suggestions (see Appendix B)
- **return_onesided**: As the input data is real-valued, the resulting spectrum is presented in a one-sided manner, excluding negative frequencies.
- **scaling = 'density':** The PSD is calculated and the results of Pxx are scaled to unit²/Hz.
- **average = 'mean'**: The parameter selects which method to use to average the periodograms. The alternative option is 'median'.

The following parameters – nperseg (window size), noverlap (overlap), nfft (FFT size) - were set according to Table 3.6.

3.1.3.2 STFT

For this purpose, the Python function '**signal.stft'** from the package '**Scipy**' was first applied to estimate the STFT coefficients, time and frequencies for RRI and SBP signals.

f, t, Zxx = signal.stft (input_signal), **fs=4, window= window_type, nperseg = window_size, noverlap = overlap_percentage, nfft = FFT_size**,
detrend=False, return_onesided=True, boundary='zeros', padded=True, axis=-1, scaling='spectrum')

Function 3: STFT computation

Function 3 returns:

Zxx: STFT of the input signal (RRI and SBP). The function returns a matrix containing complex values that represent STFT coefficients.

f: An array representing sample frequencies

t: An array representing segment times

Afterward, the PSDs of both signals were calculated by multiplying STFT coefficients of one signal with conjugated STFT of the same signal, as in (11).

$$\mathrm{psd}_{\mathrm{rri}} = \mathrm{np.multiply}\left(\mathrm{rri}_{\mathrm{stft}}, \mathrm{np.conj}\left(\mathrm{rri}_{\mathrm{stft}}\right)\right) \quad (11)$$

3.1.4 Computing CSD between SBP and RRI

3.1.4.1 Welch

For this purpose, the Python function '**signal.csd'** from the package '**Scipy**' was used to estimate the CSD in ms*mmHg/Hz using the Welch method already incorporated.

f, Pxy =
scipy.signal.csd(sbp_signal, rri_signal, fs=4.0, window='hann', nperseg=256, noverlap=128, nfft=512**,** detrend=False', return_onesided=True, scaling='density', axis=-1, average='mean')

Function 4: Welch CSD computation

Function 4 returns:

- **f:** An array of sample frequencies
- **Pxy**: A CSD of input signals RRI and SBP

All parameters mirror those described in the **scipy.signal.welch** function, maintaining identical settings. The sole distinction lies in this function's ability to handle two input signals, RRI and SBP.

3.1.4.2 STFT

The CSD between both signals was calculated by multiplying STFT coefficients of SBP signal with conjugated STFT of the RRI signal, as in (12).

$$\mathrm{csd}_{\mathrm{sbp,rri}} = \mathrm{np.multiply}\left(\mathrm{sbp}_{\mathrm{stft}}, \mathrm{np.conj}\left(\mathrm{rri}_{\mathrm{stft}}\right)\right) \quad (12)$$

3.1.5 Coherence computation

3.1.5.1 Welch

For this purpose, the Python function '**scipy.signal.coherence'** from the package '**Scipy**' was used to estimate the coherence (range 0 - 1) using the Welch method already incorporated.

f, Cxy =
scipy.signal.coherence(sbp_signal**,** rri_signal, fs=4, window='hann', nperseg=256, noverlap= 128, nfft=512, detrend=False, axis=-1)

Function 5: Welch coherence computation

Function 5 returns:

- **f:** An array of sample frequencies
- **Cxy**: A magnitude squared coherence of input signals RRI and SBP

All parameters mirror those described in the **scipy.signal.csd** function, maintaining identical settings.

3.1.5.2 STFT

The magnitude squared coherence involved dividing the squared cross-spectrum of RRI and SBP by the product of the individual auto-spectrums, as in (13). [60], [153]

$$\mathrm{coh}_{\mathrm{stft}} = \mathrm{abs}(\mathrm{csd}_{\mathrm{sbp,rri}}) ** 2/\mathrm{abs}(\mathrm{np.multiply}(\mathrm{psd}_{\mathrm{sbp}}, \mathrm{psd}_{\mathrm{rri}}) \quad (13)$$

3.1.6 Phase computation

The phase angle was computed as the angle from the complex valued cross-spectrum between SBP and RRI for both STFT and Welch methods (Function 6). [153]

Phase = numpy.angle(CSD(sbp,rri), deg = True)

Function 6: Phase computation

Function 6 returns angle in degrees in the range -180° and +180°.

3.1.7 Transfer function computation

The BRS gain (modulus) at each frequency point was computed as in (14). [60]

$$\text{BRS gain(magnitude)} = \frac{\mathrm{abs}(\mathrm{csd}_{\mathrm{sbp,rri}})}{\mathrm{abs}(\mathrm{psd}_{\mathrm{sbp}})} \quad (14)$$

3.1.8 BRS value estimation and visualization

3.1.8.1 Welch

The BRS value was estimated only in the LF band by using (15).

$$\text{BRS value} = \text{mean}\ (\Sigma\ \text{BRS gains [LF band frequency indices]}) \quad (15)$$

The coherence threshold could be adjusted if necessary but was set at 0.5 in this case. Finally, the BRS value in the LF band was visualized with and without taking the coherence criterion into consideration. (see Chapter 3.3.3.3)

3.1.8.2 STFT

The BRS values for each time instance were estimated only in the LF band according to (15) as well. However, the coherence threshold was not included in the determination of BRS values. (see Chapter 3.4.3.2)

3.2 BRS visualization alternatives

This section delineates the BRS visualization alternatives, individually for both the Welch and STFT-based approaches. Generally, BRS visualizations should include the BRS spectrum, coherence, phase and BRS values in the LF band.

3.2.1 Welch method: 2D and 3D visualizations

BRS spectrum:

- **2D plot: BRS spectrum with coherence spectrum:** The BRS spectrum (0.04 – 0.4 Hz) accompanied with the coherence spectrum was plotted and the transfer gain points for all three experimental stages (Baseline, Stress, Recovery) were included and marked separately on the spectrum.
- **3D line plot**: The BRS spectrum (0.04 – 0.4 Hz) for each experimental stage was plotted separately, but all stages were plotted together in one 3D line plot with marked transfer gain points included in the analysis.

Phase spectrum:

- **2D plot: Phase spectrum with coherence spectrum:** The phase spectrum over frequency (0.04-0.4 Hz) accompanied with the coherence spectrum was plotted.

BRS values:

- **2D plot**: Single BRS value in the LF band per experimental stage was visualized including and excluding the coherence criterion for BRS computation.

3.2.2 STFT: 2D and 3D visualizations

BRS spectrum:

The LH and HF bands (0.04-0.4 Hz) were plotted together, excluding a coherence threshold application:

- **3D contour plot:** Original (non-normalized) BRS Spectrogram
- **3D surface plot and 3D contour plot:** Normalized BRS spectrogram

Normalized BRS spectrogram (discussed in Chapter 3.4.2), was introduced to address BRS visualization challenges connected to the non-normalized spectrogram. To solve this, the normalization was implemented, which incorporates defined BRS ranges outlined in Chapter 1.4 from the study done by Suarez-Roca et al. [44]

This normalization technique facilitated improved visual comparisons of BRS gains over time and frequencies. Consequently, the color bar was segmented to depict distinct ranges: severe dysfunctional BRS (0-3 ms/mmHg), moderate dysfunctional BRS (3-6 ms/mmHg), and normal BRS (above 6 ms/mmHg). Additional color-segments were also introduced above 6 ms/mmHg to better visualize BRS variations above this value.

Phase spectrum:

- **3D contour plot:** Phase spectrogram (0.04-0.4 Hz) excluding coherence application
- **3D contour plot:** Phase spectrogram (0.04-0.4 Hz), while keeping only regions portraying the negative phase since the baroreflex function is more connected to negative phase angles in the LF band (see Chapter 2.5.4)

BRS values:

- **2D plot**: Mean BRS values in the LF band were visualized over time. This plot encompasses the entire BRS behavior across all three experimental stages, including the brief pauses between stages. The objective was to observe the continuous evolution of the BRS index throughout the entire signal duration.

Finally, the coherence spectrogram could not be visualized due to issues addressed in Chapter 3.4.3.2.

3.3 Results

Results were divided into few sections:

- **Data collection**
  - Original SBP and RRI signals (see Appendix D)
  - Preprocessed SBP and RRI signals (see Appendix E)
  - STFT: Time-Frequency resolution tradeoff (see Chapter 3.3.1)
  - STFT: Window type effect on BRS values (see Chapter 3.3.2)
- **Spectral analysis:**
  - Welch: PSD of RRI/SBP – 2D visualization (see Appendix F)
  - Welch: Coherence, phase, BRS spectrum and BRS values with different frequency resolutions (see Chapter 3.3.3)
  - STFT: PSD of RRI/SBP – 3D visualizations (see Appendix G)
  - STFT: BRS spectrogram, phase spectrograms and BRS values with different quasi time (overlaps) and frequency resolutions (see Chapters 3.3.4)
- **Results comparison** between Welch, STFT-based and sequence methods (see Chapter 3.3.5)

3.3.1 STFT: Time-Frequency resolution tradeoff

In an attempt to identify a suitable tradeoff between 'actual' time and frequency resolutions tables 3.7 - 3.9 were created to present variations in BRS values (mean ± SD) and their relative standard deviation (RSD) in the LF band under different tradeoff settings. Different hop sizes were also tested while kept fixed for different frequency resolutions in each table section for purposes of easier comparison.

The Hanning window type was kept fixed as well. Tested frequency resolutions and hop sizes were taken from Table 3.6.

Frequency resolution (Hz)	Hop size (sec)	BRS values per stage (Baseline: : Stress: Recovery)	Baseline BRS Mean ± SD	Baseline BRS RSD (%)	Stress BRS Mean ± SD	Stress BRS RSD (%)	Recovery BRS Mean ± SD	Recovery RSD (%)
0.008	60	6:3:6	11.49±1.83	15.89	12.31±1.60	13.03	17.3 ± 5.20	29.98
0.008	30	11:6:11	12.15±2.19	18.05	13.82±2.58	18.65	17.35±5.22	30.08
0.011	30	11:6:11	12.68±2.32	18.28	12.69±3.39	26.73	16.75±4.54	27.11
0.017	30	11:6:11	13.16±3.07	23.35	12.53±5.27	42.13	16.59±6.33	38.18
0.008	15	21:12:21	12.21±1.94	15.88	13.40±2.53	18.91	17.02±4.76	27.95
0.011	15	21:12:21	12.34±2.06	16.71	11.93±3.09	25.91	15.94±4.19	26.30
0.017	15	21:12:21	10.50±1.21	11.52	12.08±4.37	36.16	20.11±14.36	71.38
0.033	15	21:12:21	13.17±3.42	26.00	12.02±5.18	43.12	16.80±3.86	22.96
0.008	5	61:36:61	12.56±2.34	18.60	12.94±2.70	12.01	17.88±7.88	20.88
0.011	5	61:36:61	12.82±3.28	25.61	11.97±3.67	30.63	16.06±4.10	25.50
0.017	5	61:36:61	12.96±2.76	21.30	12.01±3.73	31.04	18.72±9.24	49.35
0.033	5	61:36:61	13.65±6.93	50.77	11.88±7.24	60.92	18.18±3.51	19.30
0.008	2	151:90:150	12.64±2.52	19.91	12.97±2.69	11.96	17.81±7.30	20.77
0.011	2	151:90:150	12.96±4.05	31.27	12.15±4.42	36.36	16.11±4.17	25.88
0.017	2	151:90:150	13.12±3.38	25.79	12.18±4.22	34.66	19.05±14.91	78.30
0.033	2	151:90:150	13.24±5.78	43.67	11.56±6.35	54.94	18.08±3.48	19.27

Table 3.7: Subject CU076: Impact of different frequency resolutions and equal hop sizes on BRS values in the LF band

Frequency resolution (Hz)	Hop size (sec)	BRS values per stage (Baseline: : Stress: Recovery)	Baseline BRS Mean± SD	Baseline BRS RSD (%)	Stress BRS Mean±SD	Stress BRS RSD (%)	Recovery BRS Mean±SD	Recovery RSD (%)
0.008	60	6:3:6	4.49±1.32	29.30	3.39±0.26	7.58	4.46±0.76	17.15
0.008	30	11:6:11	4.49±1.19	26.50	3.68±0.54	14.63	4.42±0.75	16.92
0.011	30	11:6:11	4.70±1.25	26.67	3.80±0.60	15.96	4.78±1.36	28.54
0.017	30	11:6:11	5.15±1.63	31.76	3.44±0.74	21.68	4.52±2.96	65.59
0.008	15	21:12:21	4.60±1.39	30.30	3.51±0.51	14.51	4.65±0.76	16.44
0.011	15	21:12:21	4.79±1.22	25.49	3.55±0.56	15.82	5.00±1.27	25.48
0.017	15	21:12:21	4.83±1.46	30.21	3.39±0.65	19.26	4.80±2.18	45.34
0.033	15	21:12:21	4.84±1.68	34.80	3.73±1.15	30.80	4.25±1.20	28.30
0.008	5	61:36:61	4.72±1.73	36.72	3.63±0.68	18.79	4.70±0.88	18.79
0.011	5	61:36:61	4.82±1.43	29.72	3.48±0.56	16.23	4.92±1.13	22.93
0.017	5	61:36:61	4.81±1.27	26.39	3.41±0.59	17.23	4.86±1.61	33.17
0.033	5	61:36:61	4.95±2.09	42.35	3.54±1.22	34.34	4.13±0.92	22.20
0.008	2	151:90:150	4.70±1.64	34.85	3.57±0.57	15.92	4.80±1.47	30.56
0.011	2	151:90:150	4.81±1.43	29.73	3.52±0.68	19.40	4.94±1.12	22.59
0.017	2	151:90:150	4.81±1.27	26.39	3.41±0.59	17.23	4.86±1.61	33.17
0.033	2	151:90:150	5.01 ±2.43	48.55	3.38±0.96	28.59	4.21±1.15	27.32

Table 3.8: Subject CU045: Impact of different frequency resolutions and equal hop sizes on BRS values in the LF band

Frequency resolution (Hz)	Hop size (sec)	BRS values per stage (Baseline: : Stress: Recovery)	Baseline BRS Mean ± SD	Baseline BRS RSD (%)	Stress BRS Mean ± SD	Stress BRS RSD (%)	Recovery BRS Mean ± SD	Recovery RSD (%)
0.008	60	6:3:6	42.46±7.44	17.52	37.68±9.83	26.10	30.19±2.10	6.95
0.008	30	11:6:11	49.71±19.32	38.87	37.30±7.26	19.48	28.95±2.09	7.22
0.011	30	11:6:11	45.22±14.88	32.90	42.51±11.95	28.11	30.94±4.50	14.56
0.017	30	11:6:11	45.19±14.56	32.22	36.11± 8.42	23.32	31.25±5.65	18.07
0.008	15	21:12:21	45.66±15.43	33.80	37.45±7.02	18.75	29.39±2.28	7.75
0.011	15	21:12:21	47.83±23.64	49.42	38.96±13.00	33.36	33.44±12.98	38.81
0.017	15	21:12:21	50.93±28.32	55.60	34.27±7.48	21.81	31.41±4.13	13.15
0.033	15	21:12:21	39.96±20.46	51.20	29.66±8.67	29.21	33.01±3.45	10.45
0.008	5	61:36:61	44.64±12.64	28.32	39.55±10.42	26.35	31.19±12.24	39.25
0.011	5	61:36:61	45.58±17.76	38.97	37.87±10.55	27.87	31.88±8.66	27.15
0.017	5	61:36:61	51.55±27.71	53.76	36.71±13.79	37.57	33.32±8.41	25.25
0.033	5	61:36:61	39.76±16.46	41.40	34.01±15.43	45.38	32.82±3.13	9.52
0.008	2	151:91:152	44.77±13.54	30.24	39.65±10.99	27.71	29.92±4.17	13.93
0.011	2	151:91:152	49.38±50.91	103.09	37.83±10.93	28.89	31.39±5.91	18.83
0.017	2	151:91:152	51.16±27.98	54.68	37.08±15.68	42.29	33.06±7.12	21.53
0.033	2	151:91:152	40.58±18.10	44.61	34.11±17.32	50.78	32.96±3.46	10.48

Table 3.9: Subject CU066: Impact of different frequency resolutions and equal hop sizes on BRS values in the LF band

3.3.2 Window type effect on BRS values

Table 3.10 was generated to offer more detailed insights on the impact of various window types on mean BRS values in the LF band across each experimental stage of the subject CU066. The BRS results (mean ± SD, as well as RSD) were computed for various frequency resolutions and hop sizes. Another table with results for the subject CU045 can be found in Appendix I.

Window type	Frequency resolution (Hz)	Quasi time resolution (sec)	Baseline BRS (ms/mmHg) Mean ± SD	Baseline BRS RSD (%)	Stress BRS (ms/mmHg) Mean ± SD	Stress BRS RSD (%)	Recovery BRS (ms/mmHg) Mean ± SD	Recovery BRS RSD (%)
Hanning	0.008	60	42.46±7.44	17.52	37.68±9.83	26.08	30.19±2.10	6.95
Hamming	0.008	60	40.15±5.29	13.17	37.19±8.53	22.94	30.68 ±2.91	9.48
Triangular	0.008	60	39.04±5.84	14.95	43.37±15.53	35.80	31.06±2.46	7.92
Blackman	0.008	60	48.19±22.07	45.80	36.16±7.61	21.04	30.25±2.32	7.67
Parzen	0.008	60	49.48±36.39	73.54	37.42±16.62	44.41	32.06±5.52	17.22
Hanning	0.008	30	46.61±18.31	39.28	39.53±8.36	21.15	30.36±2.63	8.66
Hamming	0.008	30	45.05±14.08	31.25	38.51±7.01	18.20	29.56±2.58	8.73
Triangular	0.008	30	45.44±13.98	30.77	40.29±11.41	28.32	29.99±2.20	7.34
Blackman	0.008	30	50.61±22.54	44.54	37.76±6.59	17.45	29.38±2.12	7.22
Parzen	0.008	30	46.61±18.31	39.28	39.53±8.36	21.15	30.36±2.63	8.66
Hanning	0.011	30	45.22±14.88	32.90	42.51±11.95	28.11	30.94±4.50	14.54
Hamming	0.011	30	44.53±11.89	26.70	49.20±27.42	55.73	30.41±3.45	11.34
Triangular	0.011	30	52.81±32.58	61.69	39.38±4.81	12.21	31.02±4.43	14.28
Blackman	0.011	30	45.55±18.35	40.28	38.31±4.28	11.17	35.80±18.00	50.28
Parzen	0.011	30	42.94±12.53	29.18	38.33±6.26	16.33	31.60±6.66	21.44
Hanning	0.008	15	45.66±15.43	33.79	37.45± 7.02	18.74	29.39±2.28	7.76
Hamming	0.008	15	43.34±11.47	26.46	38.08±6.77	17.78	29.79±2.38	7.99
Triangular	0.008	15	43.00±11.34	26.37	44.16±21.76	49.27	30.47±4.07	13.36
Blackman	0.008	15	46.34±18.25	39.38	38.88±8.88	22.84	30.94±5.78	18.68
Parzen	0.008	15	44.72±15.80	35.33	38.43±9.78	25.45	30.96±4.76	15.37
Hanning	0.011	15	47.83±23.64	49.42	38.96±13.00	33.37	33.44±12.98	38.82
Hamming	0.011	15	47.15±20.85	44.22	42.27±21.67	51.27	33.44±12.56	37.56
Triangular	0.011	15	48.56±25.68	52.88	37.23±8.03	21.57	30.69±4.19	13.65
Blackman	0.011	15	55.27±48.34	87.46	35.33±8.22	23.27	33.15±13.44	40.54
Parzen	0.011	15	48.64±26.52	54.52	35.10±8.36	23.82	31.09±5.12	16.47
Hanning	0.008	5	44.64±12.64	28.31	39.55± 10.42	26.35	31.19±12.24	39.24
Hamming	0.008	5	42.56±10.54	24.77	40.47 ± 11.91	29.43	33.00±22.54	68.30
Triangular	0.008	5	43.80±12.83	29.29	39.59±14.05	35.49	30.48±3.59	11.78
Blackman	0.008	5	45.02±14.84	32.96	39.76±10.96	27.56	30.41±4.59	15.09
Parzen	0.008	5	44.85±16.04	35.76	37.95±8.94	23.56	30.92±4.37	14.14

Hanning	0.011	5	45.58±17.76	38.96	37.87±10.55	27.86	31.88± 8.66	27.16
Hamming	0.011	5	47.60±23.45	49.26	39.11±14.60	37.33	32.21±9.26	28.75
Triangular	0.011	5	47.21±20.55	43.53	37.28±8.38	22.48	30.72±3.98	12.96
Blackman	0.011	5	48.78±31.23	64.02	38.12±18.20	47.74	34.91±19.72	56.49
Parzen	0.011	5	47.10±21.58	45.81	38.37±18.28	47.64	32.10±5.65	17.60

Table 3.10: Effect of various window sizes on mean BRS values in the LF band per stage of subject CU066

3.3.3 Welch method: 2D and 3D visualizations

This section illustrates appearance of the 2D and 3D BRS visualizations by the Welch method.

3.3.3.1 2D: BRS, phase, coherence spectrum

Fig. 3.2 is an example of a 2D visualization which depicts BRS, coherence and phase spectra of subject CU045 (low BRS) across experimental stages.

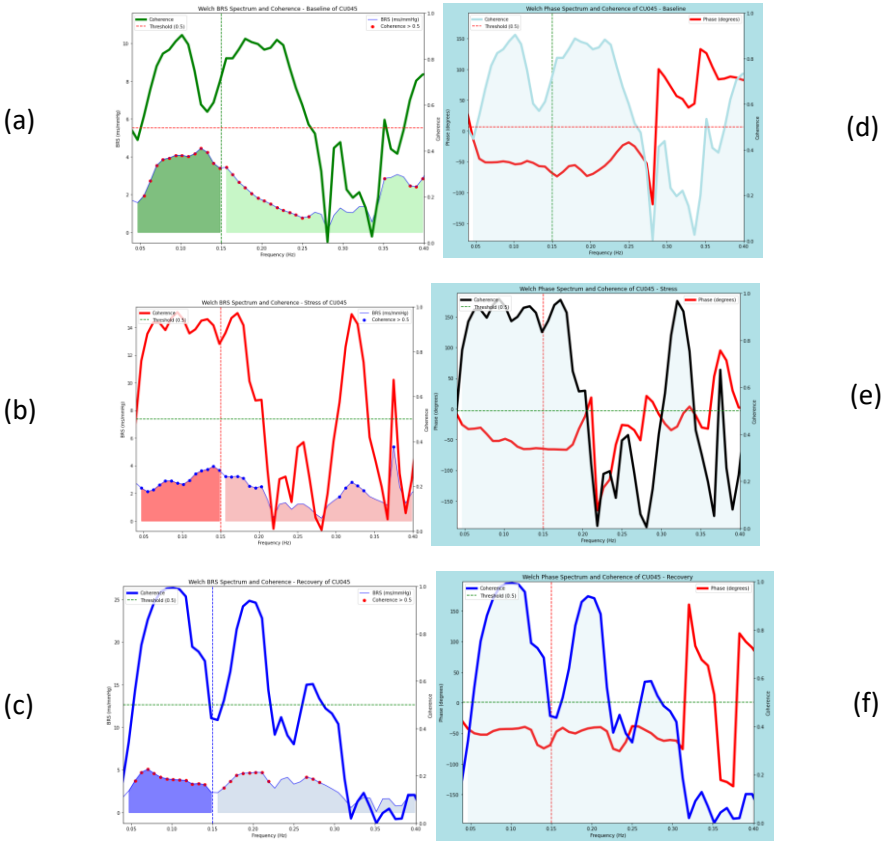

Figure 3.2: (a,b,c) BRS and coherence inc. (d,e,f) phase spectrums of subject CU045 for three different experimental stages: baseline (a, d), stress (b, e), recovery (c, f). Frequency resolution is set to 0.008 Hz; the x-axis represents frequency in Hz, y-axis indicates BRS gains in ms/mmHg or phase in degrees (red line); the mirrored y-axis represents coherence values between 0 and 1, with the dashed horizontal line indicating the applied coherence threshold (0.5). Colored circles on each BRS spectrum highlight transfer gains included in BRS value computation, as they exceeded the coherence threshold

Fig. 3.3 portrays differences in coherence and BRS gains between three subjects during the baseline stage, while Fig. 3.4 portrays the differences in phase during the recovery stage.

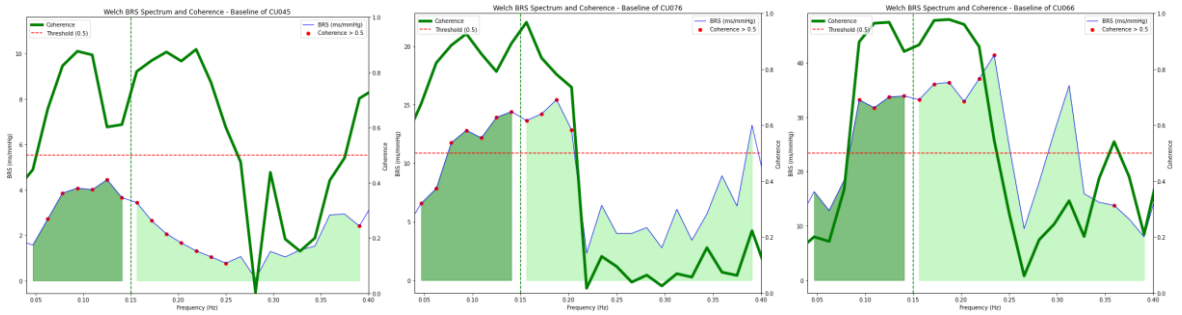

(a) (b) (c)

Figure 3.3: 2D: BRS (inc. red dots) and coherence spectra (green lines) via the Welch method during the baseline stage of subjects (a) CU045, (b) CU076, (c) CU066; fres = 0.015 Hz

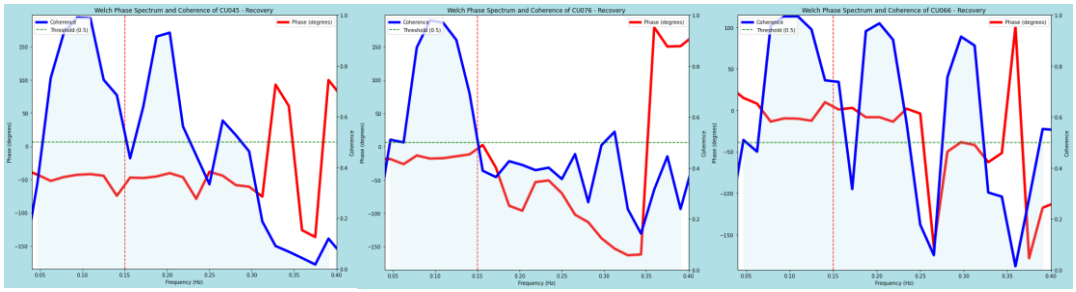

(a) (b) (c)

Figure 3.4: 2D: Phase (red lines) and coherence spectrums (blue lines) during the recovery stage (paced breathing at 0.1 Hz) via the Welch method of subjects: (a) CU045, (b) CU076, (c) CU066; fres = 0.015 Hz

3.3.3.2 3D: BRS spectrum

Fig. 3.5 portrays examples of 3D line plot visualizations by the Welch method for three subjects.

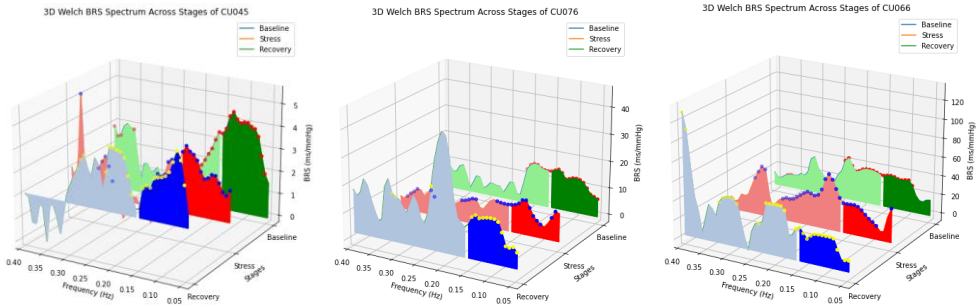

(a) (b) (c)

Figure 3.5: 3D: BRS spectra via the Welch method of subjects: (a) CU045, (b) CU076, (c) CU066. Frequency resolution set to 0.008 Hz; the x-axis represents three experimental stages, the y-axis represents frequency in Hz, and the z-axis represents BRS gains in ms/mmHg

3.3.3.3 2D: BRS values

In Fig. 3.6, BRS values in the LF band were visualized for each experimental stage with (red) and without (blue) taking into consideration the coherence threshold (> 0.5).

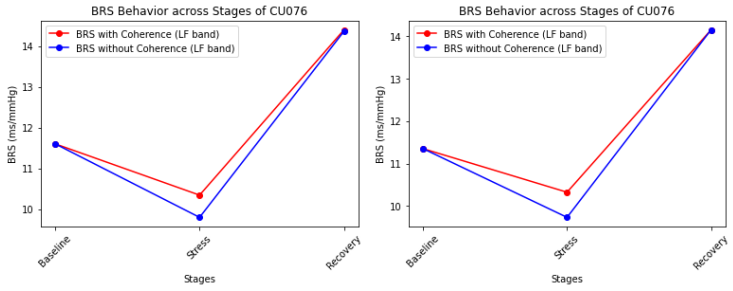

(a) (b)

Figure 3.6**:** BRS values in the LF band per experimental stage computed by the Welch method for subject CU076. Computations with (a) zero padding and (b) without zero padding. Frequency resolutions set: (a) 0.008 Hz, (b) 0.015 Hz

3.3.4 STFT: 3D visualizations

This section illustrates appearance of the STFT-based 3D BRS visualizations.

Fig. 3.7 depicts non-normalized BRS spectrogram of the subject CU076 (medium BRS).

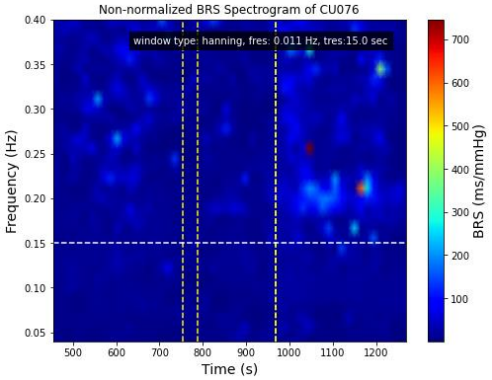

Figure 3.7: Non-normalized BRS spectrogram of subject CU076; frequency resolution of 0.011 Hz and quasi time resolution of 15 seconds; the x-axis denotes time in seconds, the y-axis represents frequency in Hz, the color bar indicates ranges of transfer function gains (BRS gains in ms/mmHg); dashed vertical lines denote transitions between experimental stages (order: baseline starts at the beginning of the plot, short adaptive period, stress, recovery), while the dashed horizontal line signifies the boundary between the LF and HF band; spectral parameter settings are detailed in the upper right corner

3.3.4.1 Normalized BRS 3D Surface plot

Fig. 3.8 depicts an alternative visualization of the BRS spectrum – a normalized 3D surface plot - of subject CU076.

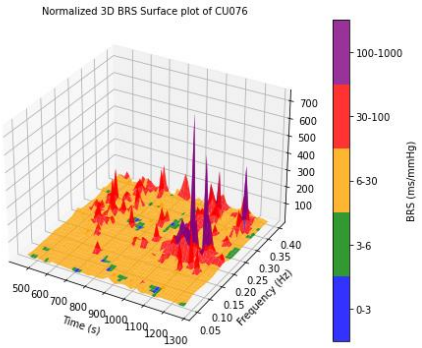

Figure 3.8**:** Normalized BRS 3D surface plot of subject CU076 with frequency resolution of 0.011 Hz and quasi time resolution of 15 seconds.; the x-axis denotes time in seconds, the y-axis represents frequency in Hz, the color bar indicates the transfer function gains ranges (BRS gains in ms/mmHg) calculated at various time points and frequencies

3.3.4.2 Normalized BRS Spectrogram

Fig. 3.9 depicts normalized BRS spectrograms (contour plots) of the subject CU076 with different frequency resolutions taken from Table 3.6 (Chapter 3.1.2.6.3).

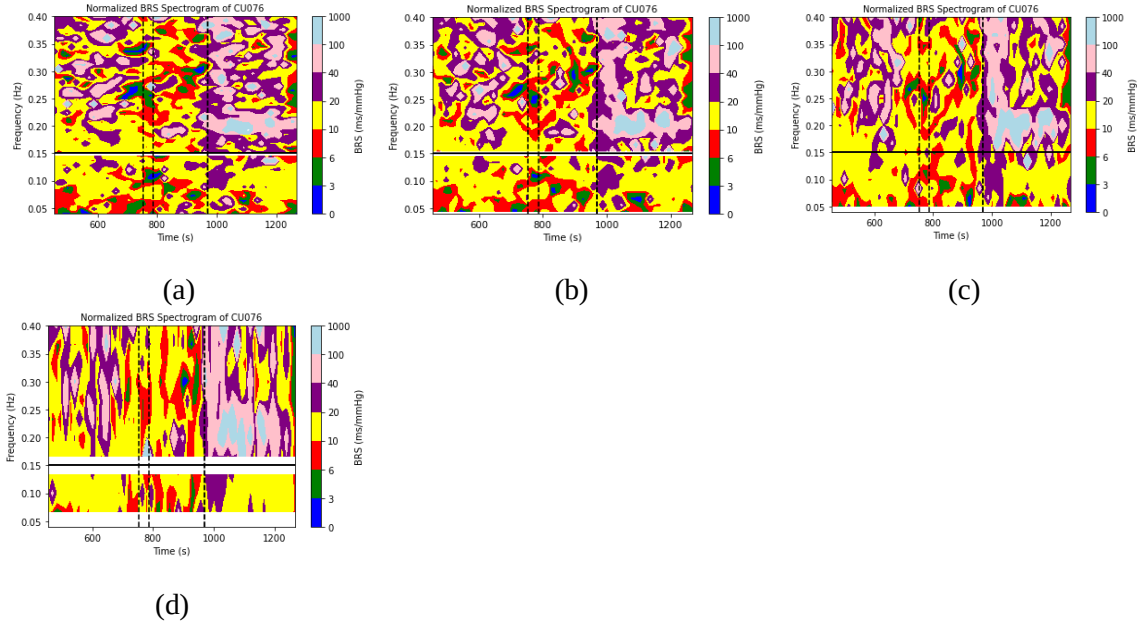

(a) (b) (c)

(d)

Figure 3.9**:** Normalized BRS spectrograms of subject CU076 with different frequency resolutions; frequency resolutions of (a) 0.008 Hz, (b) 0.011 Hz, (c) 0.017 Hz, (d) 0.033 Hz and quasi time resolution of 15 seconds; x-axis denotes time in seconds, y-axis represents frequency in Hz, the color bar indicates normalized ranges of transfer function gains (BRS gains in ms/mmHg); dashed vertical lines denote transitions between experimental stages (baseline, adaptive period, stress, recovery), while the horizontal line (0.15 Hz) signifies the boundary between the LF and HF band

Fig. 3.10 depicts normalized BRS spectrograms of the three subjects.

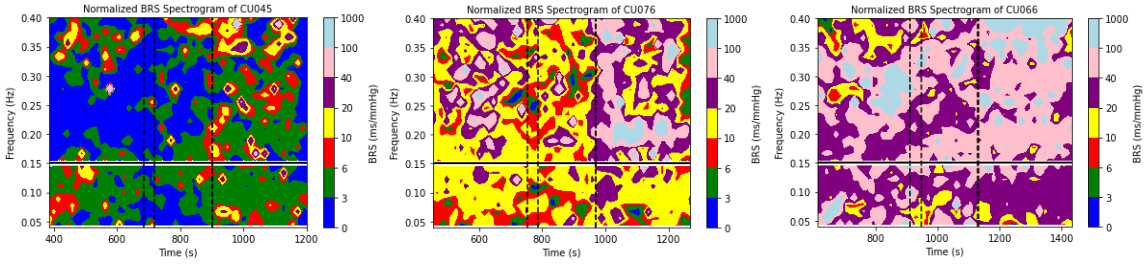

(a) (b) (c)

Figure 3.10: BRS spectrograms of subjects: (a) CU045, (b) CU076, (c) CU066 at frequency resolution of 0.011 Hz

3.3.4.3 Phase spectrogram

Fig. 3.11 portrays phase (contour plots) spectrograms and the normalized BRS spectrogram focusing solely on the negative phase of subject CU076. Additionally, Fig. 3.12 portrays phase spectrograms of subjects CU066 and CU045 and their respective normalized BRS spectrograms

including only negative phases - for simplification purposes, described here as negative phase spectrograms.

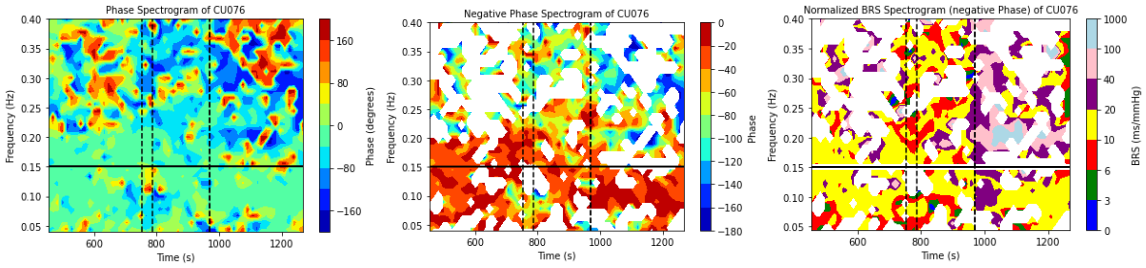

(a) (b) (c)

Figure 3.11: Phase spectrograms (excluding coherence threshold application) of subject CU076: (a) including positive and negative phases, (b) only highlighting the negative phase, (c) normalized BRS spectrogram including only the negative phase. Frequency resolution set to 0.011 Hz, quasi-time resolution to 15 seconds. Phase values are color-coded based on the degree scale presented in the color bar, spanning from -180 to 180 degrees

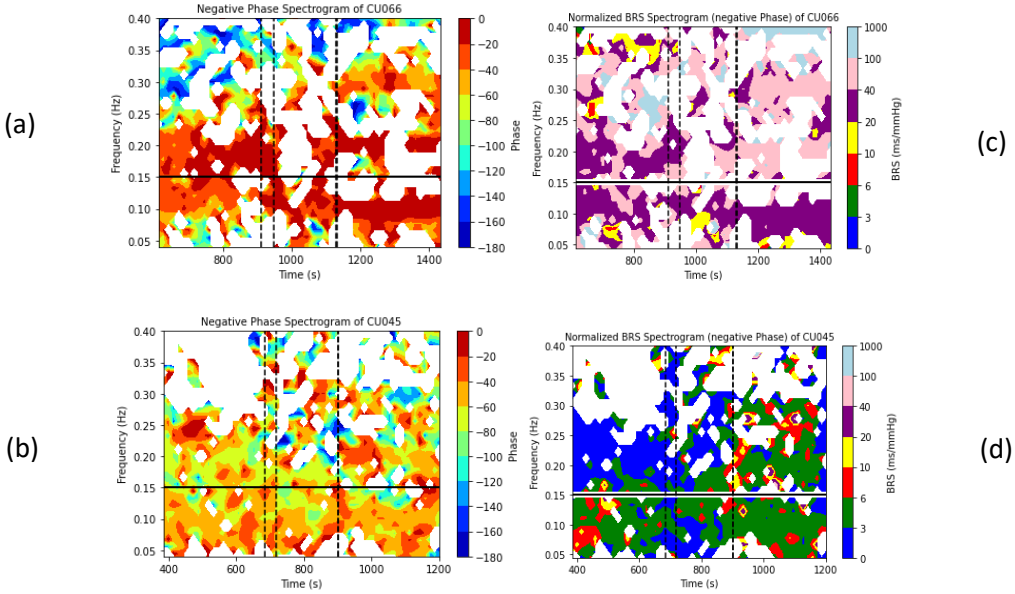

Figure 3.12: Negative phase and normalized BRS spectrograms of subjects: (a,c) CU066, (b,d) CU045

3.3.4.4 STFT: 2D visualization: BRS values

Fig. 3.13 illustrates an example of a 2D visualization of BRS values in the LF band over time across different experimental stages of the subject CU076. The frequency resolution (f_{res}) is kept fixed while the hop sizes (quasi time resolution - t_{res}) vary.

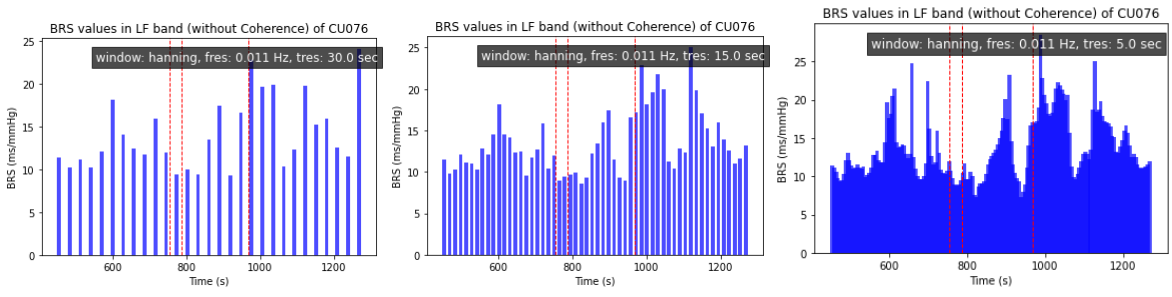

(a) (b) (c)

Figure 3.13: BRS values over time of subject CU076 with various hop sizes: (a) 30 sec, (b) 15 sec, (c) 5 sec. The red dashed lines indicate time stamps between different experimental stages (order: baseline, adaptive period, stress, recovery)

3.3.5 Comparison of BRS results: Welch, STFT, Sequence method

Fig. 3.14-3.16 were created to compare mean BRS values (LF band) and trends across different experimental stages (baseline, stress, recovery) of all patients between the Welch (f_{res}: 0.008 Hz) (with and without taking coherence criterion into consideration), STFT (excluding coherence criterion) with frequency resolutions of 0.008 Hz and 0.011 Hz and the sequence method (BRS evaluated only during the baseline stage).

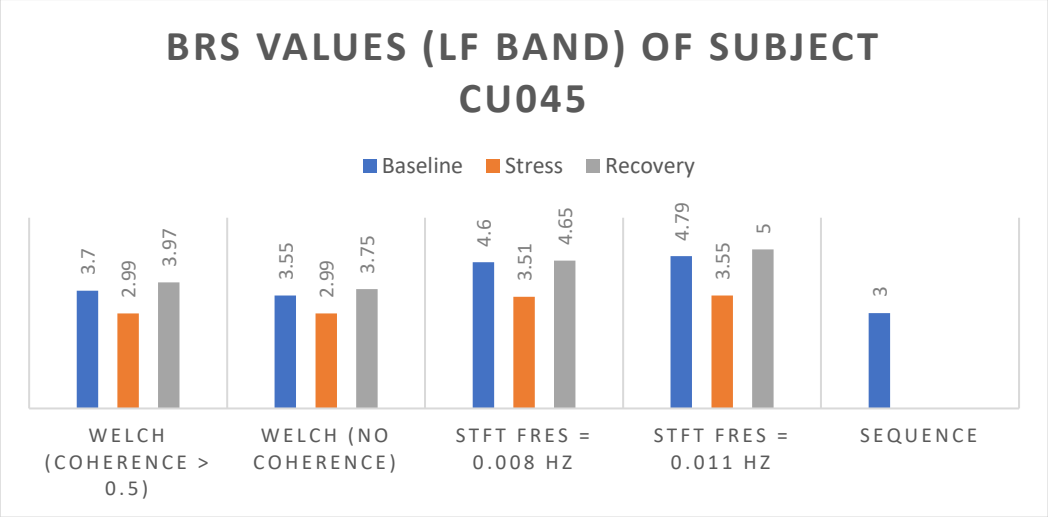

Figure 3.14: BRS values across different methods and experimental stages of subject CU045

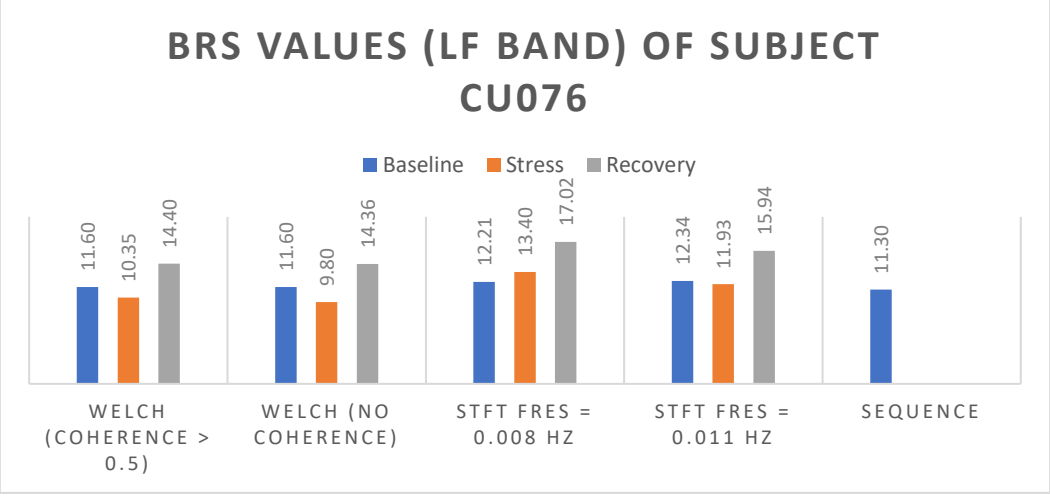

Figure 3.15**:** BRS values across different methods and experimental stages of subject CU076

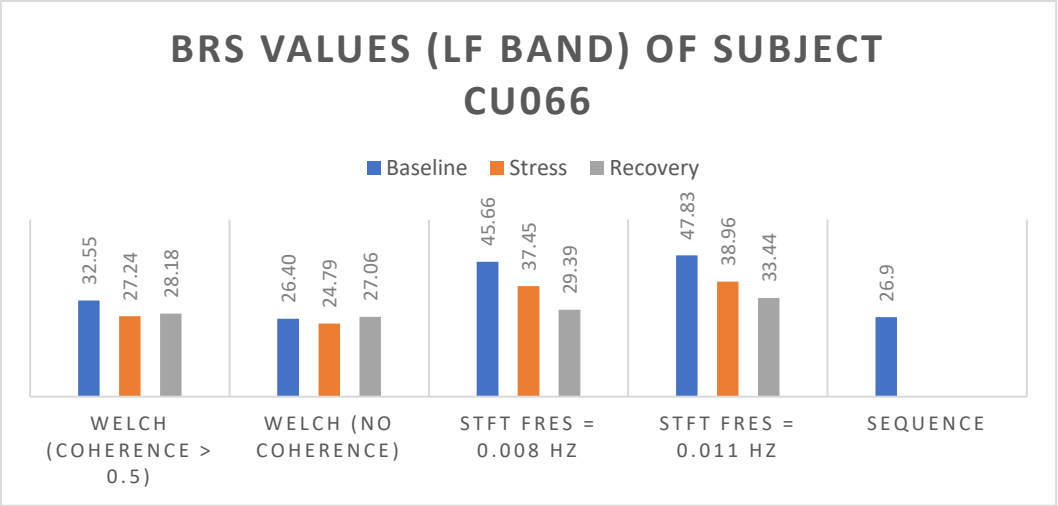

Figure 3.16: BRS values across different methods and experimental stages of subject CU066

3.4 Discussion

In short, the primary goal of the practical part of this thesis was to represent visually the BRS parameter using spectral methods, in particular focusing on FFT-based techniques such as the Welch periodogram and the STFT-based approach.

The most significant points were addressed in the subsequent sections.

3.4.1 Welch method: 2D and 3D visualizations

The difference in frequency resolutions of 0.008 Hz and 0.015 Hz has minimal effect on BRS values (LF band) per stage. (Fig 3.6) Both options are acceptable for visualization purposes. The trends of BRS values also appear similar across experimental stages for both frequency resolution options as well.

Visually, the differences in spectrum shapes between these two frequency resolutions also appear minimal (see Appendix H), since the zero padding mainly servers to smooth the spectrum.

In general, 2D visualizations of the BRS spectrum, coherence and phase (Fig. 3.2-3.4), as well as BRS value per experimental stage (Fig 3.6) are very valuable. However, the 3D visualization – experimental stages plotted together (Fig. 3.5) – does not provide any additional benefit in comparison to 2D visualizations.

3.4.2 STFT: 2D and 3D visualizations

A 3D visualization – non-normalized BRS spectrogram (Fig. 3.7) - is an ineffective method to visualize BRS gains due to the high contrast being present in BRS gains (0-700+ ms/mmHg), making it difficult to discern low BRS gains amid high random peaks. It is especially challenging to do so in the LF band. Therefore, to address this limitation, the normalized spectrogram (Fig. 3.8 – 3.10) was introduced in this thesis, offering enhanced color-coded information on BRS gain ranges and changes over time.

However, the utility of this normalized spectrogram is reduced by the absence of comparative BRS studies and the presence of very high gains in certain regions (100-1000 ms/mmHg). This is particularly visible in a 3D surface plot (Fig. 3.8), which also appears as an ineffective tool for BRS visualization. Potentially, these peaks could be mitigated if coherence were to be calculated (see Chapter 3.4.3.2), and only areas with high coherence were visualized in the spectrogram. It is plausible that high random peaks may occur more frequently in areas with low coherence and higher noise as suggested by Pinna et al. [96], although this hypothesis remains unverified.

Nevertheless, despite random peaks, normalized spectrograms appear to depict BRS gain variations effectively across different areas and their temporal and frequency dynamics. For instance, the spectrogram of the subject CU066 (Fig. 3.10) showcases heightened BRS gains represented by a diverse array of colors, while subject CU045’s spectrogram predominantly displays lower BRS gains, facilitating clear differentiation in BRS strength between these two individuals. Additionally, adjusting the color-coded values represented in a color bar - by

adding new ranges of BRS values or modifying colors - may be performed by the user depending on the specific focus of interest.

Additionally, another potential BRS visualization would be to display BRS gains only in those areas where the phase is negative (Fig. 3.11(b), 3.12(a-b)). This may be an interesting visualization option since only areas considered relevant for baroreflex activity are more enhanced this way. However, this approach to BRS estimation has yet to be fully developed, but the LF band phase behavior of the three subjects confirms the literature findings which state that the phase is known to be more negative in this frequency region. [15], [161]

Ultimately, the visualization of the normalized BRS and phase spectrogram along with 2D visualization of BRS values over time in the LF band (Fig. 3.13) allow fuller understanding of BRS fluctuations.

3.4.2.1 STFT: Time-Frequency resolution tradeoff

The optimal frequency-time resolution primarily depends on the segment length (window size) while the number of computed BRS values remains determined solely by the hop size parameter. (Fig. 3.13)

However, tables 3.7-3.9 highlight the inconclusiveness of selecting a single optimal solution for this tradeoff while taking various hop sizes (or overlaps) into consideration. Each patient demonstrates certain outliers (random peaks) in different hop size and frequency resolutions combinations, characterized by a notably high relative standard deviation (RSD > 40 % - threshold arbitrarily chosen), thus, the data is more scattered around the mean and potentially considered less reliable, therefore, this suggests a lack of a universal solution across all subjects.

Higher RSD appears more associated with inferior frequency resolutions (> 0.011 Hz) rather than higher ones, particularly for subjects with higher BRS values (CU066 and CU076). Moreover, Chao-Ecija et al. [61] already observed the issues related to using excessively small window lengths for STFT-based BRS, since they compromise frequency resolution and potentially lead to erroneous peaks or difficulty isolating the frequency band of interest.

Even though these random outliers in time-frequency estimations significantly influence the RSD value, the mean BRS values of subjects in all combinations remain relatively unaffected, as confirmed by Eckberg et al. [33] in their study of BRS variability and different window size effects.

Furthermore, Eckberg et al. [33] also note the major constant fluctuations of BRS values in subjects, who could have the ratio of maximum to minimum BRS values between 4 and 35 in different individuals even under same experimental conditions, e.g. in a supine position in this case. This phenomenon additionally complicates the interpretation of the BRS variability. Moreover, the potential inclusion of spectral BRS variation (RSD) as a separate diagnostic parameter remains an open question and this domain requires further research since there is no clinical literature on this topic.

Alternatively, if there is an interest in presenting the normalized BRS spectrogram, a frequency resolution of 0.011 Hz demonstrates greater effectiveness. (Fig. 3.9(b)) From a qualitative standpoint, lower frequency resolutions hinder the effective visualization of BRS spectrograms.

Therefore, for visualization purposes, especially concerning the BRS spectrogram as well as the phase spectrogram, higher frequency resolutions are recommended.

As mentioned previously, Eckberg et al. [33] also concluded that baroreflex oscillations appear to be organized around the frequency of 0.01 Hz (every 90 seconds); longer recordings which include more cycles would be recommended for more reliable BRS estimations.

3.4.2.2 STFT: Window type effects

To assess the impact of different window types on BRS values in the LF band, tests were performed on two subjects, CU045 and CU066, representing the highest and lowest BRS values in the dataset, respectively (Table 3.10, Appendix I).

The analysis revealed that subject CU066 demonstrates greater variability in BRS values, with the RSD fluctuating more significantly depending on the window type used, even when frequency resolution and hop size parameters remain constant.

Conversely, subject CU045 exhibits less variation in RSD under the same conditions, indicating that the choice of window type has a smaller impact on this subject's BRS values.

Outliers were observed for both subjects in some instances, with RSD exceeding 50%, based on an arbitrarily set threshold.

These findings suggest that, similar to the frequency/time resolution trade-off, the effect of window type on BRS values varies between subjects and depends and also varies with different frequency resolutions and hop sizes as well. Thus, the impact of window type appears to be subject-specific.

Given these observations, the Hanning window could be recommended for visualization purposes, as its use aligns with its application in the Welch method. This alignment may allow more consistent comparisons between the two methods and support standardization efforts. Notably, there is a lack of literature addressing the impact of window types on BRS values.

In summary, window type emerges as an insignificant parameter in the spectral analysis of BRS.

3.4.3 Difference between BRS and coherence

An essential inquiry to discuss is the distinction between coherence and BRS, given their seemingly similar calculation formulas, as in (3) and (4) – in particular to respond to the question if coherence can serve as a substitute for BRS?

The short answer is no. Coherence and BRS gain do complement each other and offer distinct information. Coherence delineates frequencies where RRI and SBP exhibit linear correlation, quantifying the extent of this linearity. Hence, coherence serves to indicate whether the signals are affected by excessive noise or nonlinearities. On the other hand, the BRS gain at a given frequency (inc. estimated BRS value) quantifies the efficiency of the autoregulatory system, which is the response of RRI on the magnitude of SBP oscillations in a particular subject. [162]

For example, examining Fig.3.3 reveals that the subject with the highest BRS (CU066) also exhibited the highest coherence value in the LF band. However, all patients exhibited coherence values above 0.5, which is considered normal, despite significant variations in their BRS gains. From a clinical perspective, the patient with low BRS (CU045) is the primary concern, as he may be at greater risk of mortality. Therefore, the minor discrepancies in coherence values among patients may not carry significant enough clinical implications, but low BRS values do.

Additionally, another question worth discussing is: Does low coherence necessarily mean low BRS?

While it seems that low coherence consistently corresponds to low BRS (Fig. 2.13(b)), the reverse is not always true—low BRS does not always imply low coherence (Fig. 2.13(a) and Fig 2.14(b)). In some cases, low BRS may simply be an age-related phenomenon, as elaborated in Chapter 1.3. However, there is no evidence in the literature that coherence is age-related as well. Nevertheless, it's worth mentioning that low BRS coupled with low coherence might indicate a more pathological situation than low BRS with higher coherence in certain patients. It is known that low coherence, due to pathological characteristics and low SNR present in RRI and SBP, for example, is often present in diabetic, CHF and POST-MI patients (see Chapter 2.3.4)) and it embodies two aspects of abnormal ANS functioning, the impaired baroreflex-HR control system and/or often depressed BPV. [95], [163] One approach to address this low coherence, suggested by Swenne et al. [148], involves inducing higher SBP and RRI oscillations with different maneuvers, such as for example through deep breathing at 0.1 Hz, since this approach should increase coherence between signals. [7] The effect of this approach is clear from Fig 3.4(a) (versus Fig 3.3(a)), where, during the recovery phase, the patient CU045 illustrates a notable increase in coherence values compared to his baseline phase. However, despite this coherence improvement, the BRS gains still remain low.

In summary, coherence alone proves insufficient in characterizing the strength of BRS but it does support the BRS estimation.

3.4.3.1 Pros and cons of using the coherence criterion

The literature suggests that the arbitrarily set coherence criterion of > 0.5 should be discarded due to its tendency to introduce a positive bias in BRS values. [95], [148] This bias may not affect normal BRS values significantly (since the baroreflex is already functioning). It could, however, pose a concern for individuals with low BRS where inclusion of the coherence criterion could cause BRS to appear higher than it really is. [148] Consequently, the coherence criterion appears unnecessary for low BRS cases where this bias should be avoided.

However, the coherence criterion is useful for reliable phase estimation. (see Chapter 3.4.3.3)

3.4.3.2 STFT: Issue with coherence computation

There is an issue with coherence estimation when employing the STFT algorithm. When applying (13), the result consistently yields 1 across all times and frequencies. Thus, the coherence was not computed nor visualized while using this algorithm. [164], [165] This issue is already known in the literature (not BRS-related) but this topic lies outside the scope of this thesis.

One potential solution to calculate BRS more reliably, while excluding coherence estimation, would be to extend the recording duration, thereby enabling the calculation of BRS with a greater number of gain points. Research suggests that a longer recording duration enhances the accuracy of BRS estimations without taking into account the coherence estimation. [33], [148]

Alternatively, the user could apply a different time-frequency algorithm to obtain the coherence, e.g. the wavelet transforms. [60], [61]

3.4.3.3 Coherence criterion and phase

A notable challenge arises with low coherence (< 0.5) or a missing coherence evaluation, in the (relatively unreliable) calculation of phase. This means that the trustworthiness of phase estimation when coherence falls below 0.5 remains uncertain.

For example, according to the Welch method (Fig 3.2(a,d)), subject CU045 demonstrates coherence above 0.5 in the LF band. Compared to two other subjects, CU045 exhibits a notably more negative phase, potentially indicating a slower baroreflex response. Interestingly, when observing the phase spectrogram (Fig. 3.12(b), 3.12(a) and Fig 3.11(b)) without considering the coherence threshold, CU045's negative phase again appears more negative compared to the other two subjects. This suggests potentially parallel results in phase estimations of both the Welch and STFT methods. However, it is important to note that due to the small sample size, definitive conclusions cannot be drawn in this case.

Nevertheless, it may be useful to visualize the (negative) phase using the STFT method, even in instances when coherence cannot be calculated.

3.4.4 Results comparison: Sequence, Welch, STFT method

Fig. 3.14 - 3.16 demonstrate that the sequence method consistently yielded slightly lower mean BRS values across all three subjects compared to the spectral methods in the LF band. The only exception was the subject CU066, whose BRS value computed via the Welch method (while excluding coherence threshold) was slightly lower than the BRS result obtained by the sequence method. (evaluated and compared only in the baseline stage)

Moreover, despite the expected differences in BRS values between various methods, all BRS values of each individual stayed within a typical range, i.e., either high, medium or low, depending on the individual.

On the other hand, the BRS trends across experimental stages when employing Welch and STFT methods varied, which made direct comparisons impossible. Finally, given the variations regarding the behavior of mean BRS values throughout different experimental protocol stages, the correct approach to determining a preferred algorithm is still an open question.

3.4.5 Welch versus STFT algorithm

This section outlines the advantages and disadvantages of BRS computations and visualizations associated with the Welch and STFT algorithms. (Table 3.11 and 3.12)

3.4.5.1 BRS Computation

Welch method		STFT method	
Pros	**Cons**	**Pros**	**Cons**
• Easy to implement • BRS spectrum could be computed • Coherence estimation possible • Reliable phase estimation possible • More robust against noise due to averaging procedure of PSD • More literature available	• Stationary signals required as input: higher signal processing effort • Time component missing • Requires 'steady-state' body positions • Single experimental stage processed at a time • Fixed window length • Slower if segment size (FFT) not power of 2 (longer processing time) • Only available in post-processing • Not recommended for ANS research • Minimum 3 minutes long recording needed per experimental stage	• Easy to implement • Non-stationary signals as input • Time component included • Able to follow many experimental stages at once • BRS spectrogram and phase could be computed • Recommended for ANS research (particularly if coherence and reliable phase could be included) • In principle available in quasi real-time, with a time delay of a window size and also in post-processing	• No coherence calculation possible without smoothing procedures or repeated trials • No reliable phase estimation possible without including coherence computation • Slower if segment size (FFT) not power of 2 (longer processing time) • Fixed window length • Susceptible to noise in signals • Clinical literature missing at this time • **Recommended:** Longer recording for better BRS estimations without including coherence estimations

Table 3.11: Pros and cons of Welch and STFT algorithms for the BRS computation

3.4.5.2 BRS Visualization

Welch method		STFT method	
Pros	**Cons**	**Pros**	**Cons**
• **2D:** Shape of BRS spectrum easier to interpret: more literature on this topic • **2D:** Phase visualization in LF and HF bands over frequency (VLF band could be also included) • **2D:** Coherence visualization in LF and HF bands over frequency (VLF band could be also included) • **2D:** BRS spectrum in LF and HF bands over frequency (VLF band could be also included) • **2D:** BRS value visualization including or excluding coherence threshold application per experimental stage	• Only single BRS value for each experimental stage generated • **3D:** Useful only if more than one experimental stage should be observed at the same time for easier visual comparison, otherwise, no real need to be used	• **3D:** Normalized BRS spectrogram visualization possible in LF, HF and VLF bands which portrays BRS gain range changes across time and frequencies simultaneously • **3D:** Negative phase spectrogram visualization possible (more reliable in subjects with higher coherence between signals) • **3D:** Phase spectrogram visualization possible in LF, and HF bands (inc. VLF) (both with positive and negative phases) • **2D:** Presents variation of BRS values over time (LF band is more clinically relevant, but HF and VLF bands could be included as well if necessary)	• No coherence spectrogram visualization • **3D:** High random peaks present in the BRS spectrogram • **3D:** Phase visualization possible but not fully reliable due to missing coherence evaluation

Table 3.12: Pros and cons of Welch and STFT algorithms for the BRS visualizations

3.4.5.3 Parameter settings suggestions for medical devices

Here is a short summary of recommendations for parameter settings concerning the Welch and STFT methods, which could enhance the user experience when integrated into medical devices. (Table 3.13) The settings are divided into “fixed” parameters and “free to adjust” that could be freely adapted by users with a goal of simplifying BRS estimation.

Parameter settings			
Welch method		**STFT method**	
Fixed	**Free to adjust**	**Fixed**	**Free to adjust**
• Hanning window • 50% overlap	• Frequency resolution (set window or FFT size) **Recommended:** 0.015 Hz or 0.008 Hz • Coherence threshold: 0-1 **Recommended:** Not to set below 0.25 and above 0.75 to avoid extremes in calculations • Choice to include or exclude coherence from BRS calculations • Choice to include or exclude visualization of the BRS value in HF or VLF band • LF, HF, and VLF band limits	• Hanning window (recommended)	• Frequency/time resolution (set window size) • Hop size (set overlap): controls number of produced BRS values (e.g. recommended hop sizes between 5 and 15 seconds for 0.011 Hz frequency resolution) • Colors or BRS ranges above 6 ms/mmHg in BRS spectrogram to observe gain variations better • LF, HF and VLF band limits • Window type (optional) • Choice to include or exclude visualization of BRS values in HF or VLF band

Table 3.13: Parameter settings: Fixed and freely adjustable for Welch and STFT algorithms

3.4.5.4 Ad hoc and online monitoring applications

In general, medical devices have the capability to compute the BRS parameter either in post-processing (ad hoc – offline modes) or 'quasi' real-time (online) modes. It should be noted that there is no BRS literature available to date on this topic of quasi real-time modes.

Ad hoc applications are valuable for conducting more detailed BRS examinations and in-depth data analysis when patient histories are retained. Online BRS estimation, on the other hand, would be more suitable for shorter appointments with clinicians, as it would enable quasi real-time BRS measurement. Consequently, advantages and disadvantages of both of these alternatives have been proposed for both approaches. (Table 3.14)

Furthermore, prior to the BRS estimation, it is crucial to acquire RRI and SBP time series and conduct automated signal preprocessing whenever feasible. This preprocessing entails identifying and/or correcting (if possible) issues such as arrhythmias, ectopic beats, or missing beats, as their presence can affect the accuracy of BRS estimations. [149] Subsequently, based on these results, a decision must be made regarding whether the measurement process could proceed or not.

Following this initial step, signal time-synchronization between SBP and RRI should be achieved, followed by the automatic calculation of sampling frequency based on beat-to-beat RRI and SBP. Additionally, linear or cubic spline interpolation and linear detrending should be applied as necessary.

Spectral BRS in medical devices			
Offline (post-processing)		**Online (quasi real-time) monitoring**	
Advantages	**Disadvantages**	**Advantages**	**Disadvantages**
• Frequency and time-frequency domain (Welch STFT, wavelet etc) possible • **Welch**: Coherence visualization possible in steady state conditions • **Welch:** Reliable phase computation possible (coherence > 0.5) in steady state conditions • **STFT, wavelet:** Good for ANS research: different experimental stages analysis followed at once, longer recording times possible • **Wavelet:** Reliable phase and coherence able to be computed in a single trial • Clinical literature available • Could be a better option if more complex signal editing is required	• Longer time required to process BRS results (pre- and post-processing) • Longer recording needed for Welch estimate than for STFT/wavelet • More storage space required • **Wavelet:** More complex to compute than STFT and Welch	• Time-frequency domain possible (e.g. STFT delayed with a window size, AR model - used on Task Force Monitor (CNSystems Medizintechnik GmbH, Graz, Austria) • Immediate results could be computed • BRS values and spectrum, coherence and phase spectrum could be computed line by line and visualized simultaneously • Good for ANS research: different experimental stages analysis followed at once	• No clinical literature available to date • Online artefact removal is necessary prior to online BRS calculation

Table 3.14: Advantages and disadvantages of postprocessing and online spectral BRS estimations for medical devices

3.5 Conclusions

The objective outlined in Chapter 1.8 of this thesis was successfully achieved.

In summary, this thesis was divided into two main phases: a literature review phase and a practical phase.

The literature review phase involved an extensive literature search followed by a thorough analysis, focusing on specific medical applications and pathological states where the BRS index is valuable. It appears from this comprehensive literature review that the three main clinical benefits of the BRS index are its roles in outcome prediction, risk stratification and diagnosis

of certain diseases which are related to the cardiovascular system, such as CHF, POST-MI state, diabetes mellitus and hypertension.

In general, among modern algorithms described, sequence method-based BRS estimations were identified as the most frequently referenced in the literature and, thus, more often used in clinical practice when compared to BRS spectral estimations, of which the transfer function method and the alpha coefficient were most commonly employed.

On the other hand, spectral estimations of BRS, despite being less common, hold significant potential since they are able to track BRS changes simultaneously across time and frequency domains. Therefore, the strengths and weaknesses of the sequence and spectral methods were presented and discussed, as the 'best' algorithm for the BRS computation does not yet exist.

Generally, the sequence method follows the BRS as a time-variant parameter and applies sequences (minimum of 3 beats) of consecutive RRI-SBP changes to compute the BRS slope (BRS value). Spectral methods, on the other hand, focus on smaller beat-to-beat changes of RRI and SBP signals to compute the BRS; therefore, these methods cannot be used interchangeably even if their results may appear to be consistent with each other. Additionally, sequence methods are easier to compute than spectral methods and the BRS slope easier to interpret. They can separate BRS values determined from positive or negative SBP changes - by computing 'up' and 'down' sequences - which spectral methods cannot do. BEI is also used as a supplementary, potentially clinically useful parameter in some cases, as it expresses the engagement rate of baroreflex during specific recording times.

However, the sequence method includes many algorithm variations due to different parameter settings employed in studies (i.e. varied sequence length, different values for minimal threshold requirement to detect changes in RRI and SBP signals, threshold for correlation coefficient between SBP and RRI (generally set to be high) and employing lags of 0 or 1 beats). For this reason, direct comparison between different studies was not possible.

Spectral methods, in contrast, differentiate the BRS changes in the LF and HF bands, and require more signal processing steps before the spectral analysis takes place, but offer additional information on autonomic system control by computing the coherence and phase between SBP and RRI. Furthermore, spectral methods require shorter recording times than the sequence method and compute more BRS gains for each recording. In some cases, it can happen that sequences cannot be found due to strict threshold criteria; yet the spectral methods also include noise in their calculations.

Finally, this thesis has shown that measurement of BRS in various pathological conditions may benefit from using different algorithms and optimizing parameter/threshold settings to fit specific applications since the BRS studies generally did not provide reasons why one algorithm or threshold employed in their studies performed better than the other in different clinical applications.

The practical phase of this thesis involved implementing the spectral method - Transfer function - for BRS computation and visualization, and comparing two FFT-based spectral decomposition techniques: the Welch method (frequency domain) and, (for the first time) in

transfer function-based BRS studies, an STFT algorithm (time-frequency domain). The strengths and weaknesses of these approaches were also clarified.

Additionally, the effects of different spectral parameters on mean BRS values in the LF band (the clinically relevant frequency range) for both algorithms were tested and discussed. In summary, the thesis identified key spectral parameters related to the TF method: the sampling frequency, window size, and FFT size, which are crucial for setting desired time/frequency resolutions. For the STFT algorithm, the overlap parameter is particularly important, since it controls the number of estimated BRS points. Furthermore, the thesis also demonstrated that the variability of spectral BRS values over time (reflected in RSD) is significantly influenced by different time/frequency resolutions and overlap parameter settings. Therefore, caution is advised when interpreting these results. Mean BRS values (i.e., time-averaged) in the LF band, in contrast, were shown to be largely unaffected by different parameter settings. Even more precisely, the differences in mean BRS results are more pronounced in higher BRS values than in the lower ranges.

Subsequently, spectral BRS visualizations in 2D and 3D, including phase and coherence visualizations - which could be useful in ANS research, despite the complex interactions of RRI and SBP signals in ANS dynamics - were presented and analyzed for their respective advantages and disadvantages. However, it should be noted that the clinical role of coherence in BRS dynamics is not yet fully researched and understood. Thus, regarding BRS spectrum visualization via the TF method, it was shown that 2D is a preferred option for the Welch method while, as introduced in this thesis, the normalized 3D BRS spectrogram appears to be a good choice when an STFT algorithm is applied. However, since the behavior of spectral BRS values over time and the BRS time-frequency spectra are not yet incorporated into the clinical literature, their potential future application at this time remains inconclusive. Nevertheless, suggestions were also provided for optimal spectral BRS parameter settings and visualization options in frequency and time-frequency domains.

Finally, the advantages and disadvantages regarding BRS incorporation into medical devices were described in the context of quasi-real-time or offline-mode parameter.

In summary, in addition to the literature review and practical work completed which led to the new insights and conclusions, this thesis also indicates the value of potential further work which could be done related to the goal of improving the quality of BRS research and simplifying its potential transition into routine clinical practice.

To pursue this objective, larger and more focused BRS studies, the use of standardized experimental protocols and agreement on BRS-related frequency bands would be necessary to support the development of optimal algorithms for specific medical conditions as well as to determine suitable parameter and threshold settings for each application.

4 Bibliography

[1] G. A. Reyes del Paso, P. de la Coba, M. Martín-Vázquez, and J. F. Thayer, "Time domain measurement of the vascular and myocardial branches of the baroreflex: A study in physically active versus sedentary individuals," *Psychophysiology*, vol. 54, no. 10, pp. 1528–1540, Oct. 2017, doi: 10.1111/psyp.12898.

[2] M. Sakamoto, D. Matsutani, and Y. Kayama, "Clinical Implications of Baroreflex Sensitivity in Type 2 Diabetes.," *Int Heart J*, vol. 60, no. 2, pp. 241–246, Mar. 2019, doi: 10.1536/ihj.18-455.

[3] G. Parati, M. Di Rienzo, and G. Mancia, "How to measure baroreflex sensitivity: from the cardiovascular laboratory to daily life.," *J Hypertens*, vol. 18, no. 1, pp. 7–19, Jan. 2000, [Online]. Available: http://www.ncbi.nlm.nih.gov/pubmed/10678538

[4] M. Di Rienzo, G. Parati, A. Radaelli, and P. Castiglioni, "Baroreflex contribution to blood pressure and heart rate oscillations: time scales, time-variant characteristics and nonlinearities," *Philosophical Transactions of the Royal Society A: Mathematical, Physical and Engineering Sciences*, vol. 367, no. 1892, pp. 1301–1318, Apr. 2009, doi: 10.1098/rsta.2008.0274.

[5] M. T. La Rovere, G. D. Pinna, and G. Raczak, "Baroreflex Sensitivity: Measurement and Clinical Implications," *Annals of Noninvasive Electrocardiology*, vol. 13, no. 2, pp. 191–207, Apr. 2008, doi: 10.1111/j.1542-474X.2008.00219.x.

[6] C. A. Swenne, "Baroreflex sensitivity: mechanisms and measurement," *Netherlands Heart Journal*, vol. 21, no. 2, pp. 58–60, Feb. 2013, doi: 10.1007/s12471-012-0346-y.

[7] J. Gerritsen, B. J. TenVoorde, J. M. Dekker, P. J. Kostense, L. M. Bouter, and R. M. Heethaar, "Baroreflex sensitivity in the elderly: influence of age, breathing and spectral methods.," *Clin Sci (Lond)*, vol. 99, no. 5, pp. 371–81, Nov. 2000.

[8] M. T. la Rovere, A. Porta, and P. J. Schwartz, "Autonomic Control of the Heart and Its Clinical Impact. A Personal Perspective," *Front Physiol*, vol. 11, Jun. 2020, doi: 10.3389/fphys.2020.00582.

[9] G. W. Pickering, P. Sleight, and H. S. Smyth, "The reflex regulation of arterial pressure during sleep in man.," *J Physiol*, vol. 194, no. 1, pp. 46P-48P, Jan. 1968, [Online]. Available: http://www.ncbi.nlm.nih.gov/pubmed/4295756

[10] J. Penttila *et al.*, "Spontaneous baroreflex sensitivity as a dynamic measure of cardiac anticholinergic drug effect," *J Auton Pharmacol*, vol. 21, no. 2, pp. 71–78, Apr. 2001, doi: 10.1046/j.1365-2680.2001.00210.x.

[11] G. A. Reyes del Paso, J. A. Hernández, and M. I. González, "Differential analysis in the time domain of the baroreceptor cardiac reflex sensitivity as a function of sequence length," *Psychophysiology*, vol. 41, no. 3, pp. 483–488, May 2004, doi: 10.1111/j.1469-8986.2004.00178.x.

[12] D. Čelovská, J. Staško, J. Gonsorčík, and A. Diab, "The Significance of Baroreflex Sensitivity in Hypertensive Subjects with Stroke," *Physiol Res*, pp. 537–543, 2010, doi: 10.33549/physiolres.931785.

[13] G. Dorantes-Mendez *et al.*, “Effects of propofol anesthesia induction on the relationship between arterial blood pressure and heart rate.,” *Annu Int Conf IEEE Eng Med Biol Soc*, vol. 2012, pp. 2835–8, 2012, doi: 10.1109/EMBC.2012.6346554.

[14] H. van de Vooren, M. G. J. Gademan, C. A. Swenne, B. J. TenVoorde, M. J. Schalij, and E. E. van der Wall, “Baroreflex sensitivity, blood pressure buffering, and resonance: what are the links? Computer simulation of healthy subjects and heart failure patients,” *J Appl Physiol*, vol. 102, no. 4, pp. 1348–1356, Apr. 2007, doi: 10.1152/japplphysiol.00158.2006.

[15] S. Carrasco-Sosa, M. J. Gaitán-González, R. González-Camarena, and O. Yáñez-Suárez, “Baroreflex sensitivity assessment and heart rate variability: relation to maneuver and technique.,” *Eur J Appl Physiol*, vol. 95, no. 4, pp. 265–75, Oct. 2005, doi: 10.1007/s00421-005-0001-z.

[16] M. T. la Rovere, J. T. Bigger, F. I. Marcus, A. Mortara, and P. J. Schwartz, “Baroreflex sensitivity and heart-rate variability in prediction of total cardiac mortality after myocardial infarction,” *The Lancet*, vol. 351, no. 9101, pp. 478–484, Feb. 1998, doi: 10.1016/S0140-6736(97)11144-8.

[17] G. D. Pinna, R. Maestri, and M. T. la Rovere, “Assessment of baroreflex sensitivity from spontaneous oscillations of blood pressure and heart rate: proven clinical value?,” *Physiol Meas*, vol. 36, no. 4, pp. 741–753, Apr. 2015, doi: 10.1088/0967-3334/36/4/741.

[18] E. J. Bowers and A. Murray, “Effects on baroreflex sensitivity measurements when different protocols are used to induce regular changes in beat-to-beat intervals and systolic pressure.,” *Physiol Meas*, vol. 25, no. 2, pp. 523–38, Apr. 2004, doi: 10.1088/0967-3334/25/2/010.

[19] M. Martín-Vázquez and G. A. Reyes del Paso, “Physical training and the dynamics of the cardiac baroreflex: A comparison when blood pressure rises and falls,” *International Journal of Psychophysiology*, vol. 76, no. 3, pp. 142–147, Jun. 2010, doi: 10.1016/j.ijpsycho.2010.03.004.

[20] M. Pagani *et al.*, “Changes in autonomic regulation induced by physical training in mild hypertension.,” *Hypertension*, vol. 12, no. 6, pp. 600–10, Dec. 1988, doi: 10.1161/01.hyp.12.6.600.

[21] D. Antonino *et al.*, “Non-invasive vagus nerve stimulation acutely improves spontaneous cardiac baroreflex sensitivity in healthy young men: A randomized placebo-controlled trial,” *Brain Stimul*, vol. 10, no. 5, pp. 875–881, Sep. 2017, doi: 10.1016/j.brs.2017.05.006.

[22] D. Celovska *et al.*, “Effect of Low Dose Atorvastatin Therapy on Baroreflex Sensitivity in Hypertensives,” *High Blood Pressure & Cardiovascular Prevention*, vol. 23, no. 2, pp. 133–140, Jun. 2016, doi: 10.1007/s40292-016-0154-3.

[23] C. T. Chan, X. S. Shen, P. Picton, and J. Floras, “Nocturnal home hemodialysis improves baroreflex effectiveness index of end-stage renal disease patients,” *J Hypertens*, vol. 26, no. 9, pp. 1795–1800, Sep. 2008, doi: 10.1097/HJH.0b013e328308b7c8.

[24] P. A. Modesti, A. Ferrari, C. Bazzini, and M. Boddi, “Time sequence of autonomic changes induced by daily slow-breathing sessions.,” *Clin Auton Res*, vol. 25, no. 2, pp. 95–104, Apr. 2015, doi: 10.1007/s10286-014-0255-9.

[25] P. Martínez-García, C. Lerma, and O. Infante, “Baroreflex sensitivity estimation by the sequence method with delayed signals,” *Clinical Autonomic Research*, vol. 22, no. 6, pp. 289–297, Dec. 2012, doi: 10.1007/s10286-012-0173-7.

[26] M. Javorka *et al.*, “Baroreflex analysis in diabetes mellitus: linear and nonlinear approaches.,” *Med Biol Eng Comput*, vol. 49, no. 3, pp. 279–88, Mar. 2011, doi: 10.1007/s11517-010-0707-x.

[27] G. Gulli, V. E. Claydon, V. L. Cooper, and R. Hainsworth, “R-R interval-blood pressure interaction in subjects with different tolerances to orthostatic stress.,” *Exp Physiol*, vol. 90, no. 3, pp. 367–75, May 2005, doi: 10.1113/expphysiol.2004.029496.

[28] V. E. Claydon and A. v. Krassioukov, “Clinical correlates of frequency analyses of cardiovascular control after spinal cord injury,” *American Journal of Physiology-Heart and Circulatory Physiology*, vol. 294, no. 2, pp. H668–H678, Feb. 2008, doi: 10.1152/ajpheart.00869.2007.

[29] M. Jíra, E. Závodná, N. Honzíková, Z. Nováková, and B. Fišer, “Baroreflex sensitivity as an individual characteristic feature,” *Physiol Res*, pp. 349–351, 2006, doi: 10.33549/physiolres.930814.

[30] G. Parati *et al.*, “Evaluation of the baroreceptor-heart rate reflex by 24-hour intra-arterial blood pressure monitoring in humans.,” *Hypertension*, vol. 12, no. 2, pp. 214–22, Aug. 1988, doi: 10.1161/01.hyp.12.2.214.

[31] S. Y. Kim and D. E. Euler, “Baroreflex Sensitivity Assessed by Complex Demodulation of Cardiovascular Variability,” *Hypertension*, vol. 29, no. 5, pp. 1119–1125, May 1997, doi: 10.1161/01.HYP.29.5.1119.

[32] R. Maestri *et al.*, “Day-by-day variability of spontaneous baroreflex sensitivity measurements: implications for their reliability in clinical and research applications.,” *J Hypertens*, vol. 27, no. 4, pp. 806–12, Apr. 2009, doi: 10.1097/HJH.0b013e328322fe4b.

[33] D. L. Eckberg and T. A. Kuusela, “Human vagal baroreflex sensitivity fluctuates widely and rhythmically at very low frequencies,” *Journal of Physiology*, vol. 567, no. 3, pp. 1011–1019, Sep. 2005, doi: 10.1113/jphysiol.2005.091090.

[34] J. Svačinová, N. Honzíková, A. Krtička, I. Tonhajzerová, K. Javorka, and M. Javorka, “Diagnostic significance of a mild decrease of baroreflex sensitivity with respect to heart rate in type 1 diabetes mellitus.,” *Physiol Res*, vol. 62, no. 6, pp. 605–13, 2013, doi: 10.33549/physiolres.932510.

[35] M. V Pitzalis *et al.*, “Age effect on phase relations between respiratory oscillations of the RR interval and systolic pressure.,” *Pacing Clin Electrophysiol*, vol. 23, no. 5, pp. 847–53, May 2000, doi: 10.1111/j.1540-8159.2000.tb00854.x.

[36] J. Tank *et al.*, “Reference values of indices of spontaneous baroreceptor reflex sensitivity,” *Am J Hypertens*, vol. 13, no. 3, pp. 268–275, Mar. 2000, doi: 10.1016/S0895-7061(99)00172-7.

[37] S. Dawson, “Older subjects show no age-related decrease in cardiac baroreceptor sensitivity,” *Age Ageing*, vol. 28, no. 4, pp. 347–353, Jul. 1999, doi: 10.1093/ageing/28.4.347.

[38] G. Piccirillo *et al.*, “Influence of aging on cardiac baroreflex sensitivity determined non-invasively by power spectral analysis.,” *Clin Sci (Lond)*, vol. 100, no. 3, pp. 267–74, Mar. 2001.

[39] D. Wichterle, V. Melenovsky, L. Necasova, J. Kautzner, and M. Malik, “Stability of the noninvasive baroreflex sensitivity assessment using cross-spectral analysis of heart rate and arterial blood pressure variabilities.,” *Clin Cardiol*, vol. 23, no. 3, pp. 201–4, Mar. 2000, doi: 10.1002/clc.4960230313.

[40] P. van de Borne, H. Nguyen, P. Biston, P. Linkowski, and J. P. Degaute, “Effects of wake and sleep stages on the 24-h autonomic control of blood pressure and heart rate in recumbent men,” *American Journal of Physiology-Heart and Circulatory Physiology*, vol. 266, no. 2, pp. H548–H554, Feb. 1994, doi: 10.1152/ajpheart.1994.266.2.H548.

[41] N. Honzikova, B. Fiser, and B. Semrad, “Critical value of baroreflex sensitivity determined by spectral analysis in risk stratification after myocardial infarction.,” *Pacing Clin Electrophysiol*, vol. 23, no. 11 Pt 2, pp. 1965–7, Nov. 2000, doi: 10.1111/j.1540-8159.2000.tb07063.x.

[42] M. S. Alnoor, H. K. Varner, I. J. Butler, L. Zhu, and M. T. Numan, “Baroreceptor activity and sensitivity: normal values in children and young adults using the head up tilt test.,” *Pediatr Res*, vol. 85, no. 6, pp. 841–847, 2019, doi: 10.1038/s41390-019-0327-6.

[43] A. Kardos, G. Watterich, R. de Menezes, M. Csanády, B. Casadei, and L. Rudas, “Determinants of Spontaneous Baroreflex Sensitivity in a Healthy Working Population,” *Hypertension*, vol. 37, no. 3, pp. 911–916, Mar. 2001, doi: 10.1161/01.HYP.37.3.911.

[44] H. Suarez-Roca *et al.*, “Contribution of Baroreceptor Function to Pain Perception and Perioperative Outcomes,” *Anesthesiology*, vol. 130, no. 4, pp. 634–650, Apr. 2019, doi: 10.1097/ALN.0000000000002510.

[45] Y. P. Wang, R. L. Shih, C. L. Huang, H. H. Huang, and S. K. Tsai, “Differential change in cardiac baroreflex sensitivity estimated by sequence and spectral analysis during etomidate anesthesia.,” *Clin Auton Res*, vol. 10, no. 3, pp. 117–21, Jun. 2000, doi: 10.1007/BF02278015.

[46] J. Gasch, M. Reimann, H. Reichmann, H. Rüdiger, and T. Ziemssen, “Determination of Baroreflex Sensitivity during the Modified Oxford Maneuver by Trigonometric Regressive Spectral Analysis,” *PLoS One*, vol. 6, no. 3, p. e18061, Mar. 2011, doi: 10.1371/journal.pone.0018061.

[47] A. C. Chao *et al.*, “Noninvasive Assessment of Spontaneous Baroreflex Sensitivity and Heart Rate Variability in Patients with Carotid Stenosis,” *Cerebrovascular Diseases*, vol. 16, no. 2, pp. 151–157, 2003, doi: 10.1159/000070595.

[48] T. G. Papaioannou *et al.*, “Assessment of arterial baroreflex sensitivity by different computational analyses of pressure wave signals alone,” *Comput Methods Programs Biomed*, vol. 172, pp. 25–34, Apr. 2019, doi: 10.1016/j.cmpb.2019.02.002.

[49] S. Tiinanen, M. Tulppo, and T. Seppanen, “Reducing the Effect of Respiration in Baroreflex Sensitivity Estimation With Adaptive Filtering,” *IEEE Trans Biomed Eng*, vol. 55, no. 1, pp. 51–59, Jan. 2008, doi: 10.1109/TBME.2007.897840.

[50] G. Parati, M. Di Rienzo, and G. Mancia, “Dynamic modulation of baroreflex sensitivity in health and disease.,” *Ann N Y Acad Sci*, vol. 940, no. 1, pp. 469–87, Jun. 2001, doi: 10.1111/j.1749-6632.2001.tb03699.x.

[51] J. Parlow, J.-P. Viale, G. Annat, R. Hughson, and L. Quintin, “Spontaneous Cardiac Baroreflex in Humans,” *Hypertension*, vol. 25, no. 5, pp. 1058–1068, May 1995, doi: 10.1161/01.HYP.25.5.1058.

[52] J. P. Fisher, S. Ogoh, C. Junor, A. Khaja, M. Northrup, and P. J. Fadel, “Spontaneous baroreflex measures are unable to detect age-related impairments in cardiac baroreflex function during dynamic exercise in humans.,” *Exp Physiol*, vol. 94, no. 4, pp. 447–58, Apr. 2009, doi: 10.1113/expphysiol.2008.044867.

[53] O. Ormezzano, J.-L. Cracowski, J.-L. Quesada, H. Pierre, J.-M. Mallion, and J.-P. Baguet, "EVAluation of the prognostic value of BARoreflex sensitivity in hypertensive patients: the EVABAR study.," *J Hypertens*, vol. 26, no. 7, pp. 1373–8, Jul. 2008, doi: 10.1097/HJH.0b013e3283015e5a.

[54] G. A. R. del Paso, "A program to assess baroreceptor cardiac reflex function," *Behavior Research Methods, Instruments, & Computers*, vol. 26, no. 1, pp. 62–64, Mar. 1994, doi: 10.3758/BF03204567.

[55] B. E. Westerhof, J. Gisolf, W. J. Stok, K. H. Wesseling, and J. M. Karemaker, "Time-domain cross-correlation baroreflex sensitivity," *J Hypertens*, vol. 22, no. 7, pp. 1371–1380, Jul. 2004, doi: 10.1097/01.hjh.0000125439.28861.ed.

[56] H. W. Robbe, L. J. Mulder, H. Rüddel, W. A. Langewitz, J. B. Veldman, and G. Mulder, "Assessment of baroreceptor reflex sensitivity by means of spectral analysis.," *Hypertension*, vol. 10, no. 5, pp. 538–543, Nov. 1987, doi: 10.1161/01.HYP.10.5.538.

[57] D. D. O'Leary, D. C. Lin, and R. L. Hughson, "Determination of baroreflex gain using auto-regressive moving-average analysis during spontaneous breathing.," *Clin Physiol*, vol. 19, no. 5, pp. 369–77, Sep. 1999, doi: 10.1046/j.1365-2281.1999.00190.x.

[58] A. Bauer *et al.*, "Bivariate phase-rectified signal averaging for assessment of spontaneous baroreflex sensitivity: pilot study of the technology.," *J Electrocardiol*, vol. 43, no. 6, pp. 649–53, doi: 10.1016/j.jelectrocard.2010.05.012.

[59] M. Ducher *et al.*, "A New Non-Invasive Statistical Method to Assess the Spontaneous Cardiac Baroreflex in Humans," *Clin Sci*, vol. 88, no. 6, pp. 651–655, Jun. 1995, doi: 10.1042/cs0880651.

[60] R. W. de Boer and J. M. Karemaker, "Cross-Wavelet Time-Frequency Analysis Reveals Sympathetic Contribution to Baroreflex Sensitivity as Cause of Variable Phase Delay Between Blood Pressure and Heart Rate," *Front Neurosci*, vol. 13, Jul. 2019, doi: 10.3389/fnins.2019.00694.

[61] A. Chao-Ecija and M. S. Dawid-Milner, "BaroWavelet: An R-based tool for dynamic baroreflex evaluation through wavelet analysis techniques," *Comput Methods Programs Biomed*, vol. 242, Dec. 2023, doi: 10.1016/j.cmpb.2023.107758.

[62] M. Orini, P. Laguna, L. T. Mainardi, and R. Bailón, "Assessment of the dynamic interactions between heart rate and arterial pressure by the cross time-frequency analysis," *Physiol Meas*, vol. 33, no. 3, pp. 315–331, 2012, doi: 10.1088/0967-3334/33/3/315.

[63] A. Kazimierska, M. M. Placek, A. Uryga, P. Wachel, M. Burzyńska, and M. Kasprowicz, "Assessment of Baroreflex Sensitivity Using Time-Frequency Analysis during Postural Change and Hypercapnia," *Comput Math Methods Med*, vol. 2019, 2019, doi: 10.1155/2019/4875231.

[64] R. Barbieri, G. Parati, and J. P. Saul, "Closed- versus open-loop assessment of heart rate baroreflex," *IEEE Engineering in Medicine and Biology Magazine*, vol. 20, no. 2, pp. 33–42, 2001, doi: 10.1109/51.917722.

[65] R. L. Hughson, L. Quintin, G. Annat, Y. Yamamoto, and C. Gharib, "Spontaneous baroreflex by sequence and power spectral methods in humans.," *Clin Physiol*, vol. 13, no. 6, pp. 663–76, Nov. 1993, doi: 10.1111/j.1475-097x.1993.tb00481.x.

[66] G. Nollo, L. Faes, A. Porta, R. Antolini, and F. Ravelli, “Exploring directionality in spontaneous heart period and systolic pressure variability interactions in humans: implications in the evaluation of baroreflex gain.,” *Am J Physiol Heart Circ Physiol*, vol. 288, no. 4, pp. H1777-85, Apr. 2005, doi: 10.1152/ajpheart.00594.2004.

[67] R. Maestri, G. D. Pinna, A. Mortara, M. T. La Rovere, and L. Tavazzi, “Assessing baroreflex sensitivity in post-myocardial infarction patients: comparison of spectral and phenylephrine techniques.,” *J Am Coll Cardiol*, vol. 31, no. 2, pp. 344–51, Feb. 1998, doi: 10.1016/s0735-1097(97)00499-3.

[68] M. T. la Rovere, R. Maestri, and G. D. Pinna, “Baroreflex Sensitivity Assessment – Latest Advances and Strategies,” *European Cardiology Review*, vol. 7, no. 2, p. 89, 2011, doi: 10.15420/ecr.2011.7.2.89.

[69] G. Nollo, A. Porta, L. Faes, M. del Greco, M. Disertori, and F. Ravelli, “Causal linear parametric model for baroreflex gain assessment in patients with recent myocardial infarction.,” *Am J Physiol Heart Circ Physiol*, vol. 280, no. 4, pp. H1830-9, Apr. 2001, doi: 10.1152/ajpheart.2001.280.4.H1830.

[70] A. Porta, V. Bari, T. Bassani, A. Marchi, V. Pistuddi, and M. Ranucci, “Model-based causal closed-loop approach to the estimate of baroreflex sensitivity during propofol anesthesia in patients undergoing coronary artery bypass graft.,” *J Appl Physiol (1985)*, vol. 115, no. 7, pp. 1032–42, Oct. 2013, doi: 10.1152/japplphysiol.00537.2013.

[71] P. B. Persson *et al.*, “Time versus frequency domain techniques for assessing baroreflex sensitivity,” *J Hypertens*, vol. 19, no. 10, pp. 1699–1705, Oct. 2001, doi: 10.1097/00004872-200110000-00001.

[72] R. De Boer, J. Karemaker, and G. Montfrans, “Determination of baroreflex sensitivity by spectral analysis of spontaneous blood-pressure and heart-rate fluctuations in man,” 1986, pp. 303–316.

[73] P. Bothová *et al.*, “Comparison of baroreflex sensitivity determined by cross-spectral analysis at respiratory and 0.1 Hz frequencies in man.,” *Physiol Res*, vol. 59 Suppl 1, pp. S103–S111, 2010, doi: 10.33549/physiolres.932009.

[74] A. P. Blaber, Y. Yamamoto, and R. L. Hughson, “Methodology of spontaneous baroreflex relationship assessed by surrogate data analysis,” *American Journal of Physiology-Heart and Circulatory Physiology*, vol. 268, no. 4, pp. H1682–H1687, Apr. 1995, doi: 10.1152/ajpheart.1995.268.4.H1682.

[75] A. P. Blaber, Y. Yamamoto, and R. L. Hughson, “Change in phase relationship between SBP and R-R interval during lower body negative pressure.,” *Am J Physiol*, vol. 268, no. 4 Pt 2, pp. H1688-93, Apr. 1995, doi: 10.1152/ajpheart.1995.268.4.H1688.

[76] G. Parati, A. Frattola, M. Di Rienzo, P. Castiglioni, A. Pedotti, and G. Mancia, “Effects of aging on 24-h dynamic baroreceptor control of heart rate in ambulant subjects.,” *Am J Physiol*, vol. 268, no. 4 Pt 2, pp. H1606-12, Apr. 1995, doi: 10.1152/ajpheart.1995.268.4.H1606.

[77] G. A. Reyes del Paso and Ma. I. González, “Modification of Baroreceptor Cardiac Reflex Function by Biofeedback,” *Appl Psychophysiol Biofeedback*, vol. 29, no. 3, pp. 197–211, Sep. 2004, doi: 10.1023/B:APBI.0000039058.68746.ad.

[78] A. Frattola *et al.*, “Time and frequency domain estimates of spontaneous baroreflex sensitivity provide early detection of autonomic dysfunction in diabetes mellitus.,” *Diabetologia*, vol. 40, no. 12, pp. 1470–5, Dec. 1997, doi: 10.1007/s001250050851.

[79] M. di Rienzo, P. Castiglioni, and G. Parati, “The sequence technique revised: additional concepts on the assessment of spontaneous baroreflex function.,” in *2010 Annual International Conference of the IEEE Engineering in Medicine and Biology*, IEEE, Aug. 2010, pp. 1703–1705. doi: 10.1109/IEMBS.2010.5626844.

[80] G. A. R. del Paso, “A biofeedback system of baroreceptor cardiac reflex sensitivity,” *Appl Psychophysiol Biofeedback*, vol. 24, no. 1, pp. 67–77, 1999, doi: 10.1023/A:1022899115220.

[81] A. Toner, N. Jenkins, and G. L. Ackland, “Baroreflex impairment and morbidity after major surgery,” *Br J Anaesth*, vol. 117, no. 3, pp. 324–331, Sep. 2016, doi: 10.1093/bja/aew257.

[82] B. de Maria *et al.*, “Separating arterial pressure increases and decreases in assessing cardiac baroreflex sensitivity via sequence and bivariate phase-rectified signal averaging techniques.,” *Med Biol Eng Comput*, vol. 56, no. 7, pp. 1241–1252, Jul. 2018, doi: 10.1007/s11517-017-1765-0.

[83] G. M. De Ferrari *et al.*, “Rapid recovery of baroreceptor reflexes in acute myocardial infarction is a marker of effective tissue reperfusion.,” *J Cardiovasc Transl Res*, vol. 7, no. 6, pp. 553–9, Aug. 2014, doi: 10.1007/s12265-014-9578-0.

[84] L. C. Davies, D. P. Francis, A. C. Scott, P. Ponikowski, M. Piepoli, and A. J. Coats, “Effect of altering conditions of the sequence method on baroreflex sensitivity.,” *J Hypertens*, vol. 19, no. 7, pp. 1279–87, Jul. 2001, doi: 10.1097/00004872-200107000-00013.

[85] D. Laude *et al.*, “Comparison of various techniques used to estimate spontaneous baroreflex sensitivity (the EuroBaVar study),” *American Journal of Physiology-Regulatory, Integrative and Comparative Physiology*, vol. 286, no. 1, pp. R226–R231, Jan. 2004, doi: 10.1152/ajpregu.00709.2002.

[86] K. H. Wesseling, “Should baroreflex sensitivity be corrected for heart rate?,” *J Hypertens*, vol. 21, no. 11, pp. 2015–2018, Nov. 2003, doi: 10.1097/00004872-200311000-00008.

[87] C. Abrahamsson, C. ??hlund, M. Nordlander, and L. Lind, “A method for heart rate-corrected estimation of baroreflex sensitivity,” *J Hypertens*, vol. 21, no. 11, pp. 2133–2140, Nov. 2003, doi: 10.1097/00004872-200311000-00023.

[88] S. Ward, S. Ryan, W. T. M. Nicholas, and C. Heneghan, “Comparison of baroreflex sensitivity measures for assessing subjects with Obstructive Sleep Apnea,” in *2006 International Conference of the IEEE Engineering in Medicine and Biology Society*, IEEE, Aug. 2006, pp. 3572–3575. doi: 10.1109/IEMBS.2006.259621.

[89] M. Di Rienzo, G. Parati, P. Castiglioni, R. Tordi, G. Mancia, and A. Pedotti, “Baroreflex effectiveness index: an additional measure of baroreflex control of heart rate in daily life,” *American Journal of Physiology-Regulatory, Integrative and Comparative Physiology*, vol. 280, no. 3, pp. R744–R751, Mar. 2001, doi: 10.1152/ajpregu.2001.280.3.R744.

[90] J. C. Watso, M. C. Babcock, K. U. Migdal, and A. T. Robinson, “The baroreflex effectiveness index as an early marker of autonomic dysfunction in heart failure,” *J Physiol*, vol. 595, no. 15, pp. 5013–5014, Aug. 2017, doi: 10.1113/JP274664.

[91] S. Wang *et al.*, “Blood pressure regulation in diabetic patients with and without peripheral neuropathy.,” *Am J Physiol Regul Integr Comp Physiol*, vol. 302, no. 5, pp. R541-50, Mar. 2012, doi: 10.1152/ajpregu.00174.2011.

[92] M. Johansson *et al.*, “Baroreflex effectiveness index and baroreflex sensitivity predict all-cause mortality and sudden death in hypertensive patients with chronic renal failure,” *J Hypertens*, vol. 25, no. 1, pp. 163–168, Jan. 2007, doi: 10.1097/01.hjh.0000254377.18983.eb.

[93] G. A. Reyes del Paso, J. A. Hernández, and M. I. González, “Differential evaluation of the baroreceptor cardiac reflex effectiveness as a function of sequence length,” *International Journal of Psychophysiology*, vol. 59, no. 2, pp. 91–96, Feb. 2006, doi: 10.1016/j.ijpsycho.2005.02.006.

[94] Y.-P. Wang, T. B. J. Kuo, C.-T. Lai, G.-S. Lee, and C. C. H. Yang, “Effects of breathing frequency on baroreflex effectiveness index and spontaneous baroreflex sensitivity derived by sequence analysis.,” *J Hypertens*, vol. 30, no. 11, pp. 2151–8, Nov. 2012, doi: 10.1097/HJH.0b013e328357ff46.

[95] G. D. Pinna, R. Maestri, G. Raczak, and M. T. La Rovere, “Measuring baroreflex sensitivity from the gain function between arterial pressure and heart period.,” *Clin Sci (Lond)*, vol. 103, no. 1, pp. 81–8, Jul. 2002, doi: 10.1042/cs1030081.

[96] G. D. Pinna and R. Maestri, “Reliability of transfer function estimates in cardiovascular variability analysis.,” *Med Biol Eng Comput*, vol. 39, no. 3, pp. 338–47, May 2001, doi: 10.1007/BF02345289.

[97] J. Frederiks *et al.*, “The importance of high-frequency paced breathing in spectral baroreflex sensitivity assessment.,” *J Hypertens*, vol. 18, no. 11, pp. 1635–44, Nov. 2000, doi: 10.1097/00004872-200018110-00015.

[98] N. Honzíková, B. Fiser, and J. Honzík, “Noninvasive determination of baroreflex sensitivity in man by means of spectral analysis.,” *Physiol Res*, vol. 41, no. 1, pp. 31–7, 1992, [Online]. Available: http://www.ncbi.nlm.nih.gov/pubmed/1610775

[99] F. Conci, M. di Rienzo, and P. Castiglioni, “Blood pressure and heart rate variability and baroreflex sensitivity before and after brain death.,” *J Neurol Neurosurg Psychiatry*, vol. 71, no. 5, pp. 621–31, Nov. 2001, doi: 10.1136/jnnp.71.5.621.

[100] R. W. deBoer, J. M. Karemaker, and J. Strackee, “Hemodynamic fluctuations and baroreflex sensitivity in humans: a beat-to-beat model,” *American Journal of Physiology-Heart and Circulatory Physiology*, vol. 253, no. 3, pp. H680–H689, Sep. 1987, doi: 10.1152/ajpheart.1987.253.3.H680.

[101] M. A. James, R. B. Panerai, and J. F. Potter, “Applicability of new techniques in the assessment of arterial baroreflex sensitivity in the elderly: a comparison with established pharmacological methods.,” *Clin Sci (Lond)*, vol. 94, no. 3, pp. 245–53, Mar. 1998, doi: 10.1042/cs0940245.

[102] G. D. Pinna, A. Porta, R. Maestri, B. De Maria, L. A. Dalla Vecchia, and M. T. La Rovere, “Different estimation methods of spontaneous baroreflex sensitivity have different predictive value in heart failure patients.,” *J Hypertens*, vol. 35, no. 8, pp. 1666–1675, 2017, doi: 10.1097/HJH.0000000000001377.

[103] J. Tank, A. Neuke, A. Mölle, J. Jordan, and M. Weck, “Spontaneous baroreflex sensitivity and heart rate variability are not superior to classic autonomic testing in older patients with type 2

diabetes.," *Am J Med Sci*, vol. 322, no. 1, pp. 24–30, Jul. 2001, doi: 10.1097/00000441-200107000-00005.

[104] R. Iida, K. Hirayanagi, K. Iwasaki, S. Ogawa, H. Suzuki, and K. Yajima, "Non-invasive assessment of human baroreflex during different body positions.," *J Auton Nerv Syst*, vol. 75, no. 2–3, pp. 164–70, Feb. 1999, doi: 10.1016/s0165-1838(98)00188-x.

[105] R. H. Clayton, A. J. Bowman, G. A. Ford, and A. Murray, "Measurement of baroreflex gain from heart rate and blood pressure spectra: a comparison of spectral estimation techniques," *Physiol Meas*, vol. 16, no. 2, pp. 131–139, May 1995, doi: 10.1088/0967-3334/16/2/005.

[106] L. Faes, M. Masè, G. Nollo, K. H. Chon, and J. P. Florian, "Measuring postural-related changes of spontaneous baroreflex sensitivity after repeated long-duration diving: Frequency domain approaches," *Auton Neurosci*, vol. 178, no. 1–2, pp. 96–102, Nov. 2013, doi: 10.1016/j.autneu.2013.03.006.

[107] L. C. Davies, D. Francis, P. Jurák, T. Kára, M. Piepoli, and A. J. Coats, "Reproducibility of methods for assessing baroreflex sensitivity in normal controls and in patients with chronic heart failure.," *Clin Sci (Lond)*, vol. 97, no. 4, pp. 515–22, Oct. 1999, [Online]. Available: http://www.ncbi.nlm.nih.gov/pubmed/10491352

[108] J. Fernandes Serôdio *et al.*, "The arterial baroreflex effectiveness index in risk stratification of chronic heart failure patients who are candidates for cardiac resynchronization therapy," *Revista Portuguesa de Cardiologia*, vol. 35, no. 6, pp. 343–350, Jun. 2016, doi: 10.1016/j.repc.2015.11.021.

[109] P. Barthel *et al.*, "Spontaneous baroreflex sensitivity: prospective validation trial of a novel technique in survivors of acute myocardial infarction.," *Heart Rhythm*, vol. 9, no. 8, pp. 1288–94, Aug. 2012, doi: 10.1016/j.hrthm.2012.04.017.

[110] B. Paleczny *et al.*, "Assessment of baroreflex sensitivity has no prognostic value in contemporary, optimally managed patients with mild-to-moderate heart failure with reduced ejection fraction: a retrospective analysis of 5-year survival.," *Eur J Heart Fail*, vol. 21, no. 1, pp. 50–58, 2019, doi: 10.1002/ejhf.1306.

[111] T. Kishi and K. Sunagawa, "Baroreflex sensitivity might predict responders to milrinone in patients with heart failure.," *Int Heart J*, vol. 51, no. 6, pp. 411–5, 2010, doi: 10.1536/ihj.51.411.

[112] L. L. Watkins, P. Grossman, and A. Sherwood, "Noninvasive assessment of baroreflex control in borderline hypertension. Comparison with the phenylephrine method.," *Hypertension*, vol. 28, no. 2, pp. 238–43, Aug. 1996, doi: 10.1161/01.hyp.28.2.238.

[113] M. Iacoviello *et al.*, "Independent role of reduced arterial baroreflex sensitivity during head-up tilt testing in predicting vasovagal syncope recurrence.," *Europace*, vol. 12, no. 8, pp. 1149–55, Aug. 2010, doi: 10.1093/europace/euq149.

[114] H. Oka, S. Mochio, M. Yoshioka, M. Morita, and K. Inoue, "Evaluation of Baroreflex Sensitivity by the Sequence Method Using Blood Pressure Oscillations and R–R Interval Changes during Deep Respiration," *Eur Neurol*, vol. 50, no. 4, pp. 230–243, 2003, doi: 10.1159/000073865.

[115] M. T. la Rovere *et al.*, "Comparison of the prognostic values of invasive and noninvasive assessments of baroreflex sensitivity in heart failure.," *J Hypertens*, vol. 29, no. 8, pp. 1546–52, Aug. 2011, doi: 10.1097/HJH.0b013e3283487827.

[116] H. Rüdiger and M. Bald, “Spontaneous baroreflex sensitivity in children and young adults calculated in the time and frequency domain,” *Autonomic Neuroscience*, vol. 93, no. 1–2, pp. 71–78, Oct. 2001, doi: 10.1016/S1566-0702(01)00326-5.

[117] G. Dorantes Mendez *et al.*, “Baroreflex sensitivity variations in response to propofol anesthesia: comparison between normotensive and hypertensive patients.,” *J Clin Monit Comput*, vol. 27, no. 4, pp. 417–26, Aug. 2013, doi: 10.1007/s10877-012-9426-1.

[118] W.-J. Shin, S.-J. Kang, Y.-K. Kim, S.-H. Seong, S.-M. Han, and G.-S. Hwang, “Link between heart rate and blood pressure Mayer wave during general anesthesia.,” *Clin Auton Res*, vol. 21, no. 5, pp. 309–17, Oct. 2011, doi: 10.1007/s10286-011-0115-9.

[119] V. Bari *et al.*, “Comparison of Different Strategies to Assess Cardiac Baroreflex Sensitivity Based on Transfer Function Technique in Patients Undergoing General Anesthesia.,” *Annu Int Conf IEEE Eng Med Biol Soc*, vol. 2018, pp. 2780–2783, Jul. 2018, doi: 10.1109/EMBC.2018.8512782.

[120] L. Bernardi *et al.*, “Slow breathing increases arterial baroreflex sensitivity in patients with chronic heart failure.,” *Circulation*, vol. 105, no. 2, pp. 143–5, Jan. 2002, doi: 10.1161/hc0202.103311.

[121] G. D. Pinna *et al.*, “Applicability and Clinical Relevance of the Transfer Function Method in the Assessment of Baroreflex Sensitivity in Heart Failure Patients,” *J Am Coll Cardiol*, vol. 46, no. 7, pp. 1314–1321, Oct. 2005, doi: 10.1016/j.jacc.2005.06.062.

[122] D. K. Kaufmann, G. Raczak, M. Szwoch, E. Wabich, M. Świątczak, and L. Daniłowicz-Szymanowicz, “Baroreflex sensitivity but not microvolt T-wave alternans can predict major adverse cardiac events in ischemic heart failure.,” *Cardiol J*, Oct. 2020, doi: 10.5603/CJ.a2020.0129.

[123] S. Gouveia, M. G. Scotto, G. D. Pinna, R. Maestri, M. T. la Rovere, and P. J. S. G. Ferreira, “Spontaneous baroreceptor reflex sensitivity for risk stratification of heart failure patients: optimal cut-off and age effects.,” *Clin Sci (Lond)*, vol. 129, no. 12, pp. 1163–72, Dec. 2015, doi: 10.1042/CS20150341.

[124] P. Lantelme *et al.*, “Spontaneous baroreflex sensitivity: toward an ideal index of cardiovascular risk in hypertension?,” *J Hypertens*, vol. 20, no. 5, pp. 935–44, May 2002, doi: 10.1097/00004872-200205000-00029.

[125] D. Lucini, N. Solaro, and M. Pagani, “May autonomic indices from cardiovascular variability help identify hypertension?,” *J Hypertens*, vol. 32, no. 2, pp. 363–73, Feb. 2014, doi: 10.1097/HJH.0000000000000020.

[126] J.-L. Kück *et al.*, “Impairment in Baroreflex Sensitivity in Recent-Onset Type 2 Diabetes Without Progression Over 5 Years.,” *Diabetes*, vol. 69, no. 5, pp. 1011–1019, 2020, doi: 10.2337/db19-0990.

[127] D. Ziegler, D. Laude, F. Akila, and J. L. Elghozi, “Time- and frequency-domain estimation of early diabetic cardiovascular autonomic neuropathy.,” *Clin Auton Res*, vol. 11, no. 6, pp. 369–76, Dec. 2001, doi: 10.1007/BF02292769.

[128] M. Ducher *et al.*, “Noninvasive exploration of cardiac autonomic neuropathy. Four reliable methods for diabetes?,” *Diabetes Care*, vol. 22, no. 3, pp. 388–393, Mar. 1999, doi: 10.2337/diacare.22.3.388.

[129] A. Boysen, M. A. Lewin, W. Hecker, H. E. Leichter, and F. Uhlemann, “Autonomic function testing in children and adolescents with diabetes mellitus.,” *Pediatr Diabetes*, vol. 8, no. 5, pp. 261–4, Oct. 2007, doi: 10.1111/j.1399-5448.2007.00254.x.

[130] P. J. Weston *et al.*, “Abnormal Baroreceptor—Cardiac Reflex Sensitivity is Not Detected by Conventional Tests of Autonomic Function in Patients with Insulin-Dependent Diabetes Mellitus,” *Clin Sci*, vol. 91, no. 1, pp. 59–64, Jul. 1996, doi: 10.1042/cs0910059.

[131] P. J. Weston, M. A. James, R. B. Panerai, P. G. McNally, J. F. Potter, and H. Thurston, “Evidence of defective cardiovascular regulation in insulin-dependent diabetic patients without clinical autonomic dysfunction.,” *Diabetes Res Clin Pract*, vol. 42, no. 3, pp. 141–8, Dec. 1998, doi: 10.1016/s0168-8227(98)00094-1.

[132] N. Honzíková, B. Semrád, B. Fiser, and R. Lábrová, “Baroreflex sensitivity determined by spectral method and heart rate variability, and two-years mortality in patients after myocardial infarction.,” *Physiol Res*, vol. 49, no. 6, pp. 643–50, 2000.

[133] R. Garcia, P. Sosner, D. Laude, S. Hadjadj, D. Herpin, and S. Ragot, “Spontaneous baroreflex sensitivity measured early after acute myocardial infarction is an independent predictor of cardiovascular mortality: results from a 12-year follow-up study.,” *Int J Cardiol*, vol. 177, no. 1, pp. 120–2, Nov. 2014, doi: 10.1016/j.ijcard.2014.09.100.

[134] M. Ranucci, A. Porta, V. Bari, V. Pistuddi, and M. T. la Rovere, “Baroreflex sensitivity and outcomes following coronary surgery.,” *PLoS One*, vol. 12, no. 4, p. e0175008, 2017, doi: 10.1371/journal.pone.0175008.

[135] M. Sykora, J. Diedler, A. Rupp, P. Turcani, A. Rocco, and T. Steiner, “Impaired baroreflex sensitivity predicts outcome of acute intracerebral hemorrhage,” *Crit Care Med*, vol. 36, no. 11, pp. 3074–3079, Nov. 2008, doi: 10.1097/CCM.0b013e31818b306d.

[136] A. Katarzynska-Szymanska *et al.*, “Shortening baroreflex delay in hypertrophic cardiomyopathy patients - an unknown effect of β-blockers,” *Br J Clin Pharmacol*, vol. 75, no. 6, pp. 1516–1524, Jun. 2013, doi: 10.1111/bcp.12027.

[137] S. Genovesi *et al.*, “Baroreceptor sensitivity and baroreceptor effectiveness index in cirrhosis: the relevance of hepatic venous pressure gradient,” *Liver International*, vol. 30, no. 2, pp. 232–239, Feb. 2010, doi: 10.1111/j.1478-3231.2009.02125.x.

[138] K. H. Wesseling *et al.*, “Validity and variability of xBRS: instantaneous cardiac baroreflex sensitivity,” *Physiol Rep*, vol. 5, no. 22, p. e13509, Nov. 2017, doi: 10.14814/phy2.13509.

[139] A. Uryga *et al.*, “Baroreflex sensitivity and heart rate variability are predictors of mortality in patients with aneurysmal subarachnoid haemorrhage.,” *J Neurol Sci*, vol. 394, pp. 112–119, 2018, doi: 10.1016/j.jns.2018.09.014.

[140] T. P. Facioli *et al.*, “The blood pressure variability and baroreflex sensitivity in healthy participants are not determined by sex or cardiorespiratory fitness,” *Blood Press Monit*, vol. 23, no. 5, pp. 260–270, Oct. 2018, doi: 10.1097/MBP.0000000000000338.

[141] A. L. Teixeira, R. Ritti-Dias, D. Antonino, M. Bottaro, P. J. Millar, and L. C. Vianna, “Sex Differences in Cardiac Baroreflex Sensitivity after Isometric Handgrip Exercise.,” *Med Sci Sports Exerc*, vol. 50, no. 4, pp. 770–777, 2018, doi: 10.1249/MSS.0000000000001487.

[142] T. Ku, S. I. Zida, L. N. Harfiya, Y.-H. Li, and Y.-D. Lin, “A Novel Method for Baroreflex Sensitivity Estimation Using Modulated Gaussian Filter,” *Sensors*, vol. 22, no. 12, p. 4618, Jun. 2022, doi: 10.3390/s22124618.

[143] A. S. S. Meel-van den Abeelen, A. H. E. A. van Beek, C. H. Slump, R. B. Panerai, and J. A. H. R. Claassen, “Transfer function analysis for the assessment of cerebral autoregulation using spontaneous oscillations in blood pressure and cerebral blood flow,” 2014, *Elsevier BV*. doi: 10.1016/j.medengphy.2014.02.001.

[144] A. Staffini, T. Svensson, U. Chung, and A. K. Svensson, “Heart Rate Modeling and Prediction Using Autoregressive Models and Deep Learning,” *Sensors*, vol. 22, no. 1, p. 34, Dec. 2021, doi: 10.3390/s22010034.

[145] K. Li, H. Rüdiger, and T. Ziemssen, “Spectral analysis of heart rate variability: Time window matters,” 2019, *Frontiers Media S.A.* doi: 10.3389/fneur.2019.00545.

[146] F. Badilini, P. Maison-Blanche, and P. Coumel, “Heart rate variability in passive tilt test: comparative evaluation of autoregressive and FFT spectral analyses.,” *Pacing Clin Electrophysiol*, vol. 21, no. 5, pp. 1122–32, May 1998, doi: 10.1111/j.1540-8159.1998.tb00159.x.

[147] D. Chemla *et al.*, “Comparison of fast Fourier transform and autoregressive spectral analysis for the study of heart rate variability in diabetic patients,” *Int J Cardiol*, vol. 104, no. 3, pp. 307–313, Oct. 2005, doi: 10.1016/j.ijcard.2004.12.018.

[148] C. A. Swenne, J. Frederiks, P. H. Fischer, W. F. C. Hardeman, M. A. C. Immerzeel-Geerlings, and B. J. Ten Voorde, “Noninvasive baroreflex sensitivity assessment in geriatric patients: feasibility and role of the coherence criterion,” in *Computers in Cardiology 2000. Vol.27 (Cat. 00CH37163)*, IEEE, pp. 45–48. doi: 10.1109/CIC.2000.898451.

[149] T. Kuusela, “Methodological Aspects of Heart Rate Variability Analysis,” in *Heart Rate Variability (HRV) Signal Analysis*, CRC Press, 2012, pp. 9–42. doi: 10.1201/b12756-4.

[150] P. Welch, “The use of fast Fourier transform for the estimation of power spectra: A method based on time averaging over short, modified periodograms,” *IEEE Transactions on Audio and Electroacoustics*, vol. 15, no. 2, pp. 70–73, Jun. 1967, doi: 10.1109/TAU.1967.1161901.

[151] B. Becerra-Luna *et al.*, “Heart rate variability assessment using time-frequency analysis in hypotensive and non-hypotensive patients in hemodialysis,” *Applied Sciences (Switzerland)*, vol. 10, no. 17, Sep. 2020, doi: 10.3390/app10176074.

[152] G. Luo, D. Zhang, Y. Koh, K. Ng, and W. Leong, “Time-frequency entropy-based partial-discharge extraction for nonintrusive measurement,” *IEEE Transactions on Power Delivery*, vol. 27, no. 4, pp. 1919–1927, 2012, doi: 10.1109/TPWRD.2012.2200911.

[153] L. J. Badra *et al.*, “Respiratory modulation of human autonomic rhythms,” *American Journal of Physiology-Heart and Circulatory Physiology*, vol. 280, no. 6, pp. H2674–H2688, Jun. 2001, doi: 10.1152/ajpheart.2001.280.6.H2674.

[154] M. V. PITZALIS *et al.*, “Age Effect on Phase Relations Between Respiratory Oscillations of the RR Interval and Systolic Pressure,” *Pacing and Clinical Electrophysiology*, vol. 23, no. 5, pp. 847–853, May 2000, doi: 10.1111/j.1540-8159.2000.tb00854.x.

[155] P. Borgnat, P. Flandrin, P. Honeine, C. Richard, and J. Xiao, “Testing stationarity with surrogates: A time-frequency approach,” *IEEE Transactions on Signal Processing*, vol. 58, no. 7, pp. 3459–3470, Jul. 2010, doi: 10.1109/TSP.2010.2043971.

[156] A. Kazimierska, M. M. Placek, A. Uryga, P. Wachel, M. Burzyńska, and M. Kasprowicz, “Assessment of Baroreflex Sensitivity Using Time-Frequency Analysis during Postural Change and Hypercapnia,” *Comput Math Methods Med*, vol. 2019, 2019, doi: 10.1155/2019/4875231.

[157] D. Singh, K. Vinod, and S. C. Saxena, “Sampling frequency of the RR interval time series for spectral analysis of heart rate variability,” *J Med Eng Technol*, vol. 28, no. 6, pp. 263–272, Nov. 2004, doi: 10.1080/03091900410001662350.

[158] A. E. Draghici and J. A. Taylor, “The physiological basis and measurement of heart rate variability in humans,” Jan. 13, 2016, *BioMed Central Ltd.* doi: 10.1186/s40101-016-0113-7.

[159] C. Gallet and C. Julien, “The significance threshold for coherence when using the Welch’s periodogram method: Effect of overlapping segments,” *Biomed Signal Process Control*, vol. 6, no. 4, pp. 405–409, Oct. 2011, doi: 10.1016/j.bspc.2010.11.004.

[160] K. Martinmäki, H. Rusko, S. Saalasti, J. Kettunen, and J. Ket, “Ability of short-time Fourier transform method to detect transient changes in vagal effects on hearts: a pharmacological blocking study,” *Am J Physiol Heart Circ Physiol*, vol. 290, pp. 2582–2589, 2006, doi: 10.1152/ajpheart.00058.2005.-Con.

[161] L. J. Badra *et al.*, “Respiratory modulation of human autonomic rhythms,” *American Journal of Physiology-Heart and Circulatory Physiology*, vol. 280, no. 6, pp. H2674–H2688, Jun. 2001, doi: 10.1152/ajpheart.2001.280.6.H2674.

[162] A. H. E. A. Van Beek, J. A. H. R. Claassen, M. G. M. O. Rikkert, and R. W. M. M. Jansen, “Cerebral autoregulation: An overview of current concepts and methodology with special focus on the elderly,” Jun. 30, 2008. doi: 10.1038/jcbfm.2008.13.

[163] G. D. Pinna, R. Maestri, G. Raczak, C. A. Swenne, and M. T. La Rovere, “Baroreflex sensitivity estimation by the transfer function method revised: Effect of changing the coherence criterion,” in *2001 Conference Proceedings of the 23rd Annual International Conference of the IEEE Engineering in Medicine and Biology Society*, IEEE, 2001, pp. 604–607. doi: 10.1109/IEMBS.2001.1019007.

[164] C. Torrence and P. J. Webster, “Interdecadal Changes in the ENSO–Monsoon System,” *J Clim*, vol. 12, no. 8, pp. 2679–2690, Aug. 1999, doi: 10.1175/1520-0442(1999)012<2679:ICITEM>2.0.CO;2.

[165] Y. Zhan, D. Halliday, P. Jiang, X. Liu, and J. Feng, “Detecting time-dependent coherence between non-stationary electrophysiological signals-A combined statistical and time-frequency approach,” *J Neurosci Methods*, vol. 156, no. 1–2, pp. 322–332, Sep. 2006, doi: 10.1016/j.jneumeth.2006.02.013.

[166] T. Akimoto, J. Sugawara, D. Ichikawa, N. Terada, P. J. Fadel, and S. Ogoh, “Enhanced open-loop but not closed-loop cardiac baroreflex sensitivity during orthostatic stress in humans.,” *Am J Physiol Regul Integr Comp Physiol*, vol. 301, no. 5, pp. R1591-8, Nov. 2011, doi: 10.1152/ajpregu.00347.2011.

[167] Y. P. Wang, R. L. Shih, C. L. Huang, H. H. Huang, and S. K. Tsai, “Differential change in cardiac baroreflex sensitivity estimated by sequence and spectral analysis during etomidate anesthesia.,” *Clin Auton Res*, vol. 10, no. 3, pp. 117–21, Jun. 2000, doi: 10.1007/BF02278015.

[168] L. L. Watkins, P. Grossman, and A. Sherwood, “Noninvasive Assessment of Baroreflex Control in Borderline Hypertension,” *Hypertension*, vol. 28, no. 2, pp. 238–243, Aug. 1996, doi: 10.1161/01.HYP.28.2.238.

[169] A. Monti, C. Medigue, H. Nedelcoux, and P. Escourrou, “Autonomic control of the cardiovascular system during sleep in normal subjects.,” *Eur J Appl Physiol*, vol. 87, no. 2, pp. 174–81, Jun. 2002, doi: 10.1007/s00421-002-0597-1.

[170] E. Zavodna *et al.*, “Can we detect the development of baroreflex sensitivity in humans between 11 and 20 years of age?,” *Can J Physiol Pharmacol*, vol. 84, no. 12, pp. 1275–1283, Dec. 2006, doi: 10.1139/y06-060.

[171] I. Bonyhay, M. Risk, and R. Freeman, “High-pass filter characteristics of the baroreflex--a comparison of frequency domain and pharmacological methods.,” *PLoS One*, vol. 8, no. 11, p. e79513, Nov. 2013, doi: 10.1371/journal.pone.0079513.

[172] G. Parati, J. P. Saul, M. Di Rienzo, and G. Mancia, “Spectral analysis of blood pressure and heart rate variability in evaluating cardiovascular regulation. A critical appraisal.,” *Hypertension*, vol. 25, no. 6, pp. 1276–86, Jun. 1995, doi: 10.1161/01.hyp.25.6.1276.

Appendix A: BRS measurement protocol recommendations in different pathological states

Recommendations regarding the BRS measurement protocol related to various pathological states when applying different BRS algorithms are listed below:

1. **CHF**

Sequence method:

The body position of a patient during measurement was most often supine [84], [110] or at a passive tilt of 70°; both are effective positions for BEI estimation. [108]

Signal recording times varied between 5 minutes [111] and 30 minutes [110], but longer recordings are preferred as they allow more time to find valid sequences and produce less biased BRS value. [111]

In all studies analyzed, the breathing pattern was spontaneous.

Thresholds applied

In articles that contained the relevant information, the lag 0 between the SBP change and RRI fluctuation was most frequently used for calculation. [102], [110] Moreover, this lag was also confirmed as the lag which produced the greatest number of sequences and the highest BRS value in CHF patients. [84] The reason for this choice was to select a quick vagal branch of the baroreflex. [102] In reality, the optimal time delay may differ between subjects and subject groups, leading to the observation that one single lag may not be equally well suited for all subjects. [107] The optimal choice for other thresholds may also differ between healthy individuals and those suffering from illness. [84]

However, according to Davies et al. [84], BRS value is not significantly affected by the lag choice, and neither is it materially affected by the correlation coefficient requirement. For this reason, it is generally suggested to use the lag that produces the highest number of sequences. The correlation coefficient criterion should be disregarded. [84]

Nevertheless, when it comes to changing the thresholds for minimal RRI and SBP change, it must be understood that this alteration has a significant effect on both the BRS value and the number of sequences found in the recording. [84] For instance, when the threshold for the RRI change is set at a high level, while at the same time the BP change threshold is set at a low level, the bias towards choosing higher BRS values exists. This maneuver can lead to the search for a specific type of sequence which is rare to find in CHF patients. Hence, the resulting BRS value may represent an artefact rather than the real BRS. [84]

WBA-TF method:

The body position of a patient during measurement was always supine, [102], [115], [123], which is also regarded as the preferred position by different sources. [102]

Signal recording times varied, and recordings shorter than 3 minutes were excluded. [121]

In all studies analyzed, the breathing was controlled outside of the LF band (> 0.15 Hz). [121]

All recordings included for BRS measurement had an ectopic rate below 5%. [123]

2. Hypertension

Sequence method:

The body position of a patient during measurement was most often supine, and this position was recommended for clinical use (instead of standing). [124]

In all studies analyzed, the breathing pattern was spontaneous and the lag of 1 beat was most often applied. [30], [101]

Alpha coefficient method:

The body position of a patient during the measurement was most often supine. This position was preferred to a standing position to identify and compare more easily hypertension to normotension. [125] More artefacts are found during the standing position measurements than in the supine position, which affect the BRS result. [124]

The breathing rate for BRS measurement was spontaneous [20], [124] or kept solely within the HF band (> 0.15 Hz). [125]

The recording time of signals varied between 5 [101] and 20 minutes [20].

3. Diabetes

Sequence method:

The body position of a patient during the measurement was most often supine. [127], [131] However, also standing [127], [131] or 70° passive tilt were used to stimulate BP regulation and heart rate increase. [91]

Signal recording times varied between 3 and 60 minutes. In all studies analyzed, the breathing pattern was spontaneous. [91], [103]

Javorka et al. suggested that, since lower synchronization between RRI and SBP might be a sign of diabetes, BRS measurement in diabetics should not be limited only to BRS gain, but also should include time delay and synchronization/similarity analyses of SBP and RRI. [26]

Thresholds applied

The lag of 1 beat between the SBP change and the following RRI fluctuation was mostly used for calculation in articles that contained this information. [26], [91]

Alpha coefficient method:

The body position of a patient during the measurement was most often supine [126], [131] but also was recorded in a standing position in one study. [131] Breathing was controlled at 0.25 Hz [131] or allowed to be spontaneous. [78], [126] However, it was noted that breathing rates below 9 bpm increases the complexity in the interpretation of power spectral curves [131] and should be avoided.

4. **Post – MI**

Sequence method:

The body position of a patient during the measurement was always supine and the breathing pattern was spontaneous. [32], [83], [109]

Signal recording times varied between 8 [32] and 60 minutes, [83] with longer recordings preferred as they allow more time to find valid sequences and produce less biased BRS value. [32]

Alpha coefficient method:

The body position of a patient during the measurement was supine. [32]

The breathing rate for BRS measurement was spontaneous and paced which improved the reliability, but only for the aHF index. [32] The recording times of signals varied between 8 [67] and 30 minutes. [109]

Original TF method:

The body position of a patient during the measurement was supine. [32], [41], [95], [132] The breathing rate for BRS measurement was paced (> 0.2 Hz) to avoid respiration influence on the LF band. [95] The recording time of signals was 8 minutes[32]

WBA-TF method:

The body position of a patient during the measurement was supine. [32] The breathing rate for BRS measurement was paced (> 0.2 Hz) to avoid respiration influence on the LF band. [32] The recording time of signals was 8 minutes. [32]

Appendix B: Parameter settings for spectral TF analysis of BRS in the literature

Table B.1(A-C) provides an overview of the various parameter settings utilized in the literature when implementing the FFT-based transfer function (TF) method and BRS visualization techniques. Only papers (regardless of BRS medical benefit) that disclosed the relevant information are referenced here, noting that many articles did not include this data or contained incomplete data.

References	FFT method	Record length	Sampling frequency (Hz)	Interpolation type	Detrending method	Segment duration (points/samples/sec)
Wang 2012 [94]	Welch	256 sec – zero padded (1024 data points)	4	cubic spline	linear	512 samples
Akimoto 2011 [166]	Welch	Minimum 10 min	2	linear	linear	256 points
Shin 2011 [118]	Welch	5 min	4	unknown	unknown	100 sec (400 samples)
Tiinanen 2008 [49]	Welch	5 min	2 and 5	-	-	1024 points
Ward 2006[88]	Welch	sleep	1	cubic spline	linear	512 samples
Carrasco- Sosa 2005 [15]	Welch	5 min	4	cubic spline	unknown	-
Badra 2001 [153]	Periodogram	ca. 5 min	5	linear	unknown	60 sec (300 samples)
Wang 2000 [167]	Welch	5 min	4	cubic spline	linear	256 seconds (1024 points) divided into 3x512 samples
Watkins 1996 [168]	Welch	5 min	4	unknown	unknown	60 sec (256 points) which included 240 sample points with zero padding
Monti 2002 [169]	Periodogram	sleep	-	-	-	128 sec (256 FFT size)
Ziegler 2001[127]	Periodogram	unknown	10	not performed	-	102.4 sec (1024 FFT)
Robbe 1987 [56]	-	4.5 min	-	-	-	-
Fisher 2009 [52]	Welch	5 min	2	linear	-	-
Dawson 1999 [37]	Periodogram	5 min	0.5 sec = 2	third order polynomial	-	512 samples
Honzikova et al. aproach						
Svacinova 2013 [34]	Not clear	42 min	10	cubic spline	linear	3 min = 180 sec
Javorka 2011 [26]	Not clear	60 min	4	linear	linear	256 samples
Zavodna 2006 [170]	Not clear	5 min	250 msec = 4	linear	least squares approximation method	240 samples
WBA-TF approach						
Pinna 2002 [95]	Blackman-Tukey	10 min	-	linear	linear	-
Bonyhay 2013 [171]	Blackman-Tukey	7 min	3	-	-	341 seconds (1024 samples)

Table B.1A**:** Transfer function method: Different spectral parameters employed in the literature

References	Window type	Window length	Overlap (% or sec)	Smoothing	Filters	Time resolution (sec)	Frequency resolution (Hz)
Wang 2012	Hanning	-	50 %	-	-	-	0.0078125
Akimoto 2011	Hamming	-	50 %	-	-	-	0.0078125
Shin 2011	Hanning	-	50 seconds (50%)	-	-	-	0.01
Tiinanen 2008 (lower value)	-	-	50 %	-	LMS	-	0.001953125 and 0.0048828125
Ward 2006	-	-	50 %	-	-	-	0.001953125
Carrasco- Sosa 2005	Hanning	32 sec zero padded to 64 sec	16 sec (50%)	-	-	-	-
Badra 2001	Hanning	60 sec	Step 1 sec (sliding window)	triangular smoothing window	low-pass filter (cut-off frequency 0.50 Hz)	-	-
Wang 2000	Hanning	-	50 %	-	-	-	0.0078125
Watkins 1996	Hanning	-	50 %	-	-	-	0.01666666666
Monti 2002	Hamming	-	50%	4-point rectangular moving average	-	64	0.0156
Ziegler 2001	Rectangular	-	-	-	-	-	-
Robbe 1987	-	-	-	-	-	-	0.01 (LF band)
Fisher 2009	-	-	-	-	-	-	-
Dawson 1999	-	-	-	13-point triangular window	low pass filter	-	-
Honzikova et al. approach							
Svacinova 2013	-	-	no overlap	-	-	-	-
Javorka 2011	Hanning	-	90 %	-	-	-	-
Zavodna 2006	Hanning	-	-	-	-	-	-
WBA-TF approach							
Pinna 2002	Parzen	0.03 Hz bandwidth	-	-	-	-	
Bonyhay 2013	Parzen	-	-	-	-	-	-

Table B.1B**:** Transfer function method: Different spectral parameters employed in the literature

References	BRS value estimation (Gain)	Coherence criterion	Phase computed	BRS spectrum visualization	LF range limits (Hz)	HF range limits (Hz)
Wang 2012	yes	>0.5	yes	-	0.05-0.15	-
Akimoto 2011	yes	-	no	-	0.05-0.20	0.20-0.30
Shin 2011	yes	>0.5	yes	2D → BRS over frequency, phase, coherence	0.04-0.15	0.20-0.30
Tiinanen 2008 (lower value)	yes	>0.5	no	-	0.04 – 0.15	-
Ward 2006	yes	>0.5 (if coherence lower, lower the threshold)	no	2D → BRS over time	0.07-0.14	0.14-0.45
Carrasco- Sosa 2005	yes	>0.5	yes	-	0.04-0.15	0.15-0.4
Badra 2001	yes	>0.5 (absolute and partial coherence)	yes	2D → BRS over time, absolute coherence and partial coherence, phase over frequency	0.05-0.15	-
Wang 2000	yes	>0.5	no	2D → BRS over frequency and coherence	0.07-0.14	0.15-0.35
Watkins 1996	yes	>0.5	no	2D → BRS over frequency and coherence	0.070 - 0.129	-
Monti 2002	yes	>0.5	no	-	0.05– 0.13	-
Ziegler 2001	yes	>0.5	no	-	0.049 - 0.137	within the 0.068 Hz bandwidth centered at the respiratory peak
Robbe 1987	yes	>0.5 (arbitrary)	no	2D → BRS over frequency and coherence	0.07-0.14	not relevant
Fisher 2009	yes	yes	yes	-	0.04-0.15	0.15-0.4
Dawson 1999	yes	>0.5	yes	2D → BRS over frequency, phase over frequency	0.05 - 0.15	0.15-0.35
Honzikova et al.						
Svacinova 2013	yes	>0.5	No	-	0.06-0.12	-
Javorka 2011	yes	>0.5	No	-	0.04-0.15	-
Zavodna 2006	yes	>0.5	No	-	0.05-0.15	-
WBA-TF approach						
Pinna 2002	yes	>0.5 (criticized)	No	2D → BRS over frequency, coherence & Interval of confidence	0.04-0.15	-
Bonyhay 2013	yes	>0.5	No	2D →BRS over frequency + SD	0.04-0.15	-

Table B.1C**:** Transfer function method: Different spectral parameters employed in the literature

Appendix C: AR model versus FFT: Spectrum shape differences

In general, spectral characteristics differ between the FFT-based and AR model approaches.

The spectrum produced by the FFT-based method encompasses the entire signal variance, which may yield specific spectral peaks as well as broadband powers lacking distinct peaks across various frequencies. [172]

In contrast, the AR approach yields more distinct spectral peaks due to the selective model order, as segments of the signal inconsistent with the model are excluded from the analysis. As a result, expertise is necessary in selecting the appropriate AR model for a given dataset, as incorrect choices can lead to inaccurate results. [172]

However, Parati et al. [172] also indicated that within BPV and HRV lie not just rhythmic oscillations, but also nonrhythmic fluctuations. They noted that these fluctuations were not clearly defined peaks in the spectrum; instead, they manifest as powers distributed across a broad frequency range. Moreover, these nonrhythmic fluctuations are also relevant in cardiovascular control mechanisms.

It is also worth noting that, under specific circumstances, both the AR and FFT-based methods can yield comparable spectral shapes. (Fig. C.1)

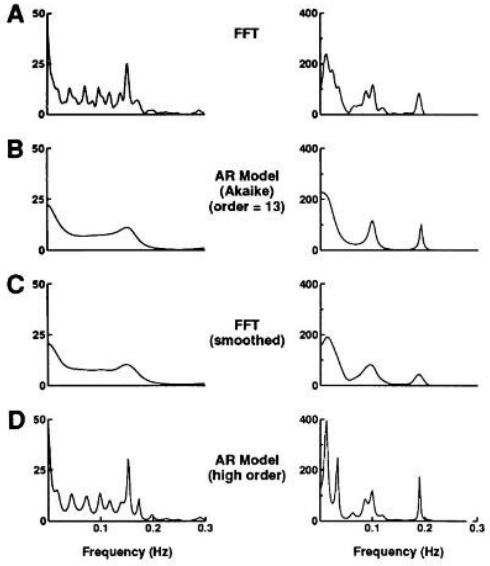

Figure C.1: Spectral shape similarities between the AR modeling and the FFT [172]

Appendix D: Data collection and characteristics

In Fig. D.1 – D.3 (A-B) the original SBP and RRI time series are represented for each subject identified as CU045, CU076 and CU066 separately. Green dashed vertical lines divide the three experimental stages (baseline, stress, recovery), with the short time period between them representing the adaptive phase. Notably, the adaptive period between stress and recovery in all subjects is missing and the adaptive period between the baseline and stress stages is relatively brief in each subject's recording.

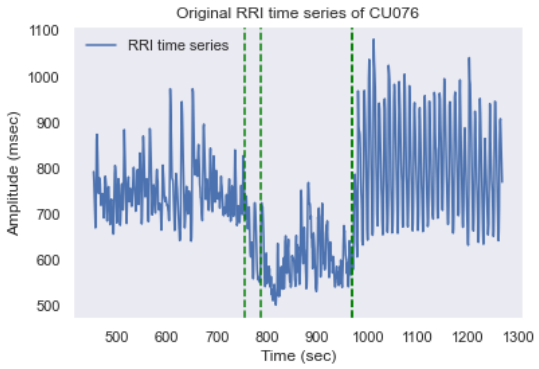

Figure D.1A: Original RRI time series of subject CU076

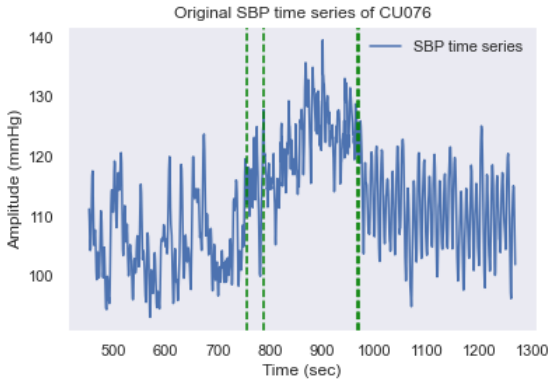

Figure D.1B: Original RRI time series of subject CU076

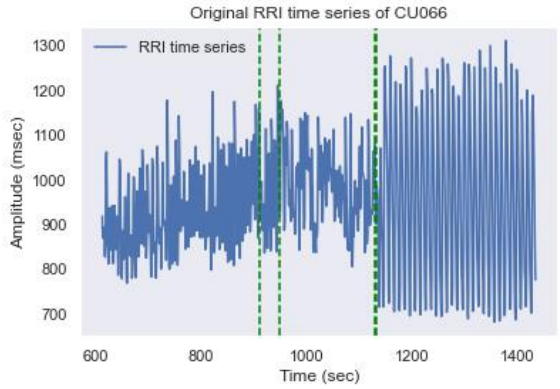

Figure D.2A: Original RRI time series of subject CU066

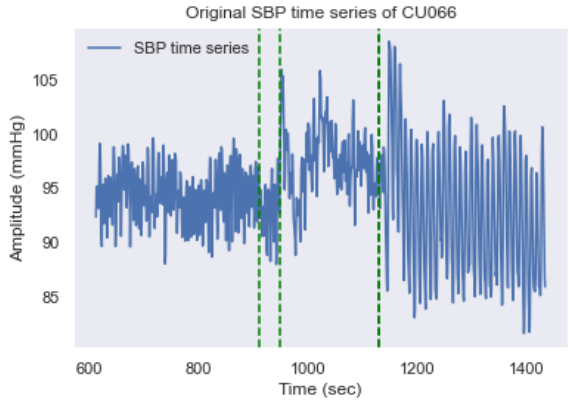

Figure D.2B: Original SBP time series of subject CU066

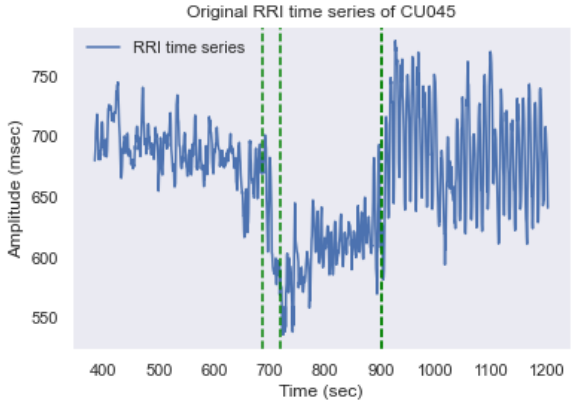

Figure D.3A: Original RRI time series of subject CU045

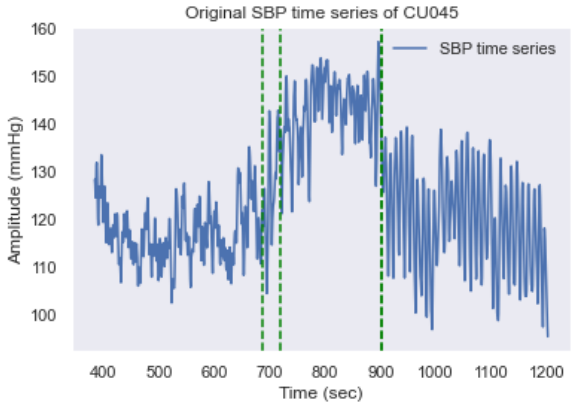

Figure D.3B: Original SBP time series of subject CU045

Table D.1 provides summarized data statistics for all subjects, represented individually by experimental stage:

Patient data ***Baseline***	**RRI Mean + SD (ms)** og	**SBP Mean + SD (mmHg)** og	**RRI CV** og	**RRI Mean + SD (ms)** int	**SBP Mean + SD (mmHg)** int	**RRI CV** int
CU045	687.42 ± 20.15	117.22±6.06	0.029	688.01+19.85	117.22±5.95	0.029
CU076	747.95 ± 55.71	105.26±6.36	0.074	751.68±56.08	105.50±6.38	0.075
CU066	918.80 ± 86.66	94.62±2.42	0.094	925.07 ± 80.88	94.71 ± 2.22	0.087
Stress						
CU045	604.98 ± 25.56	143.08±6.86	0.042	606.02±25.21	143.24±6.73	0.042
CU076	595.44 ± 54.43	122.39±5.92	0.091	600.15±55.42	122.70±5.86	0.092
CU066	977.62 ± 84.23	97.53±3.12	0.086	983.38±78.34	97.67±3.01	0.080
Recovery						
CU045	683.40±42.16	119.39±10.48	0.061	685.94±41.54	119.62±10.32	0.060
CU076	788.29±109.06	110.55±6.54	0.138	802.27±107.00	111.03±6.40	0.133
CU066	918.57±187.11	92.18±5.95	0.203	951.12±180.43	93.04±5.91	0.190

Table D.1: Data statistics (mean ± SD) of subjects CU045, CU076, CU066 outlined across baseline, stress, and recovery stages. Values presented for both the original ('og') and interpolated ('int') RRI and SBP time series. Coefficient of variation (CV) was included for the RRI signal

Appendix E: Data preprocessing steps

Fig. E.1 - E.2 present interpolated (resampled at 4 Hz) and linearly detrended RRI and SBP time series of subject CU076.

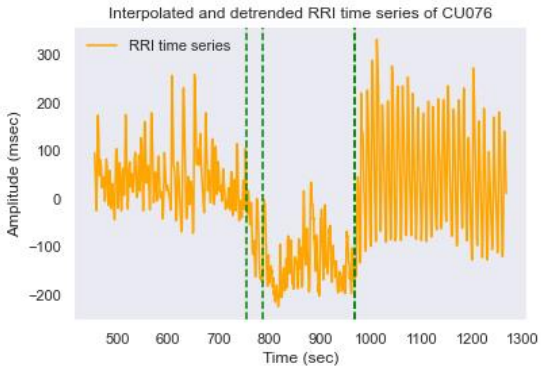

Figure E.1: Interpolated (resampled at 4 Hz) and linearly detrended RRI signal of subject CU076

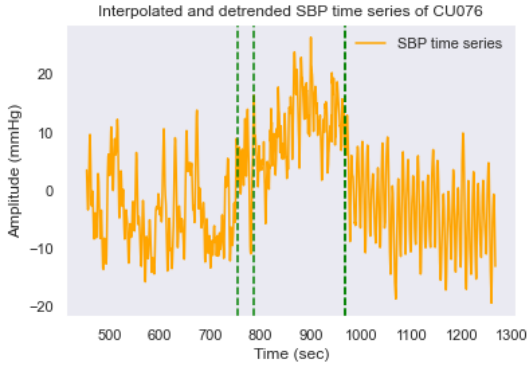

Figure E.2: Interpolated (resampled at 4 Hz) and linearly detrended SBP signal of subject CU076

Appendix F: Welch: 2D and 3D PSD spectrums

In Fig. F.1 – F.4 the PSD of RRI and SBP signals are presented for subjects CU066 and CU045 across experimental stages. The x-axis denotes frequency in Hz, while the y-axis indicates PSD in ms²/Hz or mmHg²/Hz. Notably, the frequency resolution varies among the figures. Detailed information regarding the applied parameter settings can be found in the caption accompanying each figure.

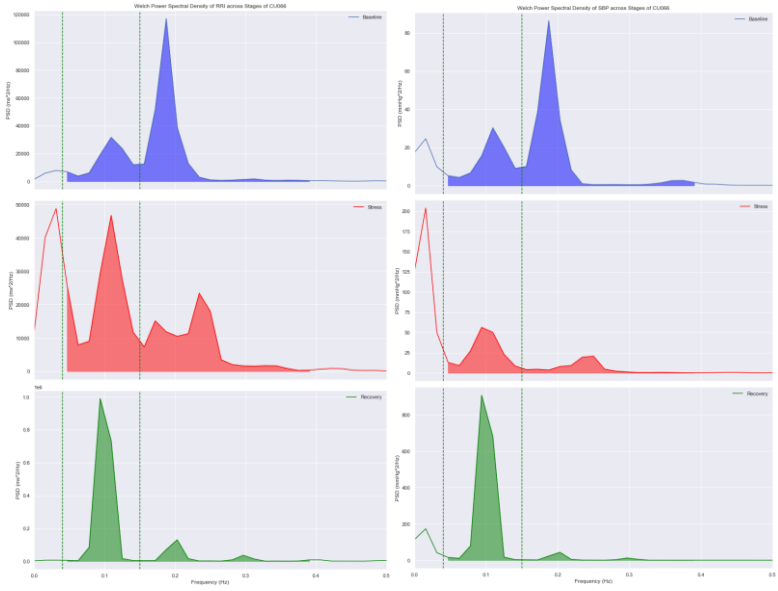

(a) (b)

Figure F.1: (a) The PSD of RRI and (b) SBP by Welch method of subject CU066 for each experimental stage: baseline (purple), stress (red), recovery (green). Frequency resolution set to 0.015 Hz, Hanning window (256 samples) applied with 50% overlap with no zero padding

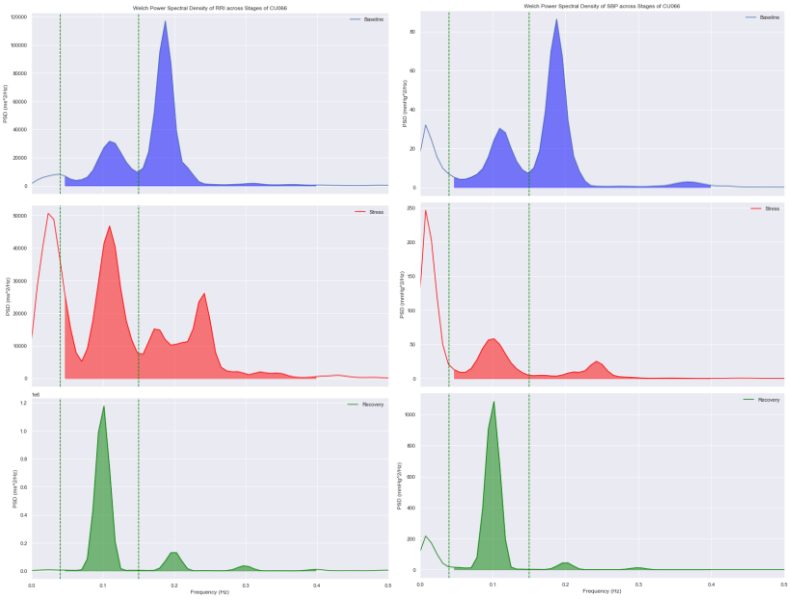

(a) (b)

Figure F.2: (a) The PSD of RRI and (b) SBP by Welch method of subject CU066 for each experimental stage: baseline (purple), stress (red), recovery (green). Frequency resolution set to 0.008 Hz. Hanning window (256 samples) applied with 50% overlap with additional zero padding (FFT size is 512 samples)

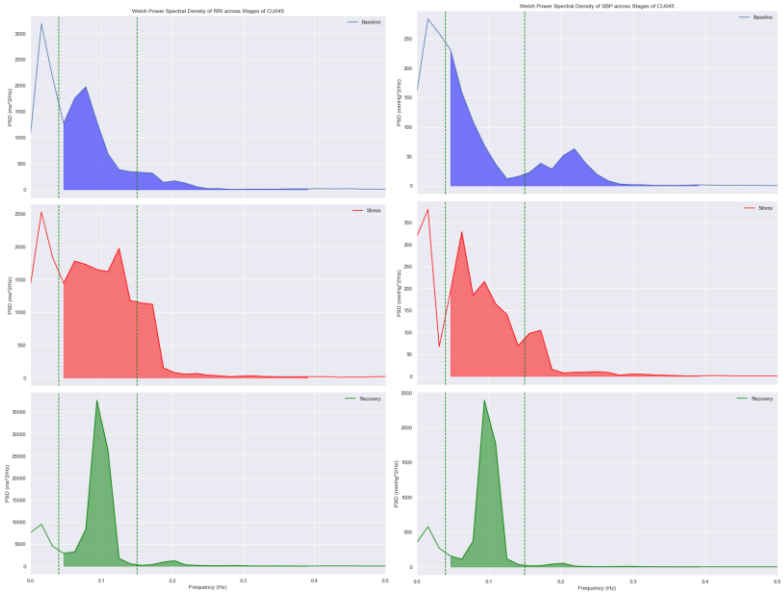

(a) (b)

Figure F.3: (a) The PSD of RRI and (b) SBP by the Welch method of subject CU045 for each experimental stage: baseline (purple), stress (red), recovery (green). Frequency resolution is 0.015 Hz. Hanning window (256 samples) applied with 50% overlap with no zero padding

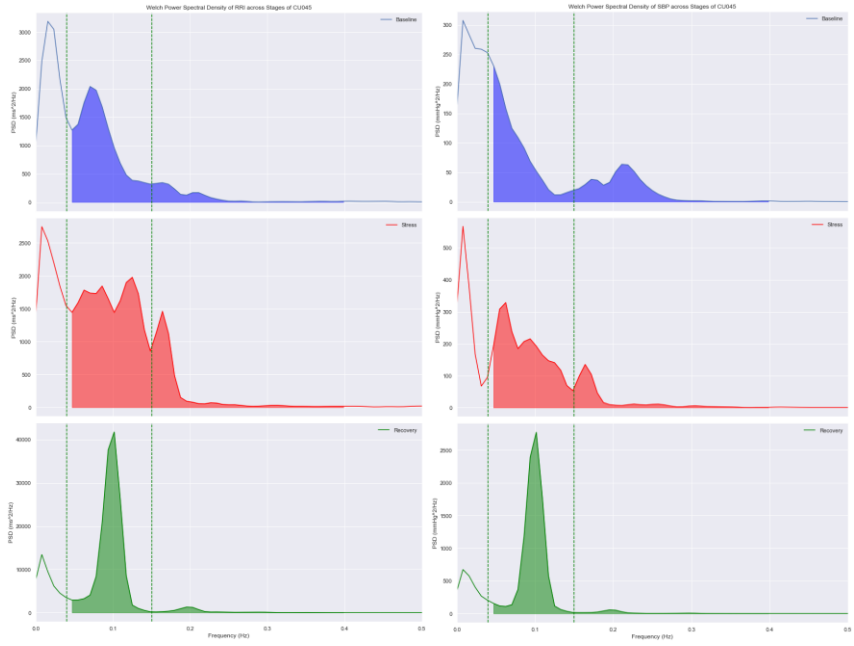

(a) (b)

Figure F.4: (a) The PSD of RRI and (b) SBP by the Welch method of subject CU045 for each experimental stage: baseline (purple), stress (red), recovery (green). Frequency resolution is 0.008 Hz. Hanning window (256 samples) applied with 50% overlap with additional zero padding (FFT size is 512 samples)

Appendix G: STFT: 3D PSD spectrum

The PSD of RRI and SBP computed by STFT-based method for subject CU045 are presented in Fig. G.1 with two different visualization alternatives, as spectrograms or 3D surface plots.

Parameter settings for each visualization are written below each figure (t_{res} – 'quasi' time resolution, f_{res} – frequency resolution, window – window type).

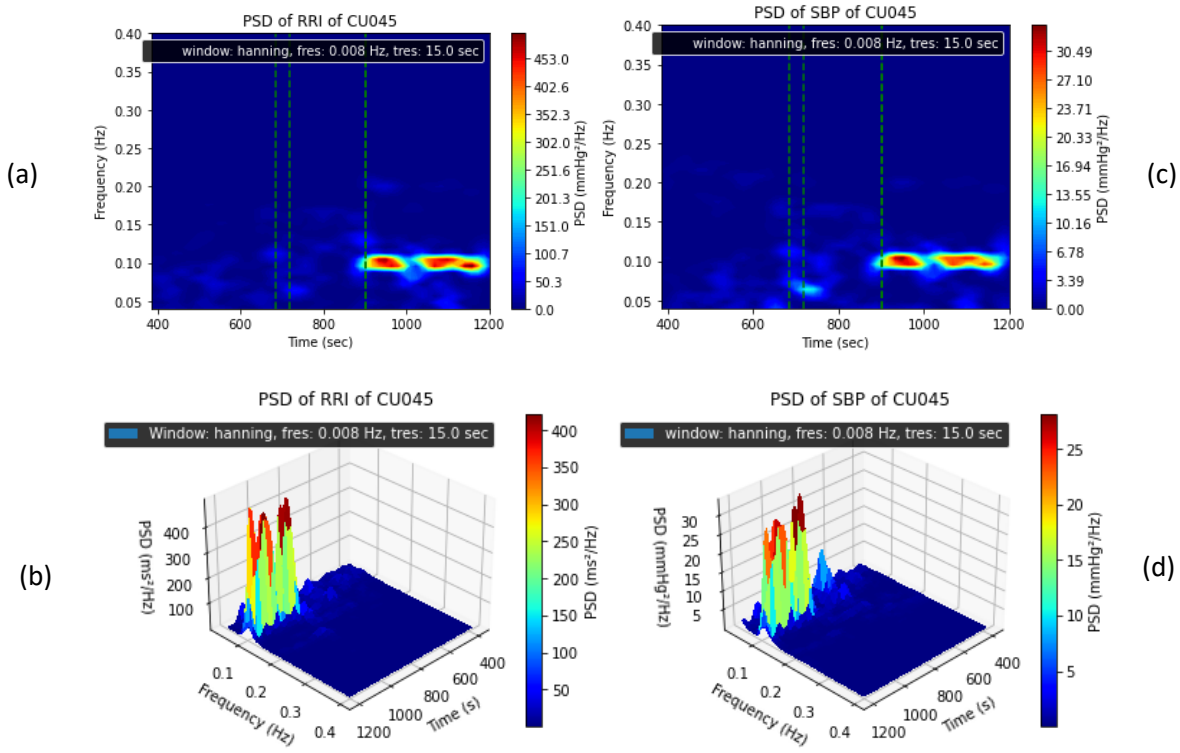

Figure G.1: The PSD of RRI (a,b) and SBP (c,d) by the STFT-based method of subject CU045 with a frequency resolution of 0.008 Hz; (a,b) 3D spectrograms, (c,d) 3D surface plots

Additionally, Fig. G.2 shows the effect of other two frequency resolutions (0.011 and 0.033 Hz) on the spectrogram visualization of subject CU045.

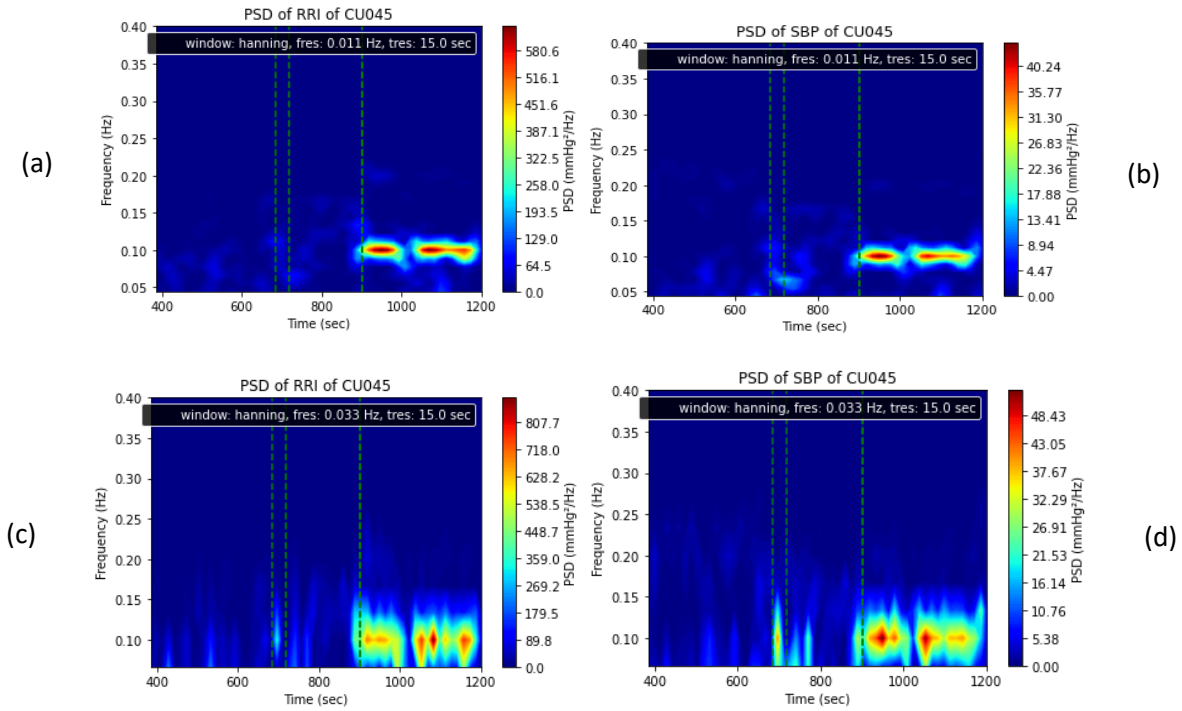

Figure G.2**:** The PSD of RRI (a,c) and SBP (b,d) by the STFT-based method of subject CU045 with different frequency resolutions: (a,b) 0.011, (c,d) 0.033 Hz

Appendix H: Welch: 2D BRS, coherence and phase spectrums

In Fig. H.1 and H.2. 2D plots depict the BRS and phase spectrum, both including coherence spectrums as well, of subject CU066 across three experimental stages.

In each figure, performing zero padding results in a frequency resolution of 0.008 Hz, whereas not performing zero padding yields a resolution of 0.015 Hz.

A

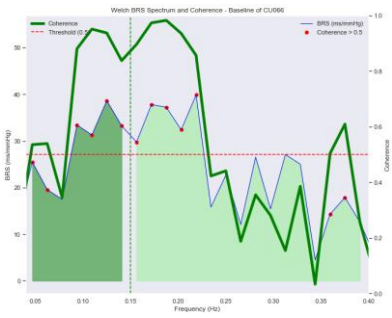

D

B

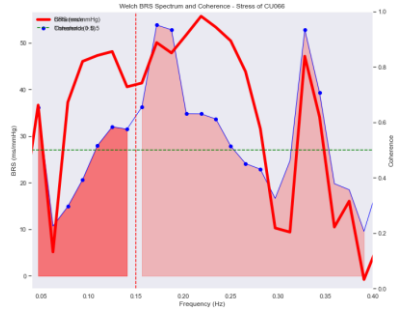

E

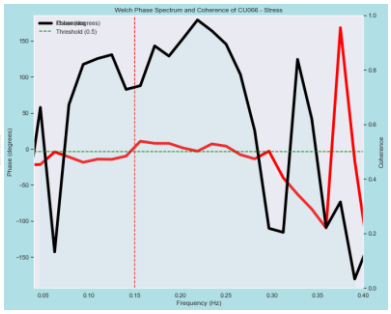

C

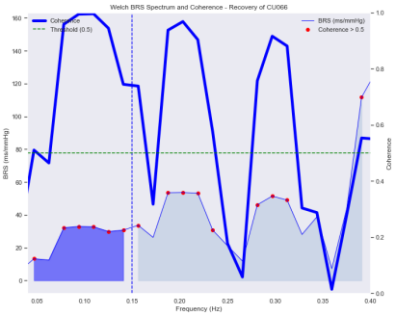

F

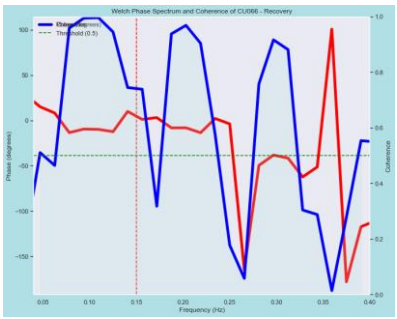

Figure H.1: 2D: BRS, coherence and phase spectrums by the Welch method of subject CU066 for three different experimental stages: (A,D) baseline, (B,E) stress, (C,F) recovery; frequency resolution at 0.015 Hz of x-axis represents frequency in Hz, y-axis indicates BRS values in ms/mmHg (A, B, C) or the phase (D, E, F) in degrees. The mirrored y-axis represents coherence values between 0 and 1, with the middle (green or red) dashed line portraying the applied coherence threshold (0.5). Colored circles on each BRS spectrum highlight transfer gains included in BRS computation, as they exceed the coherence threshold

A

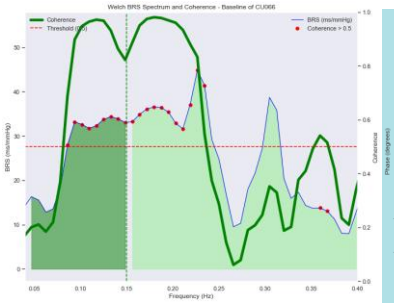

D

B

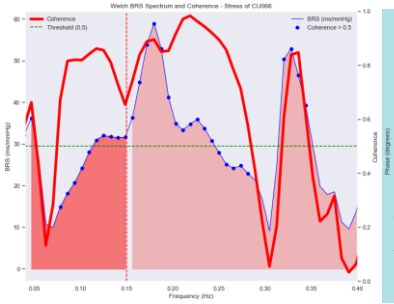

E

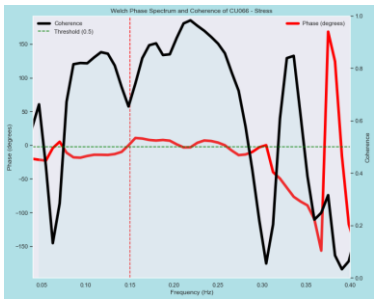

C

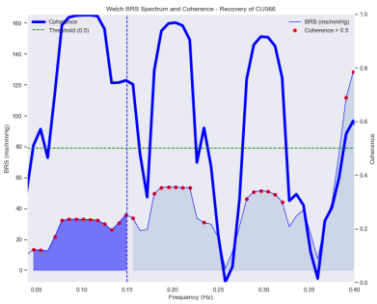

F

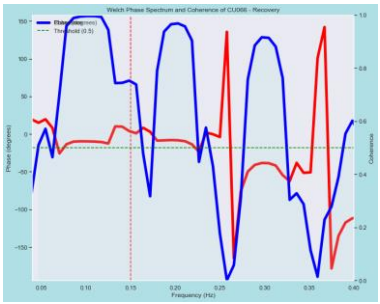

Figure H.2: 2D: BRS, coherence and phase spectrums by the Welch method of subject CU066 for three different experimental stages: (A,D) baseline, (B,E) stress, (C,F) recovery; frequency resolution at 0.015 Hz of x-axis represents frequency in Hz, y-axis indicates BRS values in ms/mmHg (A,B,C) or the phase (D,E,F) in degrees. The mirrored y-axis represents coherence values between 0 and 1, with the middle (green or red) dashed line portraying the applied coherence threshold (0.5). Colored circles on each BRS spectrum highlight transfer gains included in BRS computation, as they exceed the coherence threshold

Appendix I: Window type effects on BRS

Window type effects on mean BRS values of subject CU045 with frequency resolutions (0.008 Hz and 0.011) Hz and different hop sizes during three experimental stages (baseline, stress, recovery) are provided in Table I.1.

Window type	Frequency resolution (Hz)	Quasi time resolution (sec)	Baseline BRS (ms/mmHg) Mean ± SD	Baseline BRS RSD (%)	Stress BRS (ms/mmHg) Mean ± SD	Stress BRS RSD (%)	Recovery BRS (ms/mmHg) Mean ± SD	Recovery BRS RSD (%)
Hanning	0.008	60	4.49 ±1.32	29.30	3.39±0.26	7.58	4.46± 0.76	17.15
Hamming	0.008	60	4.49±1.33	29.52	3.23±0.29	9.01	4.51±0.63	13.92
Triangular	0.008	60	4.38± 1.19	27.23	3.26±0.44	13.38	4.26±0.49	11.47
Blackman	0.008	60	5.07±1.36	26.89	3.32±0.22	6.61	4.65±1.25	26.85
Parzen	0.008	60	5.21±1.46	27.94	3.25±0.21	6.60	4.72±1.50	31.84
Hanning	0.008	30	4.49±1.19	26.49	3.68±0.54	14.63	4.42±0.75	16.92
Hamming	0.008	30	4.50±1.22	27.10	3.53±0.56	15.78	4.86±1.25	25.60
Triangular	0.008	30	4.44±1.17	26.43	3.41±0.50	14.80	4.75±1.16	24.33
Blackman	0.008	30	4.73±1.22	25.70	3.55±0.48	13.62	4.51±1.05	23.39
Parzen	0.008	30	4.78±1.29	27.08	3.46±0.45	13.06	4.57±1.23	26.96
Hanning	0.011	30	4.70±1.25	26.67	3.80±0.61	15.96	4.78± 1.36	28.54
Hamming	0.011	30	4.80±1.32	27.61	3.84±0.63	16.33	4.71±1.37	29.03
Triangular	0.011	30	4.93±1.43	28.99	3.67±0.37	10.18	4.32±0.86	19.85
Blackman	0.011	30	4.93±1.43	28.96	3.56±0.42	11.94	4.41±1.21	27.53

Parzen	0.011	30	5.16±1.62	31.47	3.50±0.45	12.74	4.23±1.12	26.62
Hanning	0.008	15	4.60±1.39	30.30	3.51±0.51	14.51	4.65±0.76	16.44
Hamming	0.008	15	4.62±1.43	31.01	3.49±0.50	14.28	4.82±1.02	21.10
Triangular	0.008	15	4.56±1.40	30.78	3.38±0.43	12.85	4.74±0.94	19.87
Blackman	0.008	15	5.35±3.71	69.37	3.56±0.56	15.73	4.86±1.20	24.67
Parzen	0.008	15	4.91±1.56	31.76	3.54±0.53	14.83	4.98±1.30	26.04
Hanning	0.011	15	4.79±1.22	25.49	3.55±0.56	15.82	5.00±1.27	25.48
Hamming	0.011	15	4.94±1.70	34.47	3.86±1.11	28.68	4.85±1.28	26.74
Triangular	0.011	15	4.82±1.43	29.74	3.47±0.40	11.67	4.59±0.87	19.05
Blackman	0.011	15	4.77±1.20	25.26	3.46±0.41	11.89	4.79±1.00	20.99
Parzen	0.011	15	4.82±1.34	27.74	3.46±0.42	12.23	4.65± 1.10	23.69
Hanning	0.008	5	4.72±1.73	36.72	3.63±0.68	18.79	4.70±0.88	18.79
Hamming	0.008	5	4.67±1.51	32.32	3.52±0.56	15.98	4.74±0.91	19.09
Triangular	0.008	5	4.62±1.46	31.56	3.62±1.25	34.58	4.70±0.95	20.18
Blackman	0.008	5	5.01±2.63	52.57	3.55±0.50	14.07	4.84±1.07	22.16
Parzen	0.008	5	4.81±1.53	31.77	3.53±0.52	14.87	5.37±2.86	53.26
Hanning	0.011	5	4.82±1.43	29.72	3.48±0.56	16.23	4.92±1.13	22.93

Hamming	0.011	5	5.10±2.02	39.67	3.65±0.86	23.50	4.76±1.10	23.14
Triangular	0.011	5	5.00±1.96	39.22	3.92±2.58	65.79	4.67±1.16	24.86
Blackman	0.011	5	4.79±1.22	25.38	3.46±0.48	13.89	4.92±1.01	20.58
Parzen	0.011	5	4.86±1.27	26.18	3.47±0.52	15.08	5.27±4.25	80.63

Table I.1: Window type effects on mean BRS values in the LF band per stage of subject CU045. (RSD: relative standard deviation, SD: standard deviation)